UNIVERSITETET I AGDER

DESIGN, MODELING, AND FABRICATION OF THERMOELECTRIC GENERATOR FOR WASTE HEAT RECOVERY IN LOCAL PROCESS INDUSTRY.

NGENDAHAYO AIMABLE

SUPERVISOR: -Prof. Peter Hugh Middleton

CO- SUPERVISOR :-Dr. Gunstein Skomedal

This master's thesis is carried out as a part of the education at The University of Agder and is therefore approved as a part of this education. However, this does not imply that the University answers for the methods that are used or the conclusions that are drawn.

University of Agder, 2017

Faculty of Engineering and Science

Department of Engineering

ABSTRACT

The waste heat from energy company consumption sectors, when rejected into atmosphere, are useless and it contributes to global warming. Nowadays industrial activities and energy sectors (power stations, oil refineries, coke ovens, etc.) are the most energy consuming sectors worldwide and, consequently, the responsible for the release of large quantities of industrial waste heat to the environment by means of hot exhaust gases, cooling media and heat lost from hot equipment surfaces and heated products. Recovering and reusing these waste heats would provide an attractive opportunity for a low-carbon and less costly energy resource. Moreover, reducing the environmental impact.

Thermoelectric generator is the one of the method which helps to recover this waste heat, designing of thermoelectric generator was based on the range of temperature produced in industries and the objective is to generate optimum power with optimum material, Comsol Multiphysics software is the tool, which has been used to get the simulation results. High manganese silicide(HMS) has been chosen according to the properties of waste heat from industries, the simulation results shows that thermoelectric generator can be a good way to recover waste heat from local industries and converted to useful power, for instance to supply small sensing electronic equipment in the plant.

Keywords

- Thermoelectric generator;
- Waste heat recovery;
- Thermoelectric system;
- Thermoelectric manufacturing;
- Thermoelectric power generation;

Preface

This master thesis is completed for the degree of Master in Technology in Renewable Energy at the department of engineering and science, University of Agder, Grimstad campus.

The thesis is divided into two main parts. The first part discusses on west heat and the theoretical background of thermoelectric generator, the second parts talks about design of thermoelectric modules, Modeling components with usage of Comsol multiphasic software, power output and cost minimization.

I would like to thank my supervisors Professor Peter Hugh Middleton and Dr. Gunstein Skomedal, whom have been available for guidance always. Without their help and constructive feedback, the master thesis would not have been possible. Several persons have given their assistance when problems have occurred and I am grateful for all help and assistance I have received. I would also like to thank 3B fiberglass company AS for their initiative in thermoelectric power generation, and making their production plant available as a study case.

Grimstad, 19/05/2017

Aimable NGENDAHAYO

Contents

ABBREVIATIONS

TE - Thermoelectric

TEG - Thermoelectric generator

TEC - Thermoelectric cooler

Sub - Substrate

IWH-industrial waste heat

WHP-Waste heat to power

CHP-combined heat and power

HRSG -heat recovery steam generator

SYMBOLS

V - Voltage [V]

I - Current [A]

l - Length [m]

q - Heat [W]

P - Power [W]

A - Area [m^2]

ZT - Figure of merit

N - Number of thermocouples

η - Efficiency

Θ - Thermal resistance [K/W]

R - Electrical resistance [Ω]

T - Temperature [K or °C]

N -the number of couples in the module

V_{oc} - the open circuit voltage output from generator in volts

R_{TE} -The electrical resistance *of* a couple of pellets

α -the average Seebeck coefficient in volts/°K

ΔT - the temperature difference across the generator in ^{0}C

$C_{M,B}$ -cost associated with processing bulk material in ($/kg)

$C_{M,A}$ - areal manufacturing cost in ($/m^2),

C_{HX}- cost of both heat exchangers in ($/(W/K))

LIST OF TABLES

LIST OF FIGURES

1.INTRODUCTION

The manufacturing or process industry consumes vast amount of energy and around its half eventually lost as waste heat to the environment in the form of flue gases and radiant heat energy. There is a clear need to improve the situation by capturing at least some of the waste heat (harvesting) and converting it back into useful energy such as electricity to supply for instance small sensing electronic devices of the plant system, to increase the efficiency of system. Also, recuperating it, helps to reduce the emission which contributes to global warming. There are a lot of technologies which are being used to capture the waste heat; these different methods which are normally used to recover waste heat, differ each other with respect to the intensity of waste heat, for instance some of them are not adequate for low temperature, others require moving part to converts waste heat into useful energy, and others are not environmental friendly.

This study is focusing on thermoelectric generators, which use thermoelectric effects to produce power. This technology is an interesting one, for direct heat to power conversion. Thermoelectric generators present potential applications in the conversion of low level thermal energy into electrical power. Especially in the case of waste heat recovery, it is unnecessary to consider the cost of the thermal energy input, and there are additional advantages, such as energy saving and emission reduction, so the low efficiency problem is no longer the most important issue that we have to take into account [1] **.**Thermoelectric generators work even at low temperature applications**,** there are a renewable energy sources and do not produce noise. This project is focusing on the design, modelling and manufacturing thermoelectric generator for waste heat recovery applicable in local industries, by using comsol Multiphysics software as the tool. The design is based on the shape of the chimney, environment and cost of manufacturing; cost is found by considering all materials used in process, this helps to give conclusion weather the system should be adopted in local processing industries.

1.1. BACKGROUND

Energy consumption is an important parameter which reflects the influence of a certain sector on the economic growth and environmental pollution of a region. Existing reports from different energy statistics agencies and show that both industrial activities and energy sectors (power stations, oil refineries, coke ovens, etc.) are the most energy consuming sectors worldwide and, consequently, the responsible for the release of large quantities of industrial waste heat (IWH) to the environment by means of hot exhaust gases, cooling media and heat lost from hot equipment surfaces and heated products. Recovering and reusing IWH would provide an attractive opportunity for a low-carbon and less costly energy resource. Moreover, reducing the environmental impact and costs could, at the same time, improve the competitiveness of the sector [2].

Nowadays, energy problems have become worldwide focuses. Several national problems, such as, energy security, energy prices, increasingly competitive global markets and stringent environmental emission regulations, are primary driving forces in the search for efficient, sustainable and economically viable technologies for energy conversion and utilization. The process industries of the chemicals, food and drinks, steels and iron, pulps and paper are substantial energy users, which represent more than 50% of the industrial energy usage. Hendricks and Choate reported that 33% of the manufacturing industrial energy was discharged directly to the atmosphere or cooling systems as waste heat, due to the fact that most industries were incapable of recycling excessive waste heat. Moreover, the global energy demand will increase by almost 35% by 2030 compared with the 2005s level or by up to 95% without the use of energy efficient technologies. Great efforts have been made in improving the energy conversion efficiency, but a considerable amount of energy is still wasted in forms of gas, liquid and solid, which requires large scope of waste energy recovery [3] .In the French industry, 75% of the final energy is used for thermal purposes such as furnaces, reactors, boilers and dryers. However, around 30% of this heat is assumed to be wasted in the form of discharged hot exhaust gas, cooling water and heated product. In metal and non-metallic mineral product manufacturing in the United States, 20-50% of the energy is lost as waste heat. In Turkey, in cement plants 51% of the overall heat of the process is unfortunately lost. The combustion of fossil fuels, which generates carbon dioxide emissions, is considered as the primary source of heat production in the industry [4]. More than 80% of the total energy use in the Dutch industry involves the need for heat, either in fired furnaces

or in the form of steam at different pressure levels, see Figure 1. Most of this heat is eventually released to the ambient atmosphere through cooling water, cooling towers, flue gasses, and other heat losses. We call this heat loss 'Industrial waste heat'. Large energy savings are possible, if this waste heat could be reused. The total industrial waste heat in the Netherlands is estimated at more than 250 PJ (PJ = Petajoule = $1*10^{15}$J) per year [5].

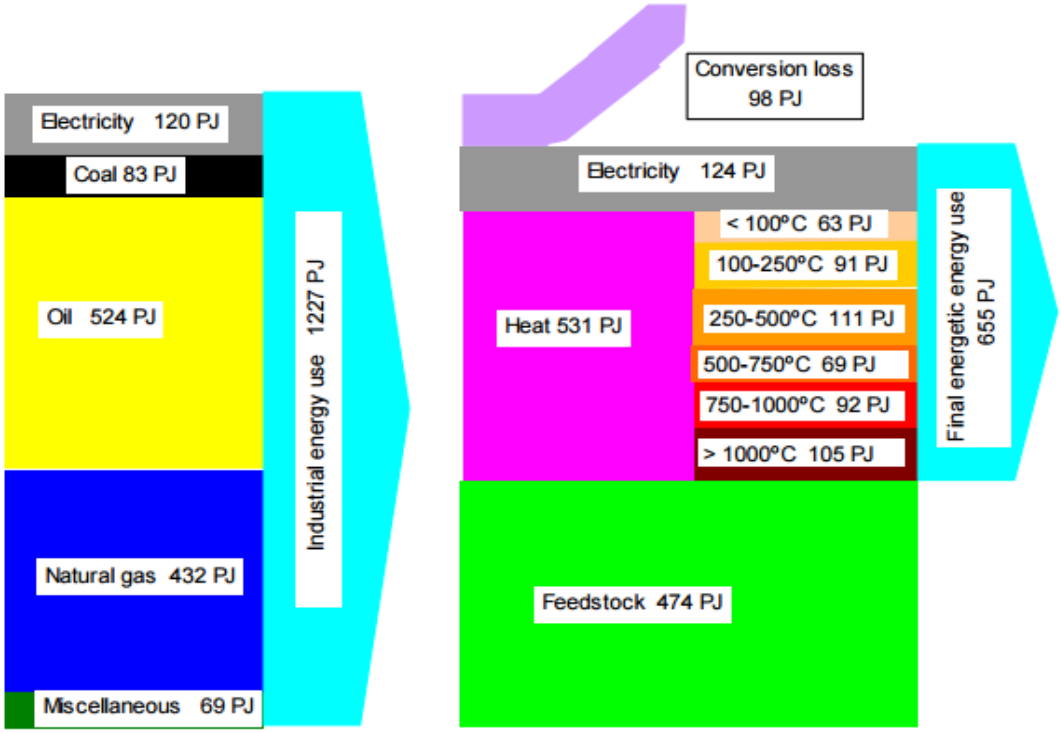

Figure 1. Energy balance of the Dutch industry, from energy carrier to end use *[5]*

For all the above-mentioned reasons, it is necessary to recover waste heat via capturing and reusing for heating or generating electrical or mechanical power in industrial processes. That way, the process efficiency will be increased, less fuel will be consumed and therefore less carbon dioxide will be emitted [4],The high and intermediate temperature waste can be directly utilized by driving steam turbine and gas turbine to generate electricity, but there are still difficulties in the utilization of waste heat in low-temperature range [3]. Thermoelectricity (TE), which is directly generated electric energy from waste heat sources shows promising results in making vital contributions to reducing greenhouse gas emissions and providing cleaner forms of energy [6] . The Thermoelectric Generator (TEG) can be used to convert heat to electricity through the Seebeck effect as illustrated in Figure 2 .

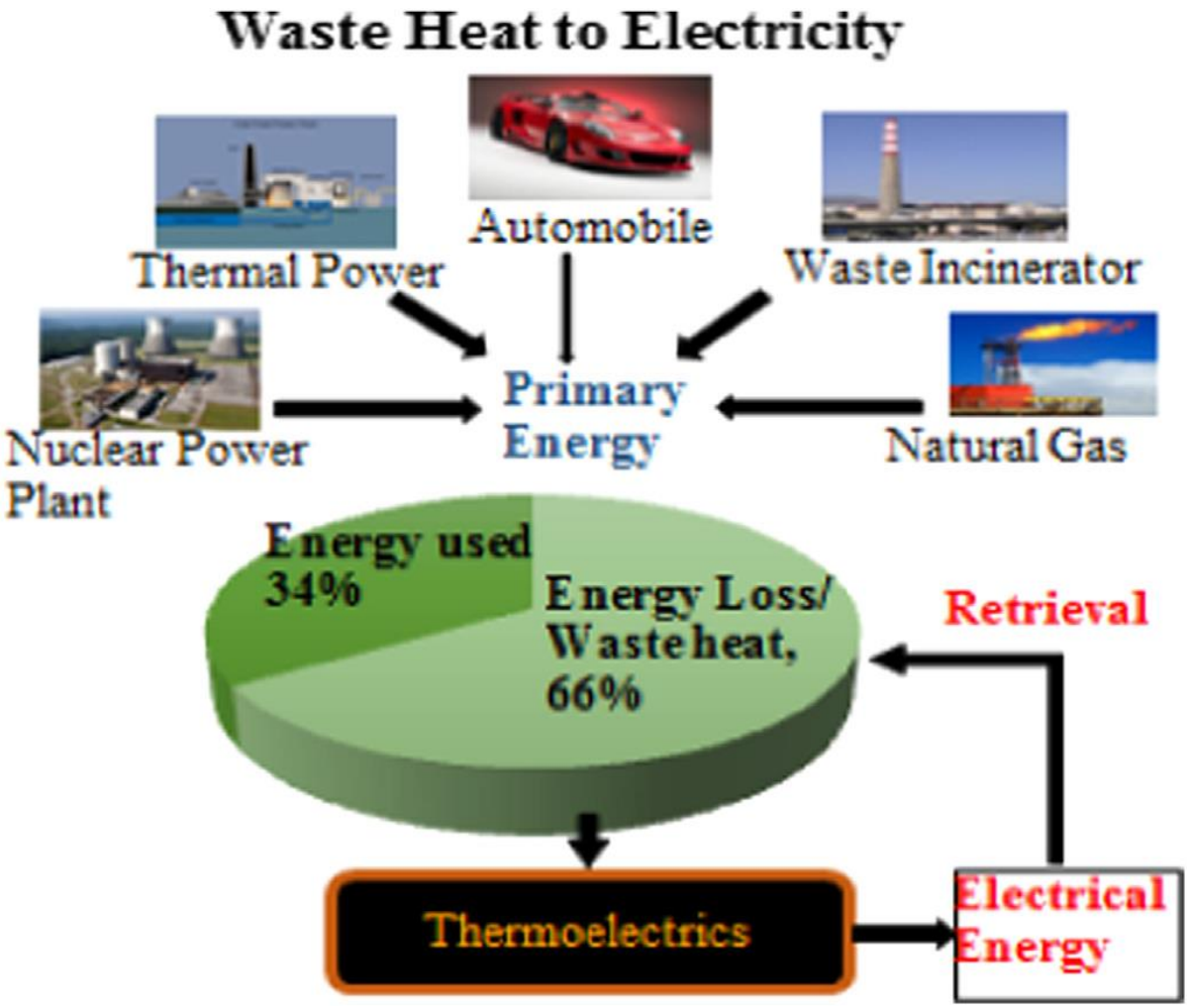

Figure 2. Thermoelectric generation of electricity offers a way to recapture some of the enormous amounts of wasted energy lost during industrial activities *[6]*

1.2. OBJECTIVES

The objective of this thesis is to design and modeling a thermoelectric generator for waste heat recovery (module and heat exchanger) and calculate the optimum power with respect to optimum materials, by means of Comsol Multiphysics software. input data are real waste heat values, from local industry which is 3B fiberglass company**.** Figure 3 shows purpose in the details, where the electricity can be produced when there is heat at one side and cold at the other side. the following points were considered to full fill the task:

- Assessing thermoelectric material
- Study how to use the waste heat as renewable energy sources

- Application of Thermoelectric in industry for waste heat recovery
- 3-D Modelling of the thermoelectric generator in Comsol Multiphysics
- Using Comsol Multiphysics to Optimize final module, considering cost per unity power.

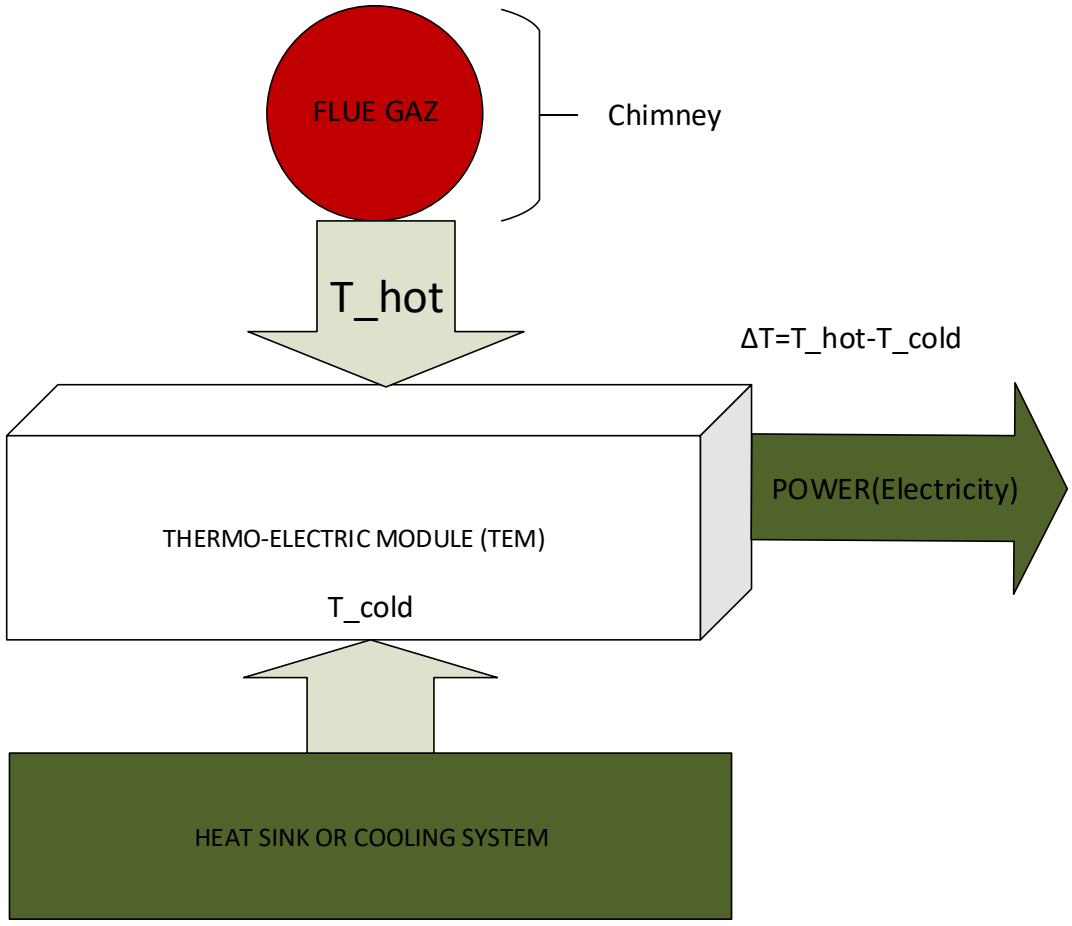

Figure 3. Block Diagram of Thermoelectric Generator Principle

1.3. KEY ASSUMPTIONS AND LIMITATIONS

The thesis will only focus on research of three thermoelectric materials in detail, skutterudites, bismuth telluride and silicide, the thermoelectric generator is modelled and sized per data from the local industry whose name is 3B fibre glass refining. Design will be focusing on a simple design by considering the heat flow as 1 Dimensional construct by considering the heat conduction in Chimney thickness as lossless.

2. THESIS OUTLINE

Chapter 3 describes west heat and how it is used, describing thermoelectricity, its application and materials. Chapter 4 talks about the design of thermoelectric generators, heat exchanger and heat sink. chapter 5 cover whole modelling both analytical and COMSOL® modelling, chapter 6 discusses the results and chapter 7concludes the thesis.

3. LITERATURE REVIEW

This part talks about waste heat, where it comes from, the way we can capture these waste heat and use it, so that to improve overall efficiency of the plant.

3.1. WASTE HEAT RECOVERY

Industrial waste heat refers to energy that is generated in industrial processes without being put to practical use. Sources of waste heat include hot combustion gases discharged to the atmosphere, heated products exiting industrial processes, and heat transfer from hot equipment surfaces. The waste heat temperature is a key factor determining waste heat recovery feasibility. Waste heat temperatures can vary significantly, with cooling water returns having low temperatures around 100- 200°F [40-90°C] and glass melting furnaces having flue temperatures above 2,400°F [1,320°C]. In order to enable heat transfer and recovery, it is necessary that the waste heat source temperature is higher than the heat sink temperature. Moreover, the magnitude of the temperature difference between the heat source and sink is an important determinant of waste heat's utility or "quality". The source and sink temperature difference influences a) the rate at which heat is transferred per unit surface area of heat exchanger, and b) the maximum theoretical efficiency of converting thermal from the heat source to another form of energy (i.e., mechanical or electrical). Finally, the temperature range has important ramifications for the selection of materials in heat exchanger designs [7]

Waste heat to power (WHP) is the process of capturing heat discarded by an existing industrial process and using that heat to generate power (see Figure 4). Energy intensive industrial processes such as those occurring at refineries, steel mills, glass furnaces, and cement kilns all release hot exhaust gases and waste streams that can be harnessed with well-established technologies to generate electricity. The recovery of industrial waste heat for power is a

largely untapped type of combined heat and power (CHP), which is the use of a single fuel source to generate both thermal energy (heating or cooling) and electricity [8]

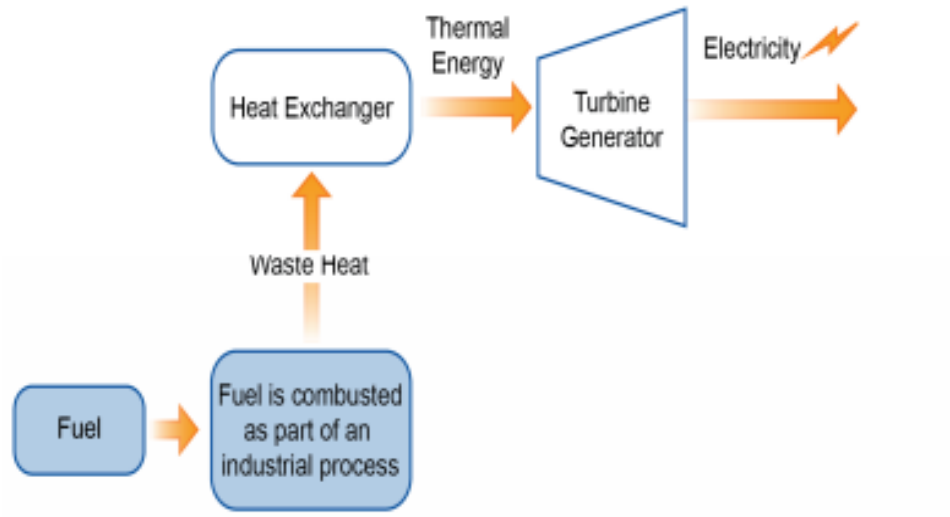

Figure 4. Waste Heat to Power Diagram *[8]*

Today, we face some significant environmental and energy problems such as global warming, urban heat island, and the precarious balance of world oil supply and demand. However, we have not yet found a satisfactory solution to these problems. Waste heat recovery is considered to be one of the best solutions because it can improve energy efficiency by converting heat exhausted from plants and machinery to electric power. This technology would also prevent atmospheric temperature increases caused by waste heat, and decrease fossil fuel consumption by recovering heat energy, thus also reducing CO_2 emissions [9].

So far, today's electrical energy production is mostly affected by generators, based on electromagnetic induction. Reciprocating steam engines, internal combustion engines, and steam and gas turbines have been coupled with such generators in utilizing chemical heat sources such as oil, coal and natural gas and nuclear heat for the production of electrical energy. Renewable energy sources like geothermal energy, solar energy and biomass energy are also being added to the list of heat sources used in modern electric power plants. Furthermore, solar energy provides hydropower indirectly. All these power plants have, however, a common disadvantage; the conversion of thermal energy into electric energy is accomplished by the utilization of moving and wear-subjected machine equipment. Some of the most widely used waste heat recovery technologies are in figure 5. The system proposed for this study is to generates electric power by providing waste heat or unharnessed thermal

energy to built-in thermoelectric modules that can convert heat into electric power. The main advantages are the low maintenance requirement, the high modularity and the possibility of utilising heat sources over a wide temperature range [10].

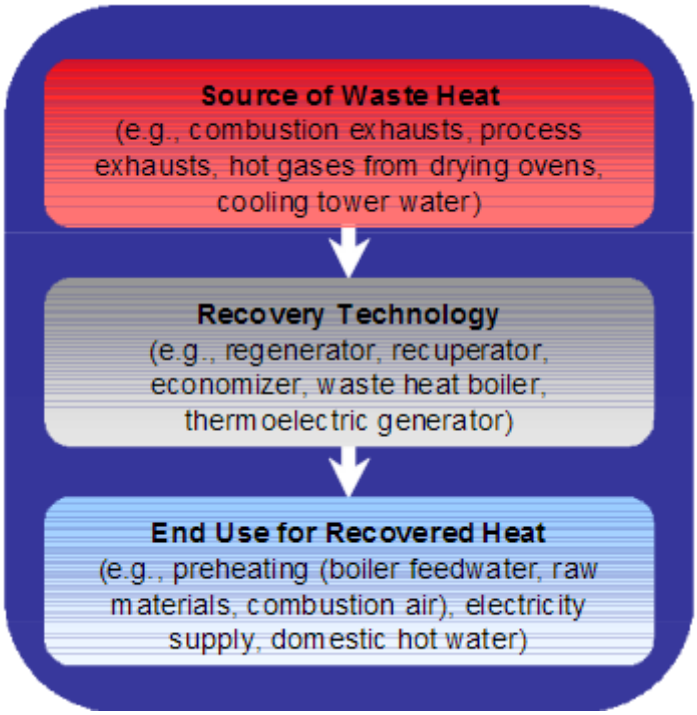

Figure 5. Three essential component are required for waste heat recovery *[7]*

3.2. THERMOELECTRICITY

The term thermoelectricity refers to the phenomena in which a flux of electric charge is caused by a temperature gradient or the opposite in which a flux of heat is caused by an electric potential gradient. (phenomena in which a temperature difference generates electricity or vice versa) These phenomena include three effects; the Seebeck, Peltier and Thomson effect. The German physicist Thomas Johann Seebeck discovered the first of the thermoelectric effects in 1821. He found that a circuit made out of two dissimilar metals would deflect a compass needle if their junctions were kept at two different temperatures. Initially, he thought that this effect was due to magnetism induced by the temperature difference, but it was realized that it was due to an induced electrical current. The second of the effects was observed by the French watchmaker Jean Charles Athanase Peltier in 1834.

He discovered the small heating or cooling effect which occurs when a current is forced through a junction of two different metals. The third effect was observed by the British physicist William Thomson (later Lord Kelvin) in 1856. He discovered that there is a heat exchange with the surroundings when there is both a temperature gradient and a flow of electric current in a conductor, this heat effect comes in addition to the Joule heating. He also recognized the interdependency between the Seebeck and Peltier effects, and by applying the theory of thermodynamics he established a relationship between the coefficients that describes the Peltier and Seebeck effects. These relations are known as the Kelvin relations. After the discovery of the thermoelectric effects, there was a slow progress in the field of thermoelectricity. Applications of the thermoelectric effects were limited to temperature measurements. New interest into the field came with the discovery of semiconductors in the 1930s. The introduction of semiconductors as thermoelectric materials in the 1950s made it possible to make Peltier refrigerators and thermoelectric generators with sufficient efficiency for special applications the interest in thermoelectricity waned until new interest was shown in the beginning of the 1990s [11].

3.2.1. THERMOELECTIC DEVICES

Thermoelectric (TE) devices have attracted much attention in recent years because they can convert waste heat into electrical energy directly. The device is made of semiconductors and is normally the shape of a rectangular parallelepiped [12].

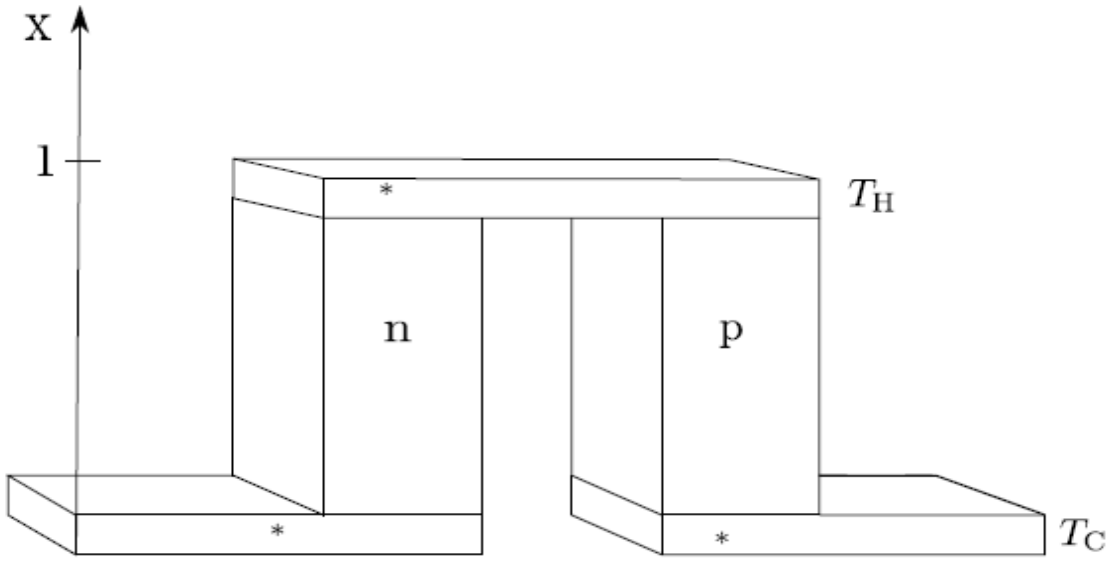

Figure 6. The basic unit of a thermoelectric device *[11]*.

A pair of n- and p-type semiconductors, called a thermocouple, is the basic unit of a thermoelectric module. A schematic drawing of the basic unit is shown in figure 6. The n-type and p-type semiconductors are connected electrically at one end. The electric conductors are marked by * in the figure. T_H and T_C are the junction temperature and base temperature, respectively. The typical semiconductor pair geometry is as shown in figure 6 and the dimensions of the semiconductors is typically in the order of millimetres [11].A thermoelectric device converts thermal energy to electrical energy by using an array of thermocouples. This device is a reliable source of power for satellites, space probes, and even unmanned facilities. Satellites that fly toward planets that are far away from the sun cannot rely exclusively on solar panels to generate electricity. In the figure 7, Electrons on the hot side of a material are more energized than on the cold side. These electrons will flow from the hot side to the cold side. If a complete circuit can be made, electricity will flow continuously. Semiconductor materials are the most efficient, and are combined in pairs of “p type” and “n type”. The electrons flow from hot to cold in the “n type,” While the electron holes flow from hot to cold in the “p type.” This allows them to be combined electrically in series. Elements are combined in series to increase voltage and power output [13]

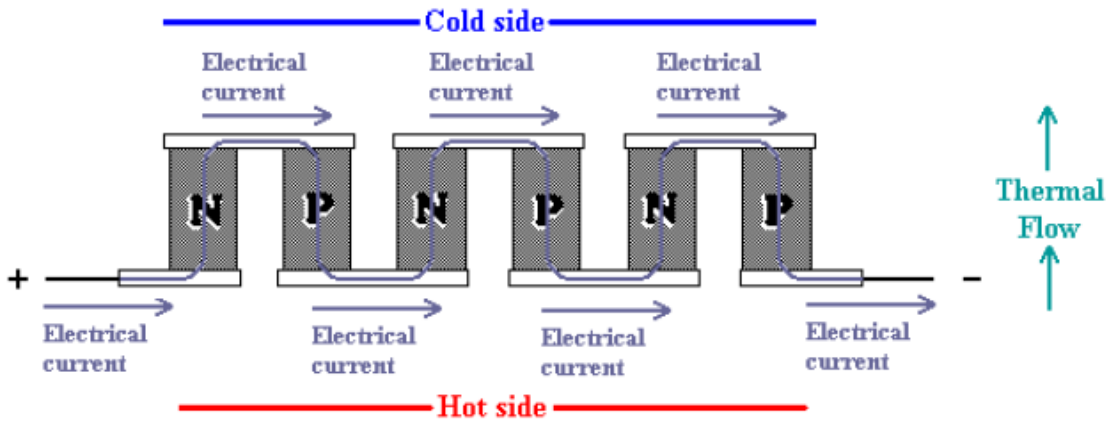

Figure 7. Thermoelectric elements in series *[13]*

3.3. THERMOELECTRIC EFFECTS

Thermoelectric effect is defined as the direct conversion of temperature differences to electric voltage and vice versa. A thermoelectric device creates a voltage when there is a different temperature applied on each side. Conversely, when a voltage is applied to such a device, it creates a temperature difference. At the atomic scale, an applied temperature

gradient causes charge carriers in the material to diffuse from the hot side to the cold side, thus inducing a thermal current, which is similar to a classical gas that expands when heated, leading a flux of the gas molecules. This effect can be used to generate electricity, measure temperature, or change the temperature of objects. Because the direction of heating and cooling is determined by the polarity of the applied voltage, thermoelectric devices are also efficient temperature controllers. The term ‘‘thermoelectric effect’’ encompasses three separately identified effects: the Seebeck effect, Peltier effect, and Thomson effect. In most textbooks, it is known as the Peltier-Seebeck effect. This name is given due to the independent discoveries of the effect by French physicist Jean Charles Athanase Peltier and Estonian-German physicist Thomas Johann Seebeck. Joule heating, a heat that is generated whenever a voltage is applied across a resistive material, is related, though it is not generally termed as thermoelectric effect. The Peltier–Seebeck and Thomson effects are thermodynamically reversible, whereas Joule heating is not [14].

3.3.1. SEEBECK EFFECT

When a conductive material is subjected to a thermal gradient, charge carriers migrate along the gradient from hot to cold; this is the Seebeck effect; if two dissimilar materials were joined together and the junctions were held at different temperatures (T and $T+\Delta T$) a voltage difference (ΔV) was developed that was proportional to the temperature difference ΔT .The ratio of the voltage developed to the temperature gradient ($\Delta V / \Delta T$) is related to an intrinsic property of the materials called the Seebeck coefficient (α) or the thermopower [15].

$$\alpha = -\frac{\Delta V}{\Delta T} = -\frac{V_{hot} - V_{cold}}{T_{hot} - T_{cold}}$$, Seebeck coefficient: α [V/K] (1)

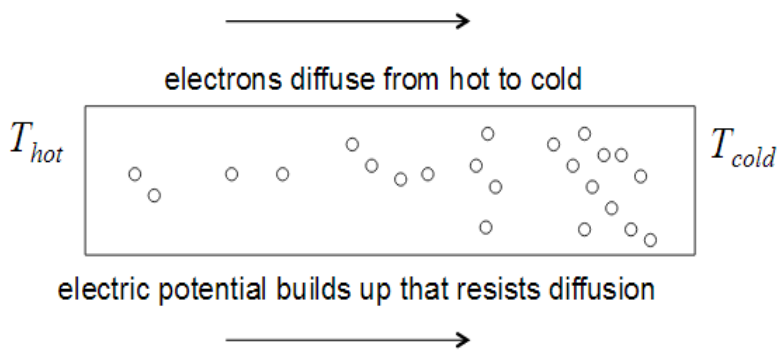

Figure 8. Motion of charge carriers *[16]*

In the open-circuit condition, Figure 8 charge carriers will accumulate in the cold region, resulting in the formation of an electric potential difference [16]. In fact, the temperature difference between top and bottom drives the electrons and holes (missing electrons) away from the hot side. This leads to an imbalance in charge between the hot and cold sides. In other words, there is a voltage difference, just like a battery, that can be used to do electrical work, e.g.: powering the radio in your car [17] (see Fig.9). The Seebeck effect describes how a temperature difference creates charge flow.

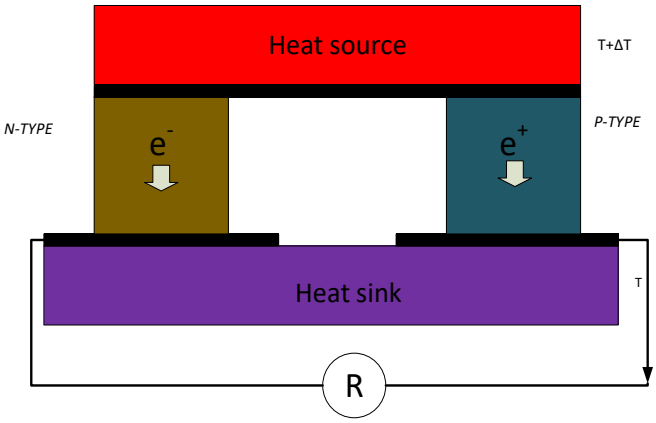

Figure 9. A single thermo-electric couple in power generation mode

The Seebeck coefficient is negative for *n*-type and positive for *p*-type materials. In degenerate semiconductors and metals, the Seebeck coefficient depends on the temperature as described in equation (2)

$$\alpha = -\frac{8\pi^2 k^2}{3eh^2} m^* T \left(\frac{\pi}{3n}\right)^{2/3} \qquad (2)$$

In equation (2), *k* is Boltzmann's constant, *h* is Planck' s constant, e is the charge of the electron which is also a constant. Then, the Seebeck coefficient is proportional to the effective mass of charge carriers, *m**. Also, a small charge carrier concentration, *n*, is needed for a large Seebeck coefficient [18].

3.3.2. PELTIER EFFECT

The reverse of the Seebeck effect is also possible: by passing a current through two junctions, you can create a temperature difference. This process was discovered in 1834 by scientist named Peltier, and thus it is called the Peltier effect. This may sound similar to Joule heating

described above, but in fact it is not. In Joule heating the current is only increasing the temperature in the material in which it flows. In Peltier effect devices, a temperature difference is created: one junction becomes cooler and one junction becomes hotter [19]. Simply Peltier has observed that if an electrical current is passed through the junction of two dissimilar materials (A and B), heat is either absorbed or rejected at the junction depending on the direction of the current see figure 10; to keep its temperature Constant [15, 20].

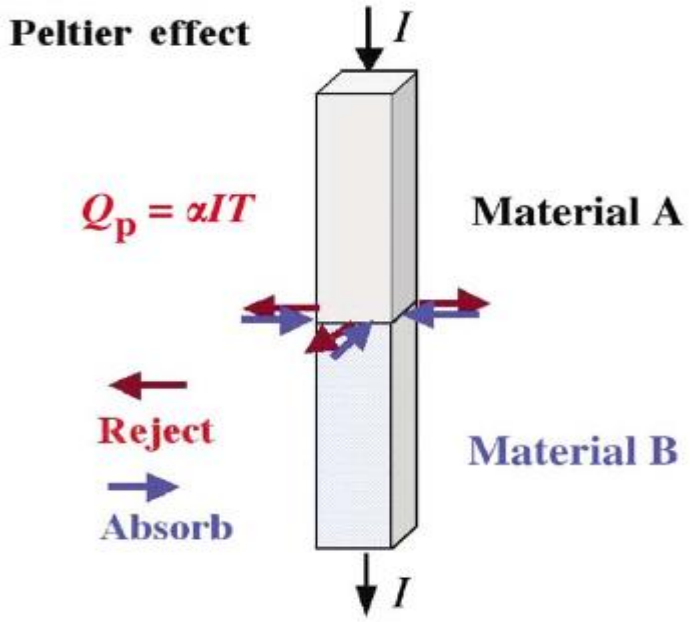

Figure 10.A schematic illustrating the Peltier effect between two dissimilar materials *[15]*.

Although Peltier coolers are not as efficient as some other types of cooling devices, they are accurate, easy to control, and easy to adjust. Peltier effect devices are used coolers for microelectronic devices such as microcontrollers and computer CPUs.This use is very common among computer hobbyists to help them in over-clocking the microprocessors for more speed without causing the CPU to overheat and break in the process [19]. The heat power associated with the Peltier phenomenon can be calculated as in equation (3)

$$Q_P = \pi I = \alpha T_j I \tag{3}$$

where,

I-the electrical current flowing in the thermoelectric module

π -Peltier coefficient that can be expressed by means of Seebeck coefficient α and last equivalence comes from the Kelvin relationship;

T_j - junction temperature

3.3.2.1. THERMOELECTRIC COOLING DEVICE

The thermoelectric devices used in thermoelectric refrigeration (or thermoelectric coolers) are based on the Peltier effect to Convert electrical energy into a temperature gradient. If a low-voltage DC power source is applied to a thermoelectric cooler, heat is transferred from one side of the thermoelectric cooler to the other side. Therefore, one face of the thermoelectric cooler is cooled and the opposite face is heated. Figure11 depicts a thermoelectric cooling module considered as a thermoelectric refrigerator, in which the electrical current flows from the N-type element to the P-type element. The temperature T_c of the cold junction decreases and the heat is transferred from the environment to the cold junction at a lower temperature. This process happens when the transport electrons pass from a low energy level inside the P-type element to a high-energy level inside the N-type element through the cold junction. At the same time, the transport electrons carry the absorbed heat to the hot junction which is at temperature T_h, The quality of a thermoelectric cooler depends on parameters such as the electric current applied at the couple of N-type and P- type thermoelements, the temperatures of the hot and cold sides, the electrical contact resistance between the cold side and the surface of the device, the thermal and electrical conductivities of the thermoelement, and the thermal resistance of the heat sink on the hot side of the thermoelectric cooler [21] .

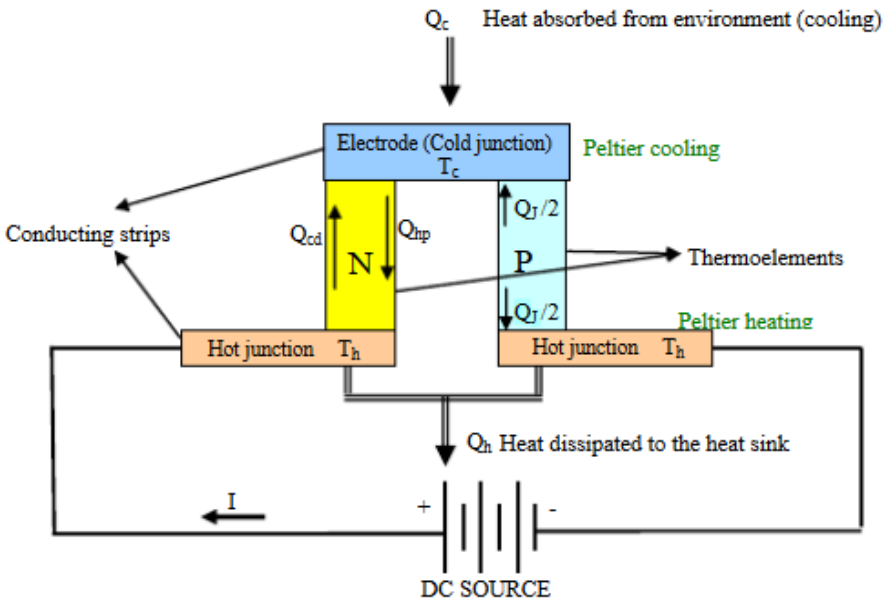

Figure 11.Schematic Diagram of a Typical Thermoelectric Cooler *[21]*

The pairs of thermoelectric cooling are made of two semiconductors elements, frequently made of bismuth telluride highly doped to create an excess (n-type) or a deficiency of electrons (p-type). The heat absorbed at the cold junction is transferred to the hot junction at a rate proportional to the current passing through the circuit and the number of semiconductors pairs [22].

3.3.3. THOMSON EFFECT

The Thomson effect can be seen as a continuous variant of the Peltier effect that is active inside the TE material, while the Peltier effect only occurs at the interfaces between different materials [23]. Thomson phenomenon takes place in presence of an electrical current flowing not through a junction of two materials as in Peltier effect but in a homogeneous electrical conductor placed between objects at two different temperatures. Depending on the direction of current flow, a heat is absorbed or dissipated from the conductor volume. For instance, if the electrons are the current carriers and move towards higher temperatures, in order to maintain thermal equilibrium, they must take an energy as heat from the outside. The reverse situation occurs in the opposite direction of the current flow. Quantitative model of this effect is described by (4) (Lovell et al., 1981) [24].

$$Q_t = \mu_T . I . \frac{dT}{dx} \tag{4}$$

Where,

μ_T -the Thomson, coefficient

The influence of Thomson effect on performance of thermoelectric devices is very weak, however, it exists and cannot be neglected for very high temperature gradients.

3.3.4. JOULE HEAT PHENOMENON

When a current flow through a material, some of the electric energy is lost and converted to heat. This is not a pure thermoelectric effect, but it exists in all materials, and it is an important, undesired effect that lowers the performance in both thermoelectric generators and Peltier coolers [23].Joule heat generation is the most commonly known phenomena associated with a current flowing in electrical circuits. Opposite to the previously described

phenomena, Joule effect is not reversible and it manifests in a heat dissipated by material with non-zero resistance in the presence of electrical current (5) [24] .

$$Q_j = I^2.R \tag{5}$$

3.3.5. POWER GENERATION

When a thermoelectric couple or a meander of serially connected, pairs is placed between two objects at two different temperatures T_c and T_h - e.g. a heat sink and a heat source , it can produce Seebeck voltage V_S, Figure12. In this case, only Seebeck effect and heat conduction phenomenon occur**.** If the electromotive force V_S is closed by a resistive load R_L then an electrical power P is generated (eq.6) and the thermoelectric module is utilizing all the described phenomena [24].

$$P = I^2 R_L = \left(\frac{V_S}{R_L + R_I}\right)^2 .R_L = \left(\frac{\alpha(T_h - T_c)}{R_L + R_I}\right)^2 .R_L \tag{6}$$

Where, R_L is the internal resistance of the thermoelectric couples

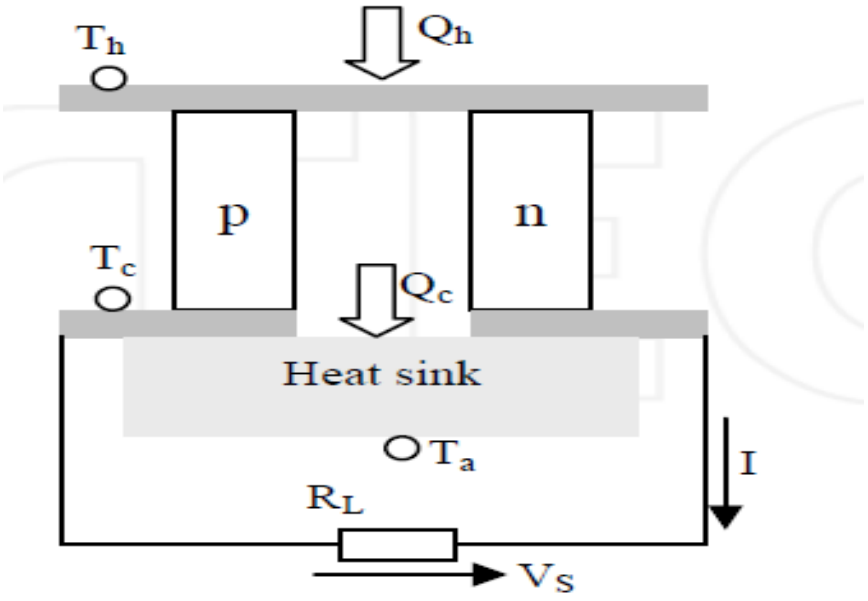

Figure 12. Power generation by a single thermocouple exposed to a temperature gradient *[24]*.

The linear voltage-current characteristic and power output are sketched in Figure 13, The maximum power output is at half-open-circuit voltage and half-short-circuit current (as with all matched loads) [25], the maximum power output is in equation (37).

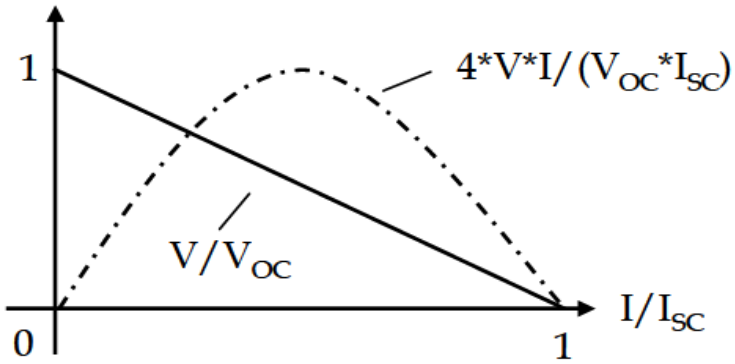

Figure 13.Voltage, current and power characteristics of the thermoelectric generator *[25]*

3.4. THERMOELECTRICITY MATERIALS

All materials exhibit thermoelectric effects but the name 'thermoelectric materials' is used to describe the materials that are good at converting heat to electricity [17].Thermoelectric materials are crucial in renewable energy conversion technologies to solve the global energy crisis. They have been proven to be suitable for high-end technological applications such as missiles and spacecraft. The thermoelectric performance of devices depends primarily on the type of materials used and their properties such as their Seebeck coefficient, electrical conductivity, thermal conductivity, and thermal stability. Classic inorganic materials have become important due to their enhanced thermoelectric responses compared with organic materials [26]. There exist a wide variety of different thermoelectric(TE) materials today some of them have been known and used for decades, while others are a result of more recent development of both understanding of the physics and more advanced production processes. Thermoelectric materials can be categorized on many different levels, such as crystal structure, conversion efficiency, cost, and temperature range [27]. Figure 14 shows the construction of a thermoelement. Modules are typically composed of around a hundred elements. Modules can be constructed as Peltier coolers or as high temperature generators. Both of these use the same materials and can be used to produce power, but they differ in how the thermoelements are soldered to the conducting strip [13] . Since Seebeck's

discovery, many materials have been considered useful to generate thermoelectricity. The first TEGs were based on electricity conductors and semiconductors, such as antimony, bismuth, copper, iron, lead, zinc and different alloys, among others. Later, in the 20th century, many other thermoelectric materials (TMs) were developed: ceramics, composites, etc. Nevertheless, the updated semiconductors continue being basic TMs for the production of thermoelectric effects. It should be emphasized that all these materials were obtained empirically, through thousands of attempts based on the personal experience of a researcher. Therefore, the essential progress in the TMs area depends mainly on the advances in fundamental knowledge related to the nature of thermoelectric effects [28].

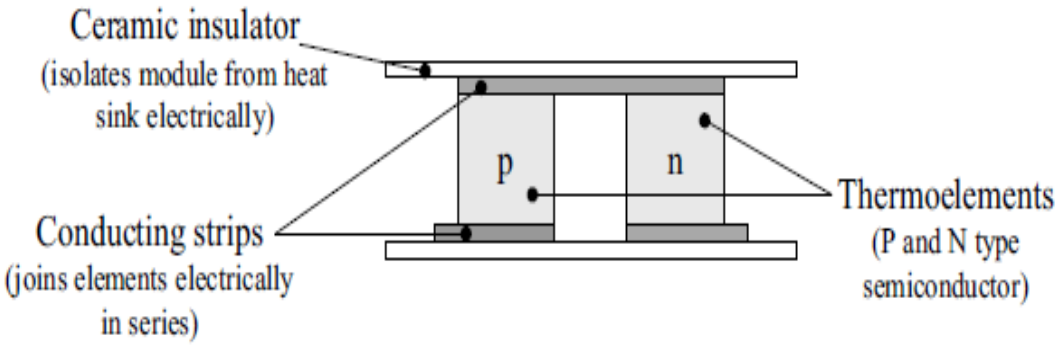

Figure 14.A Thermoelectric Materials *[13]* .

3.4.1. THERMOELECTRIC PERFORMANCE

The performance of thermoelectric devices strongly depends on the efficiency of the materials of which they are made, the material used in the construction of a TEG plays an important role in controlling the performance of these devices. The efficiency is evaluated by the thermoelectric figure of merit (*Z)*, which expresses the combination between Seebeck coefficient (α), electrical resistivity (*ρ)*, and thermal conductivity (*k)* (Equation 7) [29] **.** There are many features that describe the performance of these materials to make them suitable for use in TEG device manufacture. The potential of a material for thermoelectric applications is determined in large part to a measure of the material's figure of merit,

$$Z = \frac{\alpha^2}{k * \rho} \tag{7}$$

where,

Z - Thermoelectric material figure-of-merit,

α - Seebeck coefficient given by equation (1)

ρ -Electrical resistivity (inverse of electric conductivity σ)

k-Total thermal conductivity.

The figure-of-merit may be made dimensionless by multiplying by *T* (average absolute temperature of hot and cold plates of the thermoelectric module).

$$ZT = \frac{\alpha^2 T}{k * \rho} = \frac{\alpha^2 T \sigma}{k} \tag{8}$$

$$T = \frac{T_H + T_C}{2} \tag{9}$$

The term $\frac{\alpha^2}{\rho}$ is referred to as the electrical power factor and the thermoelectric properties yield the conversion efficiency of the material and are thus the most important properties when evaluating thermoelectric materials. All these values (Electrical Conductivity, Thermal Conductivity) are dependent on the charge carrier density of the materials, as seen in the figure 15. This is mainly because diffusion of charge carriers is the main transport mechanism to consider in materials and semiconductors. The Seebeck coefficient is a measure of the entropy transported by moving charge carriers divided by the carrier's charge, and can be described by the equation (10)

$$\alpha \sim \frac{1}{eT}\langle E - E_F \rangle \tag{10}$$

Where,

e-the electrical charge,

E_F -the Fermi energy and

$\langle E - E_F \rangle$-the average energy per carrier, excess of the fermi energy.

The diffusive movement of charge carriers will always be from the hot to the cold end. If electrons are the majority carriers, the Seebeck coefficient will become negative. This is called a n-type material. The Seebeck coefficient is inversely proportional with the number of charge carriers. This is illustrated in figure 15 [30].

3.4.2. ELECTRICAL CONDUCTIVITY

The electrical conductivity is the ability of the material to move charge carriers through the material. The formulae associated with electrical conductivity are presented in equations (11) and (12):

$$\sigma = n\mu e \tag{11}$$

$$\mu = \frac{e\tau}{m^*} \tag{12}$$

The electrical conductivity, *σ,* is proportional to the charge carrier concentration, *n,* charge of the electron *e* which is a constant, as well as the mobility of the charge carrier, μ. Mobility, in turn, is proportional to the relaxation time, τ, which is the time between collisions of charge carriers, and inversely proportional to the effective mass of charge carriers, *m**. Thus, factors that enhance the Seebeck coefficient, namely low carrier concentration and high effective mass, are factors that cause a lower electrical conductivity [18] .In metals, there are many carriers and states available for conduction, typically $n \approx 10^{22}$ carriers cm^{-3}. The electrical conductivity is then very large for metals; on the order of 10^6 $(\Omega cm)^{-1}$.Again for semiconductors, the carriers must be thermally excited across a gap for conduction to occur. The conductivity can occur through the contributions of both holes and electrons

$$\sigma = n\mu_e + pe\mu_h \tag{13}$$

Where,

n - electron concentration

μ_e - electron mobility

p- hole concentration and,

μ_h - hole mobility.

There are two primary ways to achieve a high conductivity in a semiconductor, either by having a very small gap to excite across ($E_G<k_B T$) where k_B is the Boltzmann constant and energy gap E_G, or by having very high mobility carriers. Typical values of the electrical conductivity lie between 10^{-4} and 10^4 $(\Omega cm)^{-1}$, however these are somewhat arbitrary boundaries [15].

3.4.3. THERMAL CONDUCTIVITY

The thermal conductivity describes the materials ability to conduct heat through the material. There are two components to thermal conductivity which can be seen in formula (14):

$$k_{total} = k_e + k_l + k_{bp} \tag{14}$$

The total thermal conductivity consists of the electronic component of thermal conductivity, k_e , which describes heat carried by the charge carriers and the lattice component of thermal conductivity, k_l , which describes heat transferred through lattice vibrations (phonons) and k_{bp} is the bipolar thermal conductivity due to the formation and recombination of electron-hole pairs .Wiedemann-Franz law describes the electronic contribution of thermal conductivity in metals and narrow band gap semiconductor. The law states that the thermal conductivity is related to electrical conductivity via the relationship described in equation (15):

$$k_e = L\sigma T \tag{15}$$

It can be seen that the electronic component of thermal conductivity is directly proportional to electrical conductivity. where the constant of proportionality L is called the Lorenz number.

Qualitatively, this relationship is based upon the fact that the heat and electrical transport both involve the free electrons in the metal. The thermal conductivity increases with the average particle velocity since that increases the forward transport of energy. However, the electrical conductivity decreases with particle velocity increases because the collisions divert the electrons from forward transport of charge. This means that the ratio of thermal to electrical conductivity depends upon the average velocity squared, which is proportional to the kinetic temperature [18, 31]. From these equations, it can be seen how the electronic contribution of the thermal conductivity is linearly dependent on the electric conductivity. Since the ratio $\frac{\sigma}{k_e}$ should be maximized to increase the ZT value, k_l must be reduced. This has led to the optimal thermoelectric material being called a "Phonon-glass, electron-crystal" where the phonons are disrupted as in a glass (amorphous material) while the electrons can move more freely as in a crystalline material [30]. The lattice thermal conductivity arises from the lattice vibration; therefore, its value strongly depends on the vibration mode. Atomic vibrations exist in all crystalline systems at above 0 K. The concept of phonon is considered as the quantized energy of lattice vibrations, related to both vibration frequency and temperature. As the temperature is raised, the amplitude of atomic agitations is increased, which means the number of phonons in the systems increases. For a simple crystalline solid, the lattice thermal conductivity is based on Debye's equation (16), treating lattice vibrations as a phonon gas, where C_V is the volume heat capacity, v is the average phonon group velocity (velocity of sound), and λ is the phonon mean free path [29].

$$k_l = \frac{1}{3} C_v v \lambda \qquad (16)$$

The bipolar thermal conductivity exists in the temperature range of intrinsic excitations, in which both electrons and holes contribute to the heat conduction. For thermoelectric materials in operation, this conduction happens because a larger number of electron-hole pairs are generated at the hot side more than the cold side when the material is subjected to a temperature gradient. Additionally, the recombination happening at the cold side releases a certain amount of energy, corresponding to the materials' bandgap, which contributes to the total thermal conduction [29]. The bipolar thermal conductivity is calculated according to equation 17, where e and h indicate the contribution of electrons and holes, respectively

$$k_{bp} = \left(\frac{k_B}{e}\right)^2 \frac{1}{\rho_e + \rho_h}(s_e + s_h)T \tag{17}$$

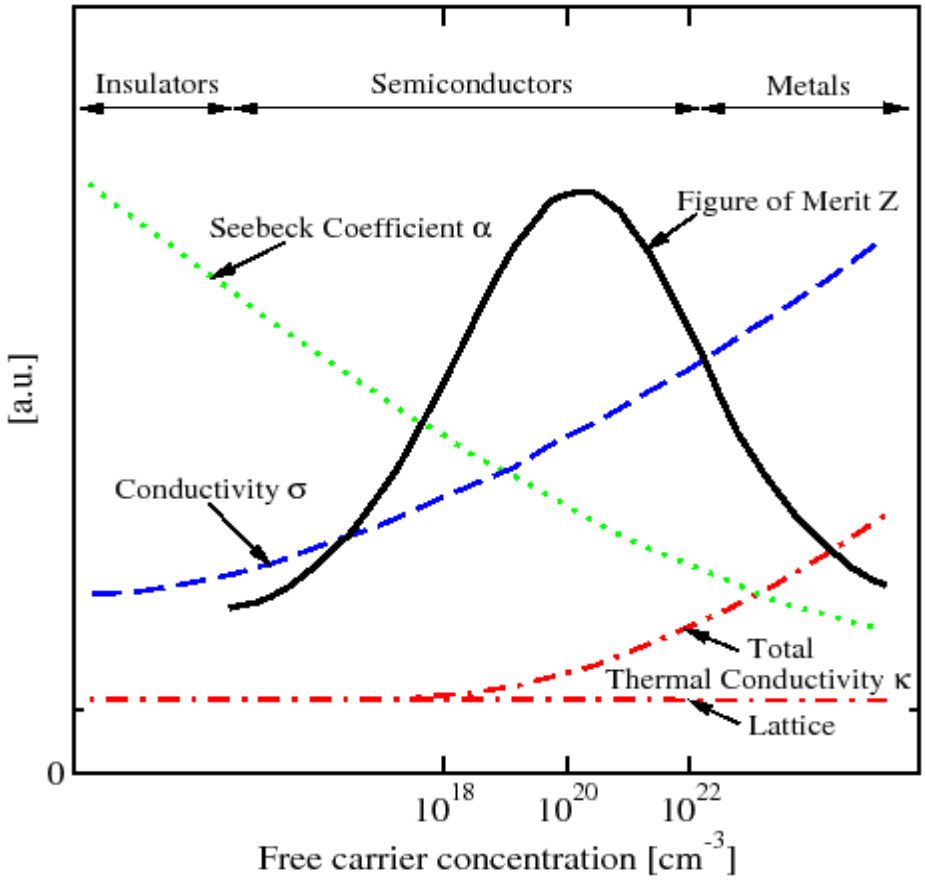

Figure 15. ZT as a function of charge carrier concentration (a.u: arbitrary units) *[18]*.

Materials with a high figure-of-merit display good thermoelectric properties. From the *ZT* equation, it is evident that a material which displays high Seebeck coefficient, high electrical conductivity and low thermal conductivity is suited to thermoelectric applications. Figure 15 illustrates different materials and their relationship to *ZT* and shows that metals have good electrical conductivity but low Seebeck coefficient due to high carrier concentration. Furthermore, metals also have high thermal conductivity; therefore, metals are not good thermoelectric materials. Insulators, on the other hand, have very low thermal conductivity and high Seebeck coefficient but are poor electrical conductors. Hence, insulators cannot be used for thermoelectric applications either. Semiconductors however, are ideal

thermoelectric materials [18]. The efficiency of thermoelectric devices is calculated from the temperature difference between the hot and cold side, and the figure of merit of materials, which is limited by the Carnot efficiency (equation 45) where T_H and T_C are the hot and cold side temperature, respectively, and T the mean temperature (Figure 16).

$$\eta_{\max} = \left(1 - \frac{T_C}{T_h}\right) \frac{\sqrt{1+ZT} - 1}{\sqrt{1+ZT} + \frac{T_C}{T_h}} \tag{18}$$

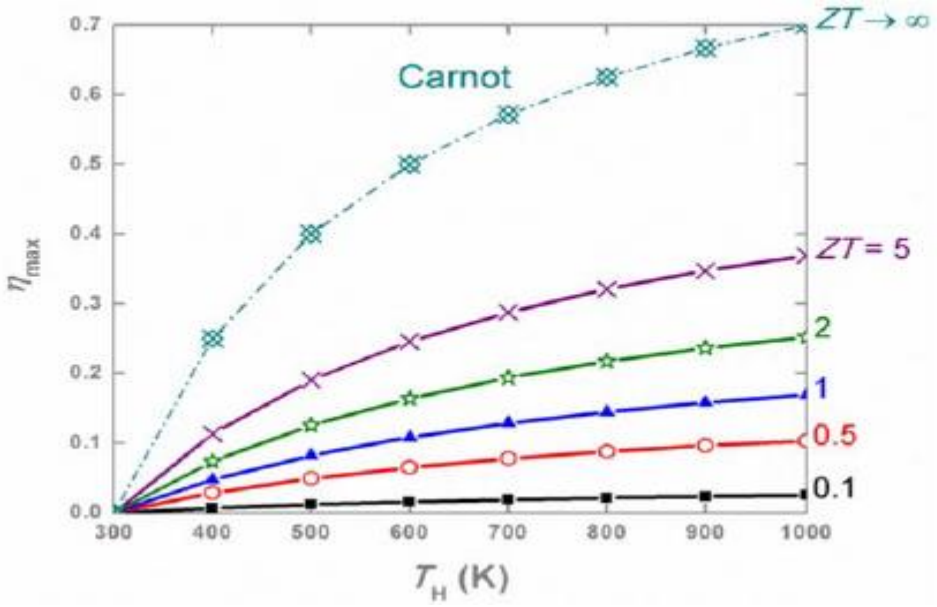

Figure 16. The efficiency of thermoelectric devices as a function of hot-side temperature for different materials with the cold side is kept at 300 K *[29]*.

In addition to *ZT*, according to the theory, the ultimate efficiency of a TEG is determined and capped by the so-called Carnot efficiency $\eta_c = (T_h - T_c)/T_h$. If T_c is kept at a constant temperature, for example, room temperature, then higher T_h will lead to higher ultimate efficiencies of TEGs. In other words, big temperature gradient across the TEG could yield a high-efficiency outcome [32].The value of the figure-of-merit is usually proportional to the conversion efficiency. The dimensionless term *ZT* is Therefore, a very convenient figure for comparing the potential conversion efficiency of modules using different thermoelectric materials. The conversion efficiency as a function of operating temperature difference and for a range of values of the thermoelectric material's figure-of-merit is shown in Figure (16).

It is evident that an increase in ΔT provides a corresponding increase in available heat for conversion as dictated by the Carnot efficiency, so large ΔT is advantageous [33].More details on efficiency are in modeling chapter.

3.4.4. APPROACHES TO INCREASING THE THERMOELECTRIC FIGURE OF MERIT

As shown in equation (8), the thermoelectric figure of merit is the square of the Seebeck coefficient multiplied by electrical conductivity and divided by thermal conductivity; the result is multiplied by absolute temperature. The Seebeck coefficient and electrical conductivity both depend on charge carrier density and cannot be simultaneously increased in a practical manner. There is an optimum charge carrier density that delivers the highest nominator (power factor) of the thermoelectric figure of merit. Only one parameter can be changed independently of charge carrier density; this is the thermal conductivity, which consists of two parts-phonon and electron. These parts can be altered more or less independently. The method of creating solid solutions allows significant reductions in thermal conductivity. In this method, the solution of two isovalent materials with the same crystal structure could be used to increase phonon scattering, thereby reducing thermal conductivity. Maximizing ZT requires minimal thermal conductivity. Another method to increasing the figure of merit is to increase the density of states (DOS). This is very difficult to achieve in some materials, because the density of states is typically dependent only on the band structure of a material, for which there is no means to produce such a change. However, in solid solutions, it is sometimes possible to alter the band structure to increase the figure of merit. [34]

3.5. THERMOELECTRIC MATERIALS

There exist a wide variety of different thermoelectric (TE) materials today. Some of them have been known and used for decades, while others are a result of more recent developments of both understanding of the physics and more advanced production processes. TE materials can be categorized on many different levels, such as crystal structure, conversion efficiency, cost and temperature range [27]. Conventional TE materials can be classified into three groups in terms of the temperature range of their operation: low temperature materials (200-500 K), medium temperature materials (500-800 K), and high temperature materials (800 K). It is sometimes found that nanocomposite TEs exhibit shifts of the optimum temperature

range to certain extent by effectively changing the temperature dependency of the Seebeck coefficient, the electrical conductivity and thermal conductivity. However, such shifts are typically relatively small and do not normally move the maximum ZT from one temperature range to another. Figure 17 summarizes recent achievements in TE nanocomposites with embedded nanoinclusions grouped in the three temperature ranges of operation mentioned above [35].

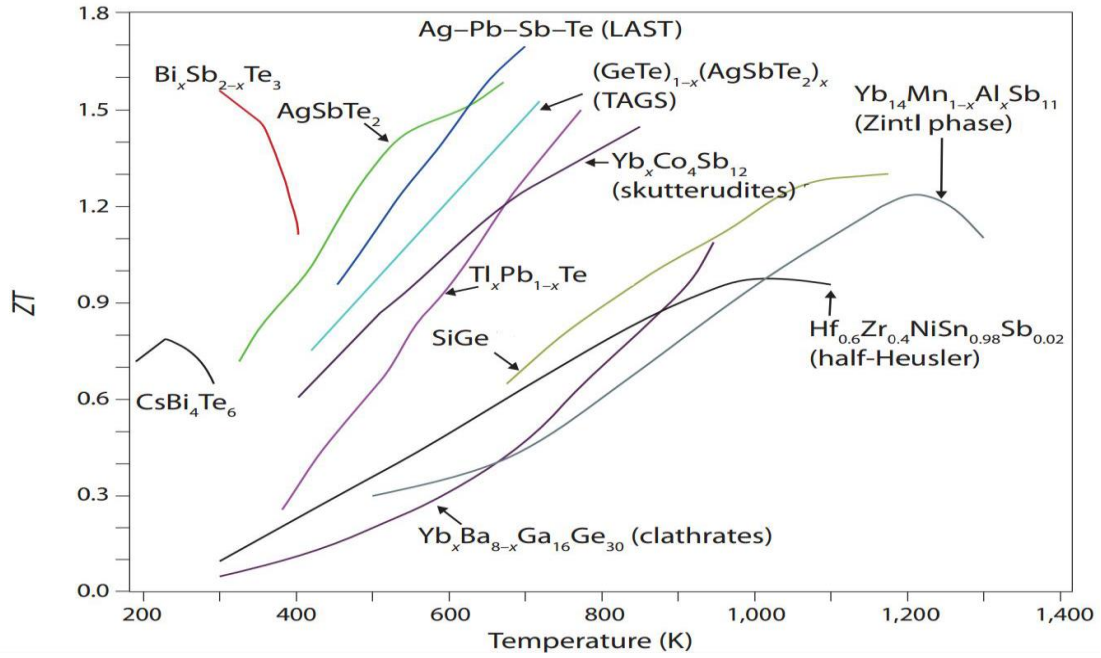

Figure 17. Overview over the ZT of different materials as a function of temperature [27]

3.6. LOW TEMPERATURE MATERIALS

Alloys of Bi_2Te_3-Sb_2Te_3 are state-of-the-art TE materials operating in the temperature range of 200-400 K. Due to their relatively high ZT values of around 1 compared to other bulk materials around room temperature, Bi_2Te_3-Sb_2Te_3 alloys have been the material of choice in a variety of commercial TE devices with applications in refrigeration and temperature regulation of scientific instrumentation, drinking fountains, and car seats. Additional applications of Bi_2Te_3-based materials lie in the recovery of low quality waste heat from combustion processes or even from electronic circuits.

A dramatic improvement in material performance was achieved by Poudel et al. in 2008 when they obtained a ZT value of 1.4 at 373 K by introducing nanoscale crystalline features in a bulk p- type $Bi_xSb_{2-x}Te_3$ alloy. This sample was prepared by hot-pressing nanopowders, which were

obtained by ball-milling commercial ingots of Bi_2Te_3 and Sb_2Te_3 under Ar atmosphere. The enhanced ZT was a result of a significant decrease in the lattice thermal conductivity of the material, most likely due to the increased phonon scattering at the nano-grain boundaries of Sb-rich phases and Te precipitates as revealed by high resolution microscopic analysis. This work motivated a series of studies on tailoring the grain structure of $Bi_xSb_{2-x}Te_3$ alloys with various nanoinclusions. Heterogeneous nanocomposites of $Bi_xSb_{2-x}Te_3$ with SiC, ZnAlO, PbTe and Zn_4Sb_3nanoinclusions were fabricated by other researchers, and their TE properties were characterized and evaluated in relation to the effect of the nanoinclusions. It was found that, in general, the presence of nanoinclusions increases the phonon scattering at their grain boundaries and consequently decreases the lattice thermal conductivity of the nanocomposites. However, for some cases, there is also a significant decrease in the electrical transport properties which more than compensates for the decreased lattice thermal conductivity, resulting in a decreased ZT. One such example was reported for the addition of PbTe nanoparticles into the $Bi_xSb_{2-x}Te_3$ matrix, which was found to cause an unfavorable doping effect that increased the carrier concentration due to incorporation of Pb_2 from the PbTe nanoparticles. Likewise, similar studies have been performed on n-type binary Bi_2Te_3 alloys. Zhao et al. conducted a series of experiments of dispersing SiC nanoparticles in bulk Bi_2Te_3. Their results showed that the addition of those nanoparticles not only increased the figure of merit by18 % with respect to the bulk reference without SiC, but also effectively improved the mechanical properties including Vickers hardness, Young's modulus, and fracture toughness, improving the materials attractiveness for device fabrication [35].

3.7. MEDIUM TEMPERATURE MATERIALS

TE materials with stable and high conversion efficiency in the medium temperature range of operation is a hot research topic, because such materials could significantly impact waste heat recovery for the transportation sector and exhaust heat generating industries. The most prominent representatives of medium temperature TE materials are skutterudites, lead chalcogenides, half-Heusler, clathrates, Zn_4Sb_3, and Mg_2Si-based. Here, we review the use of nanoinclusions with these materials to further enhance their performance [35].

3.7.1. SKUTTERUDITES

Skutterudites are crystal structures that are based on the mineral $CoAs_3$.in Figure 18, These crystal structures have hollows in the center of the body, which can be used to accommodate large metal atoms to form filled skutterudites. These metal atoms can manipulate the phonon scattering, which results in a reduction of the lattice's thermal conductivity and consequently increases the ZT values. In fact, filled skutterudites like $Ce_{0.9}Fe_3CoSb_{12}$ and $Ba_{0.30}Ni_{0.05}Co_{3.95}Sb_{12}$ reach ZT higher than 1 for temperatures over 500^0C [36].

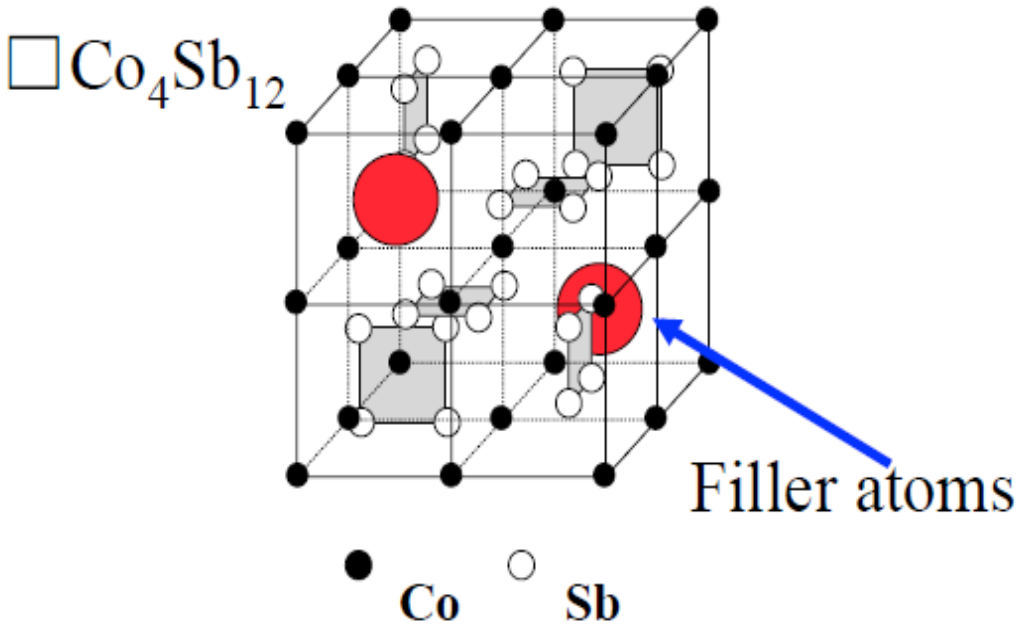

Figure 18. basic structure of Skutterudites *[37]*

Skutterudite is the name of a cobalt and arsenic based mineral that was extensively mined in the region of Skutterud, Norway. This compound has the formula $CoAs_3$ and serves as the prototype. More generally MX_3 (*M* = Fe, Co, Rh, Ir, Ni *X*= P, As, Sb) compounds with the same cubic crystal structure have since been known as 'skutterudites' [38]. Generally, binary skutterudites are semiconductors with small bandgaps ~0.1 eV, high carrier mobilities and modest Seebeck Coefficients but very high thermal conductivities. The open structure is the key to their potential for thermoelectric applications. Filling the voids with foreign atoms could possibly depress the lattice thermal conductivity dramatically and modify the electronic properties to enhance the figure of merit [39]

3.7.2. CHALCOGENIDE

chalcogenide compounds are group of potential thermoelectric materials, which are semiconductors with high stability in air and high melting points. Because of their strong flexibility in hosting other elements and the small difference in electronegativity among sulfur, selenium, and tellurium, it is highly potential to synthesize chalcogenide semiconductors with energy gaps (e.g.0.1–0.8 eV) suitable for thermoelectric applications over a wide range of temperature. Among various chalcogenide compounds, Bi_2Te_3, together with its solid solutions, such as p-type $Bi_{2-x}Sb_xTe_3$ and n-type $Bi2Te_{3-x}Se_x$, is the most widely used thermoelectric materials for large-scale cooling applications. PbTe is another important example of chalcogenide compounds, with a maximum ZT of about 0.8 at 770 K, which is thus used for power generation at intermediate temperatures. Recent studies have shown that germanium-based TAGS (Te-Ag-Ge-Sb) has higher performance than PbTe, but its high sublimation rate, high cost, and the presence of a low-temperature phase transition could be obstacles for their practical applications [14].

3.7.3. CLATHRATE

Clathrate are characterized by open frameworks composed of tetrahedrally coordinated Al, Ga, Si, Ge, or Sn, thus having low thermal conductivity. Within the framework structure, there are various cages that can incorporate large electropositive atoms. There are two main types of structure, Type I and Type II, with Type I being more commonly encountered. The Type I structure can be represented by a general formula $X_2Y_6E_{46}$ (Figure 19, Na_8Si_{46} for example), where X and Y are ‘‘guest’’ atoms encapsulated in two different polyhedral cages E_{20} and E_{24}, with E representing tetrahedrally coordinated framework atoms. The Type II structure is composed of E_{20} and E_{28} cages. It has been accepted that the presence of the guest atoms in these cages that can rattle and scatter lattice phonons, together with the open nature of the framework, effectively decrease the lattice thermal conductivity [14].

In a recent study, TiO_2 nanoparticles were incorporated in a bulk $Ba_8Ga_{16}Ge_{30}$ matrix, where the composites were made by mixing of powders followed by SPS (Spark plasma sintering). A large reduction of the thermal conductivity was observed in the materials with increasing content of TiO_2 nanoparticles but this was unfortunately accompanied by a large reduction in

the electrical conductivity. An optimum performance was, however, found at 0.4 vol.% TiO_2, where the overall effect on ZT was positive. Hall measurements showed an increased carrier concentration for the best performing composite material, which was interpreted to be due to a doping effect originating from the inclusion of the nanoparticles. Likely, a part or most of the TiO_2 has been reduced through the sintering process and elemental Ti has entered the matrix to act as a dopant. When the TiO_2 content became too high, this reduction process was not as effective and thus the performance of the material decreased resulting in the presence of the optimum concentration of nanoinclusions [40].

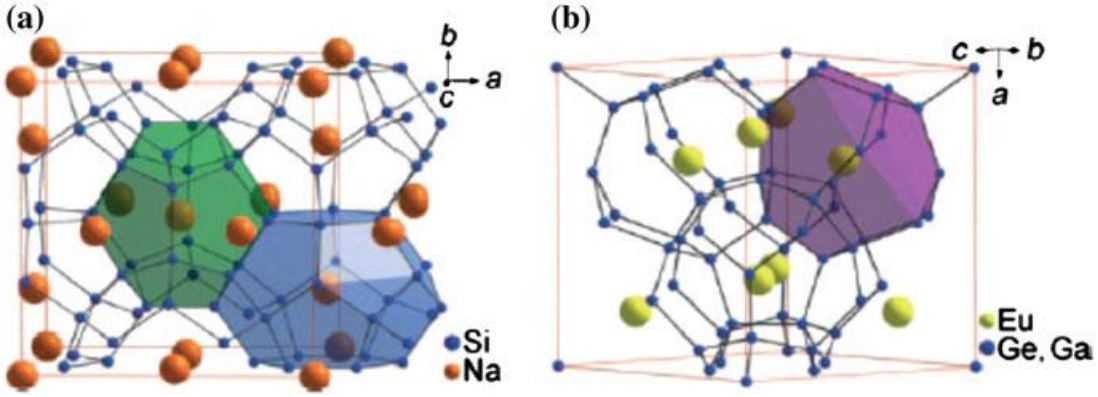

Figure 19. a) Crystal structure of the Type I clathrate, Na_8Si_{46}. Framework composed of Si atoms(blue) and two different cages with guest Na atoms, the tetrakaidecahedral cage; blue) and the pentagonal dodecahedral cage (green). b) Crystal structure of the Type VIII clathrate, $Eu_8Ga_{16}Ge_{30}$. The framework (violet) is composed of Ge and Ga atoms. ([Ax]: A = number of vertices, x = number of faces). Reproduced with permission from *[14]*.

3.7.4. HALF-HEUSSLER COMPOUNDS

One of the most versatile class of compounds are the so called Heusler compounds [38], which are named after their discoverer Fritz Heusler. Today, the class of Heusler materials includes more than 1,500 different compounds and can be divided into Heusler (general formula X_2YZ) and half-Heusler (XYZ) compounds, X and Y are transition metals and Z is a main group element [14, 38] Today the research for good thermoelectric compounds within the class of half-Heusler compounds is especially focused on two systems based on NiTiSn for the *n*-type and CoTiSb for the *p*-type materials. These compounds can easily be doped with other elements, and thus the band structure can be changed. For NiTi (Sn, Sb) materials, power factors up to 70 µW/cm K at 650 K can be reached, nevertheless due to the comparatively high thermal conductivity of about 10 µW/mK, a figure of merit of only 0.45 at 650 K was achieved. One of the highest figures of merit of 1.5 at 700 K was reported for Sb-doped $NiTi_{0.50}Zr_{0.25}Hf_{0.25}Sn$. Further substitutions with other main-group and transition metals have

been made for the optimization of the thermoelectric performance (see Fig. 20). The main challenge for this compound is the reduction of the thermal conductivity. This can be easily be done by introducing grain boundaries into the system, which will considerably influence the phonon scattering. One way is based on exploiting a phase separation of the solid solution $CoMn_{(1-x)}$ Ti_xSb into the compounds CoTiSb and CoMnSb. Another way is the introduction of nanostructures by creating nanopowders by ball milling bulk samples and finally obtaining dense bulk material by hot pressing. This lead to an enhancement of 60% *ZT* with a *ZT* of 0.8 at 700^0C for the $Zr_{0.5}Hf_{0.5}CoSn_{0.8}Sb_{0.2}$ Heusler compound. An advantage of the half-Heulser compounds are the similar chemical and physical properties of the *n*- and *p*-type compounds, making them attractive for thermoelectric modules [38].

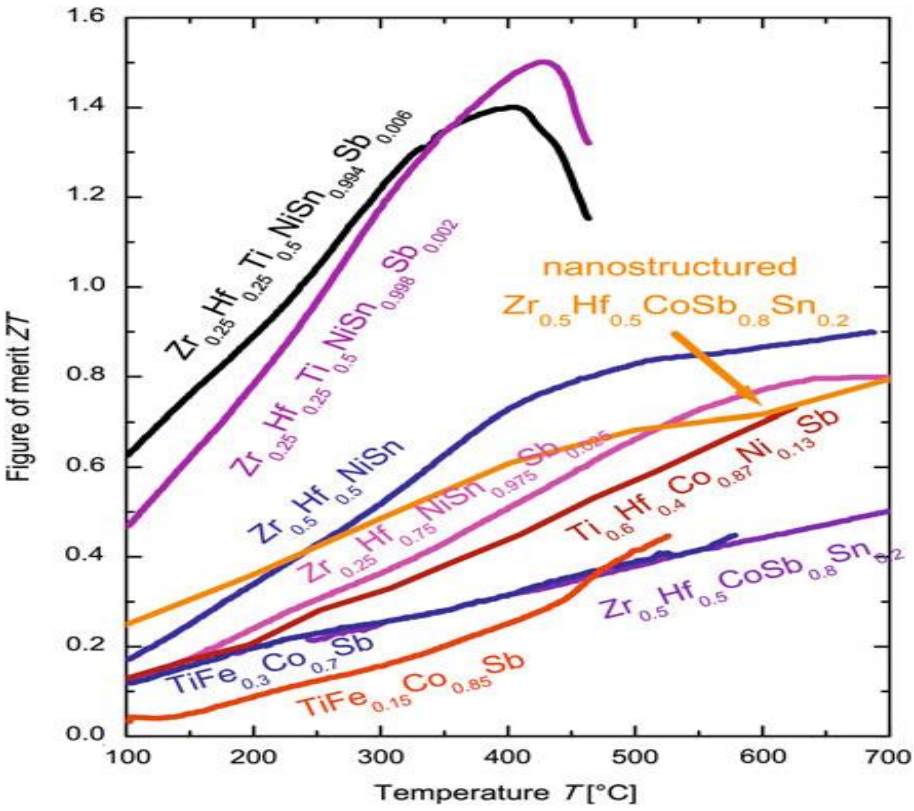

Figure 20. State of the art thermoelectric figure of merit ZT of half-Heusler materials *[38]*.

3.7.5. SILICIDES

The Silicides are an interesting material group for thermoelectric power generation as they not only show good thermoelectric properties, but also make use of cheaper raw materials and offers good mechanical and chemical stability. Higher manganese silicide (HMS, $MnSi_x$, x=1.70-1.77) is the most promising TE-material of the silicide group. It is an example of

material with complex and large crystal structure. This often leads to an amorphous behavior of the lattice part of the thermal conductivity as the phonons are scattered effectively by the large distance between atoms. The c-axis of the crystal structure is more than three times the length of the perpendicular axes leading to a strong anisotropy of the crystal and thus also on the thermoelectric and mechanical properties. The ZT curve of a HMS material is found in Figure 21. Chromium disilicide, $CrSi_2$, is another interesting silicide material. It has a hexagonal crystal structure similar to HMS, but has still not been made with higher ZT values than approximately 0.3. Other types of silicide are $FeSi_2$, Ru_2Si_3 and CoSi [30]. Silicide based thermoelectric materials has high potential as silicide is one of the most common materials in the world, the only more common element in the earth's crust is oxygen. This makes it cheap to produce compared to other scarce thermoelectric materials. That the silicide is abundant is not the only positive, it is also ecologically friendly and does not contain rare or toxic elements [41].

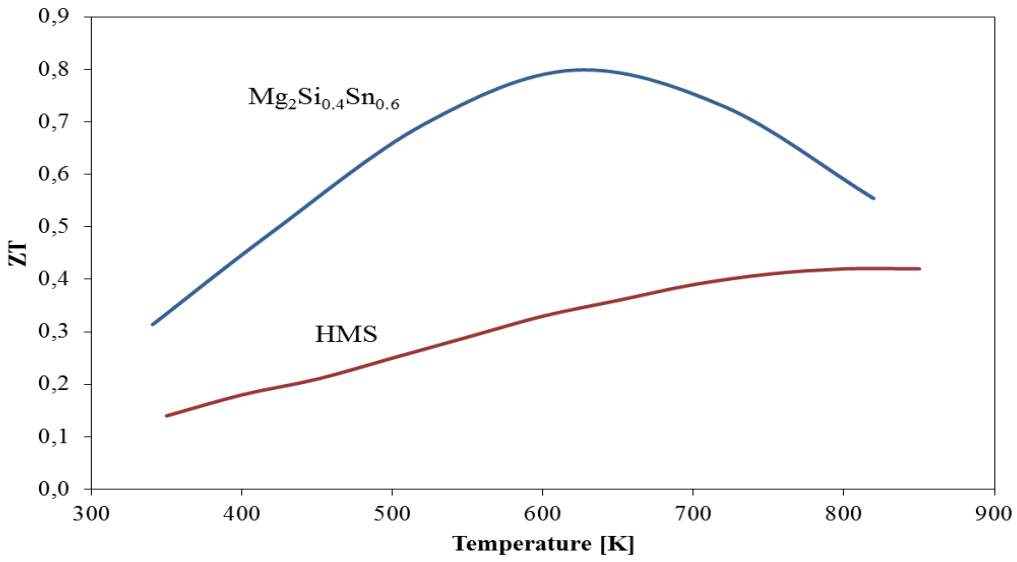

Figure 21 .ZT values of $Mg_2Si_{0.4}Sn_{0.6}$ solid solution and HMS as a function of temperature. These materials have been used as n- and p-type materials for a demonstration module *[30]*.

3.7.5.1. HIGHER MANGANESE SILICIDES (Mg_2Si-based material)

An ideal TE material should not only have a high ZT value, but should also be composed of elements that are abundant and non-toxic. Therefore Mg_2Si-based materials have drawn much attention recently. A ZT_{max} value of 1.1 was obtained in $MgSi_{0.4}Sn_{0.6}$ solid solutions at 800 K [40]. Higher manganese silicide is one of the most interesting materials from the point

of view of its structure and thermoelectric properties. Careful study of the phase diagram of the Mn-Si system shows that higher manganese silicide (HMS) can be produced in aperitectic reaction at 1 428 K and its composition was determined to be $MnSi_{1.72}$. The homogeneity region of HMS has been found to be very narrow (not more than 0.3%). The method of HMS formation has been confirmed by other researchers; however, the composition of HMS was reported to be different in different papers and the consensus is that HMS can exist over the composition range of $MnSi_{1.70}$ to $MnSi_{1.77}$ [42].

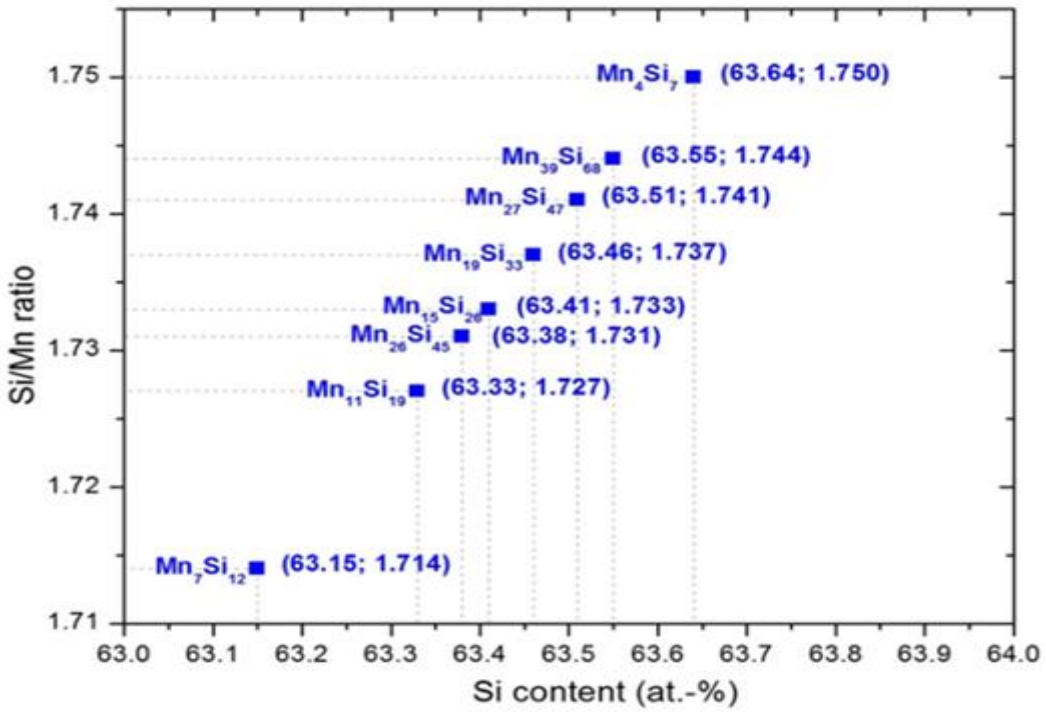

Figure 22. Different structural formulas of HMS with the corresponding Si/Mn ratios and Si contents *[29]*

The compositional formula of HMS was mistakenly believed to be $MnSi_2$ in the early days. In 1968, a process of making crack-free Mn_4Si_7 with improved thermoelectric performance compared to MnSi and $MnSi_2$ was patented, which included melting the mixture, solidifying the melt, crushing the solid melt, and hot pressing the finely divided particles. Since then, HMS have attracted a lot of attention from material researchers all over the world as potential candidates for thermoelectric applications. Figure 22 shows that, Higher Manganese Silicides (HMS) are the only known compounds in which the Si amounts (63-64 at. -%) exceeds that of Mn. The first glimpse at the phase diagram gives an impression that HMS are the solid solutions with continuous compositions. [26] Distinct compounds with different structural formulas exist, including Mn_7Si_{12}, $Mn_{11}Si_{19}$, $Mn_{26}Si_{45}$, $Mn_{15}Si_{26}$, $Mn_{19}Si_{33}$, $Mn_{27}Si_{47}$, $Mn_{39}Si_{68}$, and Mn_4Si_7 [29].

The HMS compounds are potential materials to fabricate thermoelectric modules with high stability during heating cycles in various atmospheres for several reasons. First, the constituent elements of manganese and silicon are nontoxic and inexpensive. Second, these compounds can be used in high heat sources up to 1100 K with no sublimation in vacuum, and they are strongly resistant to oxidation at high temperature [29]. The best Silicides meet these claims. Really: Si- is the fourth element among the most widespread elements of the Earth's crust. Si and majority components of the best silicide thermoelectrics are cheap, do not contain rare or toxic elements and are ecologically friendly. Moreover, they represent various mechanisms of electron transport, so among them representatives of new classes of thermoelectrics could be found**.** Figure 23 magnesium silicide based thermoelectric is the best in the temperature range 600-850 K in comparison with the other thermoelectrics of *n*-type [43].

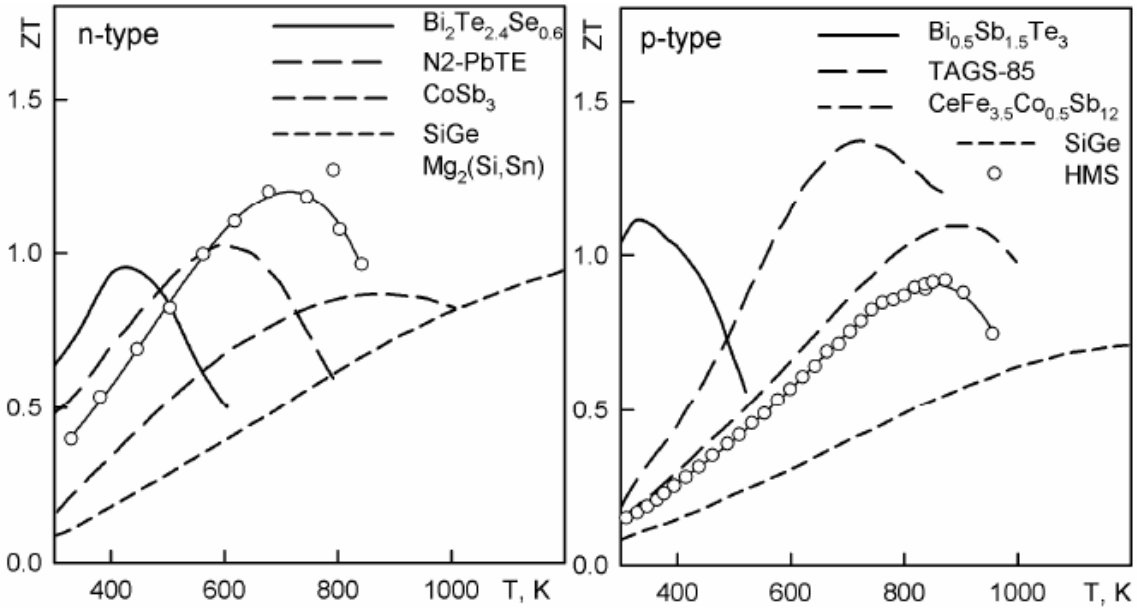

Figure 23. The thermoelectric Figure of merit of the best representatives of silicide thermoelectrics in comparison with the other thermoelectrics, having the highest ZT in their temperature range *[43]*

3.7.6. HIGH TEMPERATURE MATERIALS

TE materials that function at a temperature range above 800 K are of particular interest for power generators used in probes for deep space exploration. Silicon-germanium (SiGe) alloys and lanthanum chalcogenides are the primary candidates that have been studied and utilized in high temperature TE devices in the past decades due to their good thermal stability and relatively high ZT values. Recent efforts to improve their properties include reducing the grain

size of the alloys by means of compressing ball-milled nanopowders. Little attention has been drawn to the use of nanoinclusions in this area, although a theoretical model has been provided by Jeng et al.in 2008 to study the effects of nanoparticles on the thermal conductivity of SiGe alloys. It can reasonably well be anticipated that nanoinclusions will help to enhance the performance also of the high temperature TE materials as an improved physical understanding of the effects of nanoinclusions is reached [35]. Figure 24 is showing Cleary some thermoelectric material application with respect to range of temperature of waste heat.

3.7.7. OXIDES

Thermoelectric material application, in terms of the temperature range of operation and the abundance and environmental friendliness of constituent elements, are represented in figure 24 a); Although ZT of oxides is still low compared with the current state-of-the-art TE materials, oxides possess several inherent merits from fundamental and application points of view. First, the high chemical and thermal stability of oxides allows for a large temperature gradient to be applied across the materials in air in Figure 24(a), thereby leading to a high Carnot efficiency in Equation (18) that somewhat compensates the low ZT. Second, the large temperature gradient may induce novel nonlinear, nonlocal TE effects (e.g., the Benedicks effect) that may be thermoelectrically favorable. Third, oxides are featured by their chemical versatility and structural intricacy, which offering a great flexibility of structural and compositional tailoring. Finally, oxides are decidedly advantageous in terms of the cost of raw materials and the environmental friendliness. For any large-scale application of thermoelectricity, the cost of raw material is a major consideration after performance. For example, the increasing price of Te somewhat vitiates the enhancement of ZT in the Te-containing high-performance nanostructured TE materials. Hence, high-performance TE materials based on abundantly available Figure 24(b) and nontoxic elements with high chemical and thermal stability are crucial for any viable large-scale applications. As shown in Fig. 24 (a), oxides are particularly suitable for high temperature power generation in air [44].

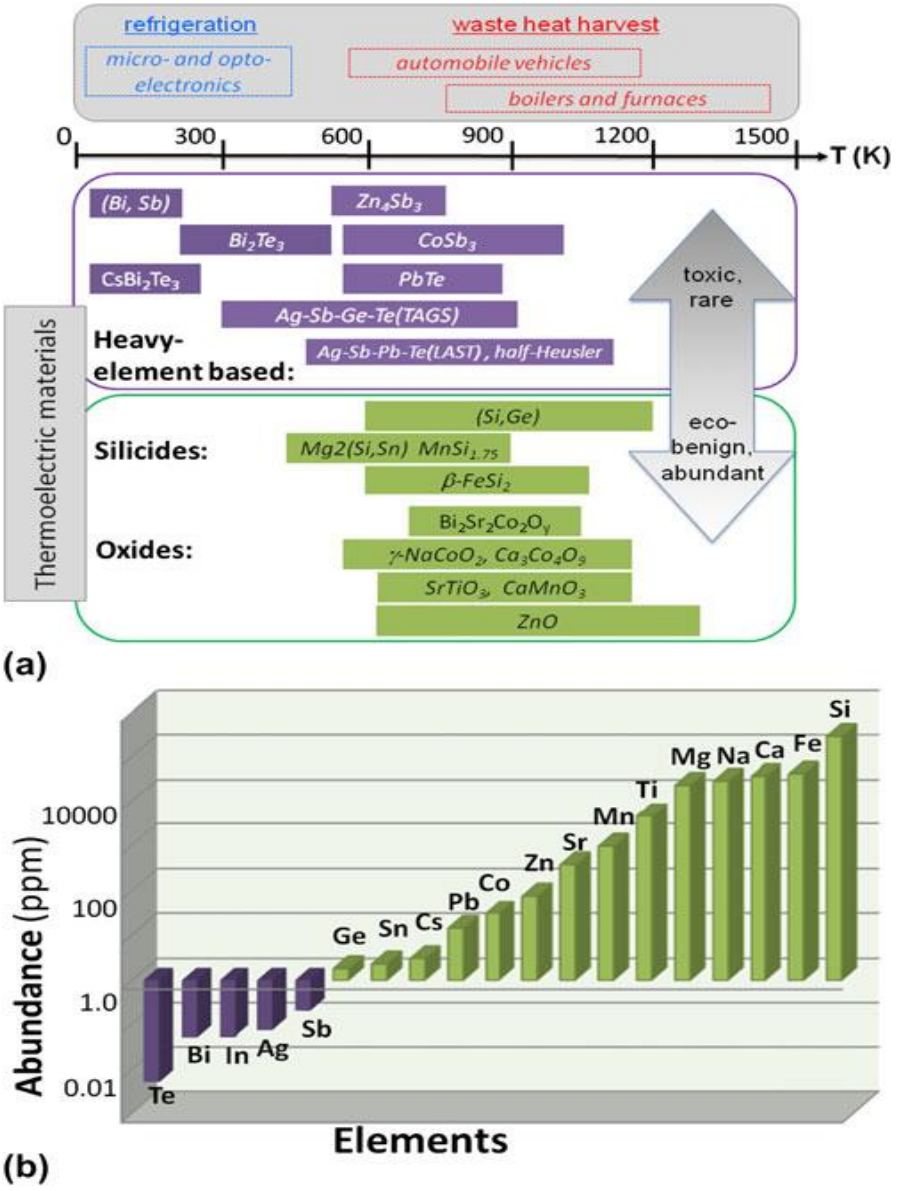

Figure 24. (a) Schematic comparison of various thermoelectric (TE) materials for applications of waste heat harvest and refrigeration. (b) The abundance of elements used in TE materials *[44]*.

3.8. MANUFACTURING

The manufacturing process for thermoelectric devices varies based on the type of thermoelectric material employed. The overview provided here applies to bulk materials and the most traditional manufacturing process. It is not comprehensive for all types of TE materials and devices but is provided as a reference to enhance understanding about engineering challenges commonly experienced with materials. A schematic of a TE device manufacturing process is shown in Figure 25 [45] .

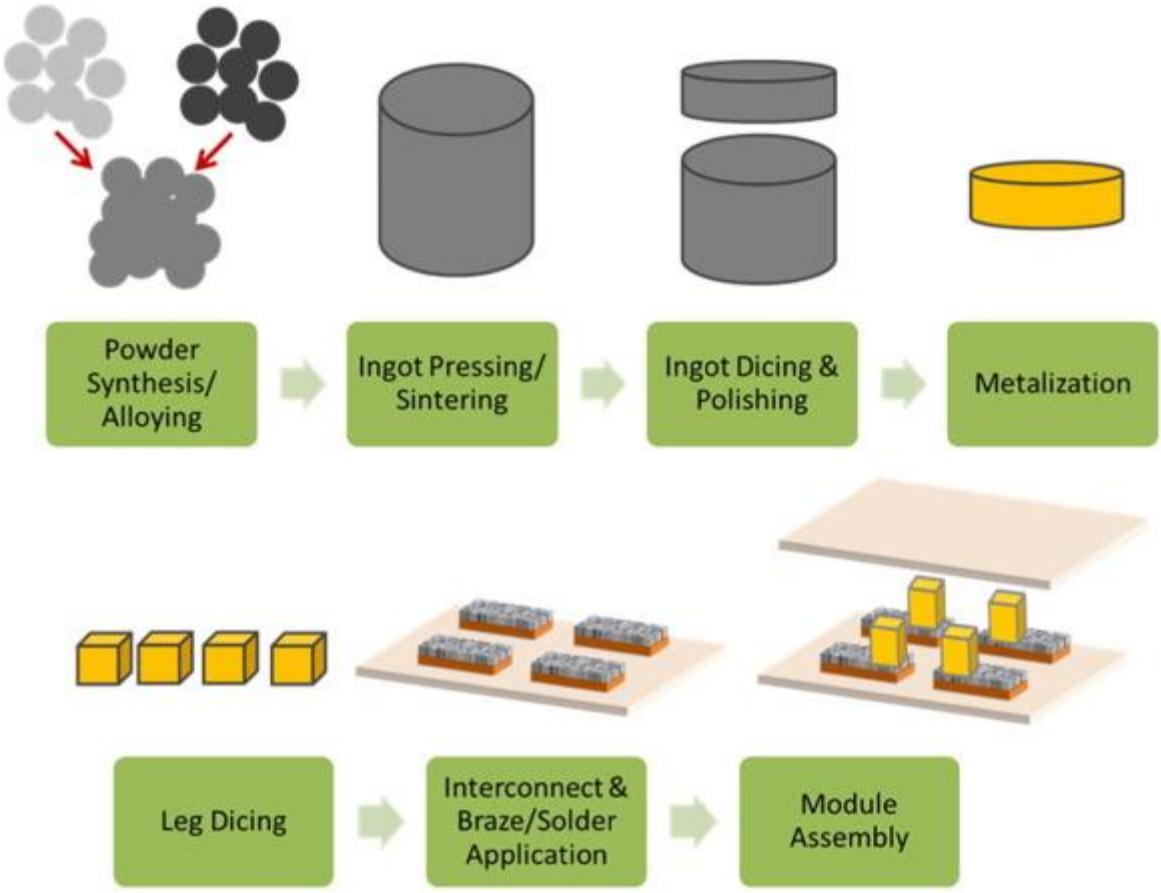

Figure 25.Schematic showing typical steps for manufacturing of thermoelectric module *[45]*

Process yield is a significant consideration for the manufacture of TE devices. As opposed to materials development and characterization where the primary yield concern corresponds to material synthesis and the number of samples which can be characterized, there are many more steps in the device manufacturing process. Thermoelectric material synthesis is commonly accomplished through ball milling powders of the constituent elements. While this can be a lengthy process, it is fairly repeatable with high yield once a processing recipe is established. However, establishing the process to repeatedly achieve a specific composition can be challenging. Complete mixing is required, and sufficient energy must be imparted to the powder particles. Thermoelectric materials can also be made through melting processes. Phase diagrams of TE materials demonstrate the narrow process windows in which each phase is achieved, and the thermoelectric material properties depend on the phase. For instance, $AgSbTe_2$ is in PbTe-based materials such as TAGS and LAST thermoelectric materials in which microstructures reportedly improve thermoelectric performance. The phase diagram for $AgSbTe_2$ (Figure 26) demonstrates the complex variations in phase, and thus

microstructures, which may arise due to process parameters. Hence, process fluctuations can result in variations of phase, microstructure formation, repeatability of the synthesis process, and resulting material properties.

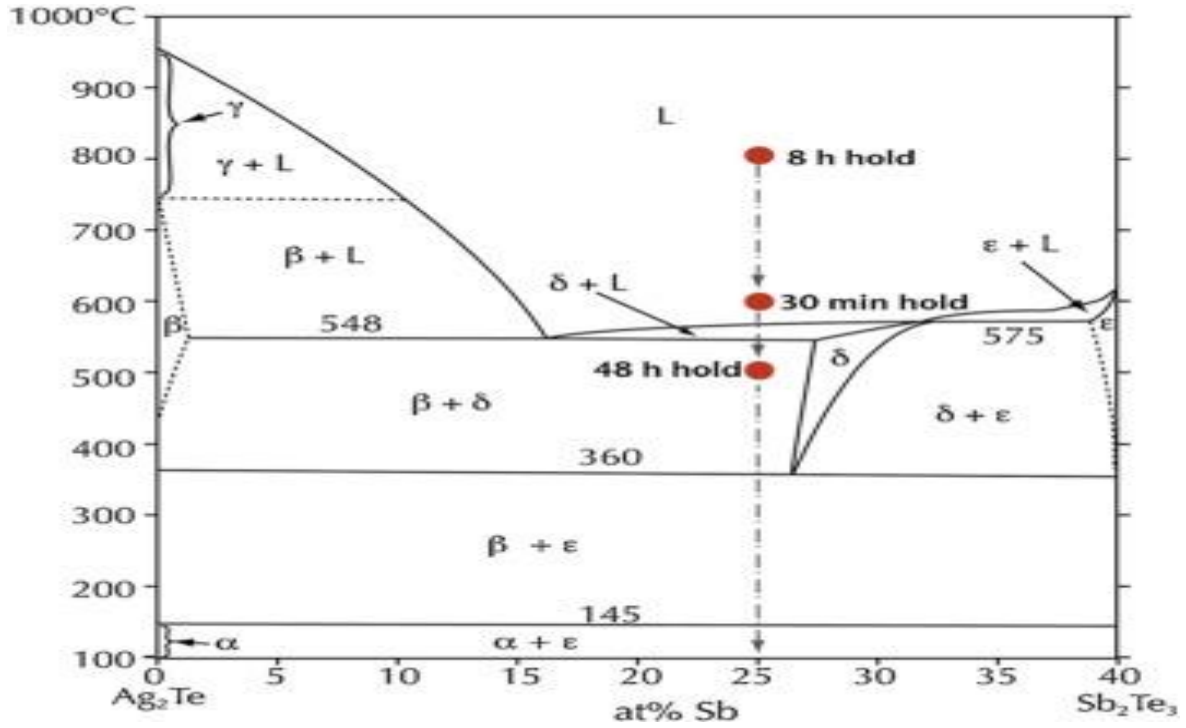

Figure 26.Phase diagram of $AgSbTe_2$, a common component in microstructured PbTe-based thermoelectric materials. The complexity and uncertainties about the bounds of the phase diagram demonstrates how small process fluctuations can affect thermoelectric material formation *[45]* .

Once the TE material is synthesized in powder or particle form, it is consolidated into ingots, typically through hot pressing or spark plasma sintering. As discussed in the materials overview section, sublimation and stability/reactivity in the process gas environment must be considered. While a given TE material might be stable at the application's operating temperature, the consolidation process (or other manufacturing processes) may occur at a higher temperature in order to densify the material.

The ingots are then diced to form the thermoelectric legs, and the material brittleness is a primary concern in this process step. Any chipping of a thermoelectric leg changes the leg surface area and influences both the leg's thermal and electrical resistance. This in turn affects system performance, particularly when the geometry of each leg is not the same. Chipped legs would not be used in a device, reducing the manufacturing process yield. Moreover,

dicing and subsequent chipping can lead to crack initiation. These cracks can propagate in subsequent process steps, or worse yet, during TE device operation. Even microcracks can affect thermal and electrical transport in the TE material. The dicing step also constrains the achievable leg dimensions since the post-dicing leg dimensions depend on the dicing equipment capabilities (e.g. saw blade width, dicing depth). The advent of thin film thermoelectrics has introduced manufacturing processes which are commonly associated with the semiconductor industry. Structures such as superlattices and nanowires have been proposed and are made with deposition, growth, and/or etching micro/nanofabrication processes including molecular beam epitaxy, chemical vapor deposition, vapor–liquid–solid growth, and electroless etching. Additionally, recent demonstrations of thermoelectric materials formed through solution processing techniques have been shown for both inorganic and organic materials. Since these approaches to making thin film thermoelectrics are quite varied, a generalizable, standard manufacturing process flow is not yet available. Material characterization during manufacturing poses a unique challenge. Both standard and custom-built equipment exist to characterize thermoelectric properties of TE materials. However, these are designed to accommodate individual samples of TE material (e.g. an ingot or one TE leg), and specialized contacts must be made to the sample. Hence, the techniques are destructive in that the characterization sample cannot subsequently be used for a TE device. The characterization process is also time-consuming, so it becomes a bottleneck in the overall manufacturing process stream. Standard, in-line characterization techniques which could be implemented within the manufacturing process would be valuable. They would enable characterization of the material as it is incorporated into the device as well as the effective properties of the material combined with its electrical and thermal contacts to other device components. In-line characterization could also increase process yield and reduce waste since defective devices would be detected earlier in the manufacturing process [45] .

3.9. THERMOELECTRIC MODULES

In this section, a description and functionality of the constituents of the thermoelectric modules are discussed. Thermoelectric generators (TEGs) are renewable energy devices made of a semiconductor that directly convert the temperature difference between surfaces into electrical energy [46]. The thermoelectric generator (TEG) is the system used to generate power from low temperatures that is less than 1000K as heat input. It is best method for recovery of exhaust heat. It can be used in many fields such as automobiles, boilers wood

stoves etc. The efficiency of a TEG depends on the thermoelectric materials. The main research of the world is to use the renewable energy. The main advantage of TEG is that it uses green energy. The TEG is mainly based on the principle of Seebeck effect. The efficiency of a thermoelectric generator is about 5%. A heat source provides the high temperature, and the heat flows through a thermoelectric converter to a heat sink, which is maintained at a temperature below that of the source [47].

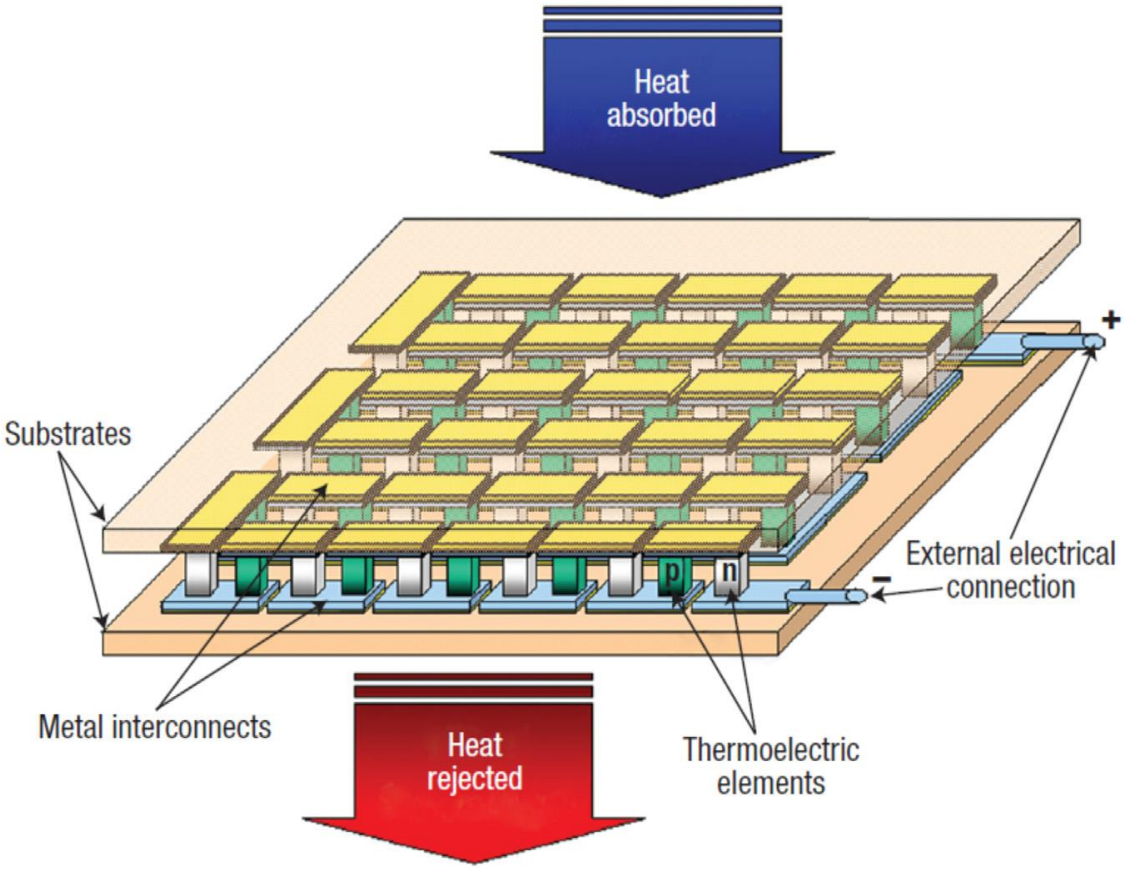

Figure 27. Constituents of a thermoelectric module *[48]*

The modules are the basic building blocks within thermoelectric power generators or coolers. Modules are a matrix of semiconductor thermoelectric couples that are connected electrically in series and thermally in parallel. The thermoelectric couples and their electrical interconnects are sandwiched between two ceramic substrates. Figure 27 shows the arrangement of the different constituents of a thermoelectric module. The main constituents of a thermoelectric module are (1) thermoelectric elements (or legs), (2) ceramic substrates, (3) metal interconnects, and (4) external electrical connections [49].

The thermoelectric elements (or legs) are the couples used for generating electricity in thermoelectric modules. They are formed out of materials such as bismuth-telluride, lead-

telluride, antimony telluride, silicon-germanium semiconductor alloys. The selection of material depends on the field of application and operating temperature range. The thermoelectric legs are arranged in a regular matrix within the module, as shown in figure 27. Ceramic substrates are used to electrically insulate the thermoelectric module from external mounting surfaces. The substrates must also have good thermal conductance to provide heat transfer with minimal thermal resistance. A common ceramic substrate is aluminium oxide (Al_2O_3). The metal interconnects serve as electrical contacts between thermoelectric legs. The contacts are arranged in such a way that all the legs are connected electrically in series. External electrical connections are used to connect the module to an electrical load in case of power generation or to an electrical source in case of the module being used for thermoelectric cooling. The thermoelectric modules in conjunction with heat exchangers are used to build systems for TPG (Thermoelectric power generation) [49].

3.9.1. CONTACT RESISTANCES

Between two solid materials, the interface is never in perfect contact. Even if the surfaces look perfectly smooth, there will always be microscopic roughness on the surfaces that will form air-filled voids when the surfaces are pressed together. These voids decrease the surface area that is actually in contact, how much depends on surface roughness, the softness of the materials, and the contact pressure. Potential surface coatings, such as oxides or other impurities, might affect both the thermal and the electrical conductivity over an interface. The magnitude of the thermal contact resistances can be decreased by minimizing the area of the voids, either by smoothing or softening the surfaces, or by increasing contact pressure. Another way to lower contact resistances is to fill the voids with a material with high conductivity. A thin layer of thermal grease or graphite is commonly used to fill the voids and enhance thermal contacts. Such a material has far better thermal conductivity than air, but much lower than metals. A common method for lowering electrical contact resistances is to cover the surface with a soft, electrically conducting material that is resistant to oxidization. A technically beneficial but expensive choice of coating material is gold. The thickness of the gold layer is important, and Nagaraju has shown that a gold layer that is too thin will increase rather than decrease contact resistance. The most important contact resistances are the electrical resistances on both sides of thermoelectric pellets, and the thermal resistances

between the connectors and the ceramic plates. There may also be thermal contact resistance between the pellets and the metal connectors. The locations of thermal and electrical contact resistances are highlighted in Figure28 [23].

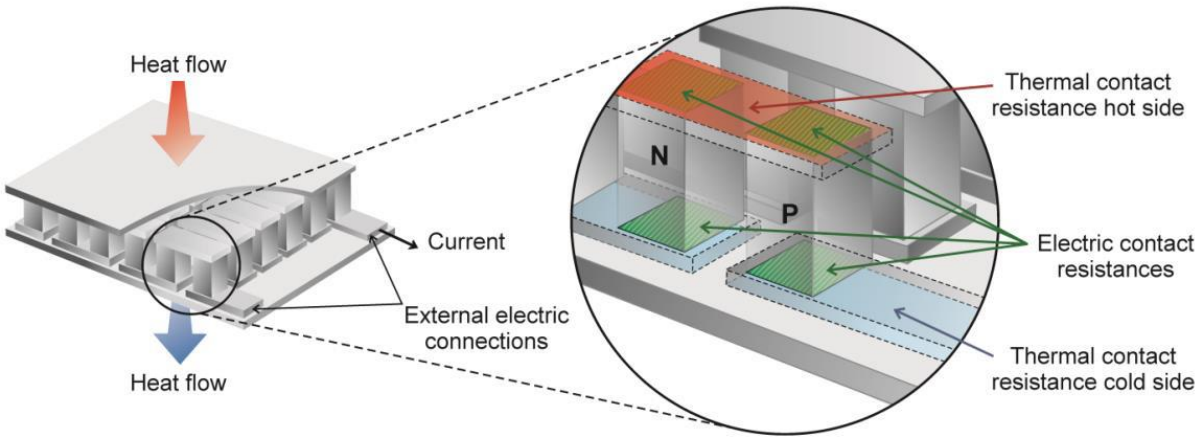

Figure 28. Contact resistances within a TE module *[23]*

3.9.2. THERMOELECTRIC ENERGY HARVESTING

Although the thermoelectric output voltage, current, and electrical power generated by a standard thermoelectric module is relatively small, the thermoelectric output voltage can be boosted to a useful and stable level by using a boost converter and low power DC to DC converter. If the electrical power output from the DC to DC converter is then accumulated and stored for future use in a supercapacitor, it is possible to increase the potential output current of the system, and hence the overall electrical power output of the thermoelectric energy harvesting system. A simplified block diagram of a thermoelectric energy harvesting system is shown in Figure 29. It is not always necessary to use a boost converter, although in many applications, the output voltage from a single thermoelectric module is too low to directly operate a DC to DC converter. The output of the DC to DC converter can also be connected directly to an electrical load in order to power other low power electronic systems, to recharge a battery, or as shown -connected to a supercapacitor for electrical storage purposes. The energy stored in the supercapacitor can then be accumulated over time, and released to the load when required. The addition of the supercapacitor in the system enables much higher levels of current to be drawn by a load, if only for a short period of time, and makes the system more versatile. Commercially available boost converters and low power DC

to DC converters can operate from very low thermoelectric output voltages of 20mV, outputting a DC output voltage of between 2.2V to 5V [50].

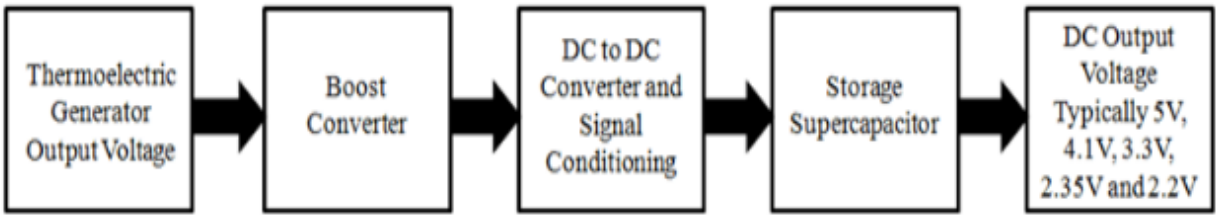

Figure 29. A generic thermoelectric energy harvesting system block diagram *[50]*

3.9.3. ADVANTAGES OF THERMOELECTRIC GENERATOR

Thermoelectric power generators offer several distinct advantages over other technologies, [51] one of them are these:

- They are extremely reliable (typically exceed 100,000 hours of steady-state operation) and silent in operation since they have no mechanical moving parts and require considerably less maintenance;
- They are simple, compact and safe;
- They have very small size and virtually weightless;
- They are capable of operating at elevated temperatures;
- They are suited for small-scale and remote applications typical of rural power supply, where there is limited or no electricity;
- They are environmentally friendly;
- They are not position-dependent;

3.9.4. APPLICATIONS OF THERMOELECTRIC GENERATOR

Thermoelectric generators(TEGs) find use in aerospace, military and automobiles applications. Automobile industries are trying coupling of the TEGs with combustion engines for improving fuel efficiency of the vehicles and for generating of the electrical energy from the waste heat. The higher fuel efficiency gives good mileage for automobiles and the electrical energy produced can be used for vehicle lights. Thermoelectric generators are also used to power space vehicles [52]

4. THEORETICAL OUTLINE FOR DESIGNERS AND MODELLING

The conventional design of a power generating thermoelectric module is usually based upon a set of formulae derived using a simple model in which the thermal and electrical contact resistances of the module are neglected. An expression is derived for the conversion efficiency which is independent of module geometry. Consequently, the design of the thermoelectric generator is guided solely by matching the load resistance to achieve either of the two limiting cases: maximum conversion efficiency or maximum power output. However, both power output and conversion efficiency of a thermoelectric module are dependent upon the thermoelement length for a given figure-of-merit, contact properties and temperature difference of operation. The optimum length necessary to obtain maximum power output differs from that for maximum conversion efficiency. Evidently, an appropriate thermoelement length for power generation will be a compromise between the requirements for maximum power output and maximum conversion efficiency. The module construction cost is closely related to the power output, while its conversion efficiency determines the running cost. The module geometry for power generation should then be optimized to minimize the cost of the generated electricity. In this project an attempt is made to provide the necessary formulae and graphs to achieve an optimized module design [53].

4.1. DESIGN

Design is generally regarded as a creative process by which new methods, devices, and techniques are developed to solve new or existing problems. Though many professions are concerned with creativity leading to new arrangements, structures, or artifacts, design is an essential element in engineering education and practice. Due to increasing worldwide competition and the need to develop new, improved, and more efficient processes and techniques, a growing emphasis is being placed on design [54] .

4.1.1. STEPS IN THE DESIGN PROCESS

The conceptual design yields the basic approach and the general features of the system. These form the basis of the subsequent quantitative design process. The starting or initial design is then specified in terms of the configuration of the system, the given quantities from the problem statement, and an appropriate selection of the design variables. This initial selection

of the design variables is based on information available from other similar designs, on current engineering practice, and on experience. Employing approximations and idealizations, a simplified model may then be developed for this initial design of the system so that its behavior and characteristics may be analyzed. Generally, the system behavior under a variety of conditions is investigated on the computer, by a process known as *simulation*, because of the complexity of the governing equations in typical thermal systems. An experimental or physical model may also be employed in some cases.

The outputs from the modeling and simulation effort allow the designer to evaluate the design with respect to the requirements and constraints given in the problem statement. If an acceptable design that satisfies these requirements and constraints is obtained, the process may be terminated or other designs may be sought with a view to improve or optimize the system. If an acceptable design is not obtained, the design is varied and the processes of modeling, simulation, and design evaluation repeated. These steps are carried out until a satisfactory design is obtained. Different strategies may be adopted to improve the efficiency of this iterative procedure. Figure 30 shows a typical overall design procedure, starting with the conceptual design, and indicating some of the steps mentioned here. Usually, the engineering design process focuses on the quantitative design aspects after the problem statement and the conceptual design have been obtained. Then, the design process starts with the initial design of the physical system and ends with communication of the design to fabrication and assembly facilities involved in developing the system. The formulation of the design problem and conceptual design are precursors to this process and play a major role at various stages. Thus, the main steps that constitute the design and optimization process may be listed as [54]:

1. Initial physical system
2. Modeling of the system
3. Simulation of the system
4. Evaluation of different designs
5. Iteration and obtaining an acceptable design
6. Optimization of the system design
7. Automation and control
8. Communicating the final design

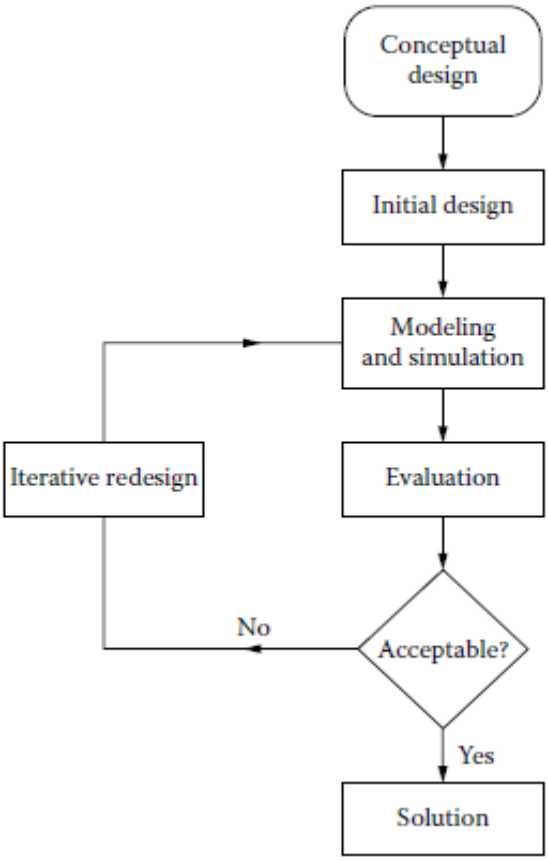

Figure 30. Iterative process to obtain an acceptable design *[54]*

Three principal points considered during designing a thermoelectric generator [53]:

1) Specifications: the operating temperatures T_C, T_H and the required power output P (and or output voltage or current I).
2) Materials parameters: the thermoelectric properties of thermoelement materials Z ($\alpha\ \rho\ \gamma$), and the electrical and thermos contact properties of the module.
3) Design parameters: the thermoelement length L, the cross-sectional area A and the number of thermocouples N.

The materials to be used is referred to Figure 24;It shows thermoelectric materials for industrial application (Boiler band furnaces), environmental friendly materials and abundance based. In this case silicide material is chosen; where HMS (high manganese silicide materials) for P-types, $Mg_2Si_{0.4}Sn_{0.6}$ for N-types materials, copper for conduction materials (between Seebeck materials and substrates) and alumina(Al_2O_3) for substrates. Output power should

be optimum with respect to the cost of materials. The desired cold temperature is 10^0C, while hot side temperature has been taken from measurement done from 3B The fiberglass company, Where the set of Pitot tube and thermometer were used, figure 31 shows the process. Down near the furnace the temperature was 800^0C, up on the top of the roof at 10.3m from the furnace; the temperature of 230^0C has been measured; these temperatures changing, proves that there is a loss, this loss is the one to be the input to the module. in addition, the mean velocity flow measured, is 12m/s. from the measured values heat flux has been calculated.

Figure 31. Data collecting action at top of roof (3B the fiberglass company)

4.1.2. HEAT LOSS CALCULATION

Heat loss calculated between two point of the chimney is the source of heat for thermoelectric generator, the flues gas properties are in table1, assuming steady state flow. thermal energy equation at any point in chimney is

$$Q_X = C_p \times V \times \rho \times A_c \times T_x \quad (19)$$

Where;

C_p - specific heat capacity of air (J/(Kg-K))

T_x -Temperature at any location

V - Flue velocity(m/s)

A_c - Cross section area(m^2)

ρ - density (air) 1.223 Kg/m^3

ν - kinematic viscosity [m^2/s]

μ - dynamic viscosity

Table 1.This table is for flue gases. It gives values of some physical properties - density and viscosity in relation to the temperature of gases [55]

t	ρ	C_P	$\mu*10^6$	$\nu*10^6$
^0C]	[kg/m^3]	[kj/kg K]	[Pas]	[m^2/s]
0	1.295	1.042	15.8	12.2
100	0.95	1.068	20.4	21.54
200	0.748	1.097	24.5	32.8
300	0.617	1.122	28.2	45.81
400	0.525	1.151	31.7	60.38
500	0.457	1.185	34.8	76.3
600	0.405	1.214	37.9	93.61
700	0.363	1.239	40.7	112.1
800	0.33	1.264	43.4	131.8
900	0.301	1.29	45.9	152.5
1000	0.275	1.306	48.4	174.3
1100	0.257	1.323	50.7	197.1
1200	0.24	1.34	53	221

In the calculation, the flow has been assumed to be laminar, chimney is smooth, thermo-convection of the flue gas is equal to conduction through the thickness, I mean lossless has been considered and uniformly distributed in all direction. From the equation (19), the heat flow axially into the chimney, using the data from table1, at 800^0 C the heat flux is $Q_{1073\ K}$=

1517.7kw, heat out axially from the chimney at 210^0 C is Q_{483K} =1133. 9kw.Refer to figure 32, the temperature loss is 590^0C, this, is the hot temperature or input to the module. For the same way, the heat loss, is calculated by making the difference, which is 383.8 kw. The length(L) between the two points of chimney is 10.2 m, the surface area or lateral area is 19.4 m^2 then the average heat flux is 19.783 kw/m^2, this value is the one which is the input to thermoelectric module.

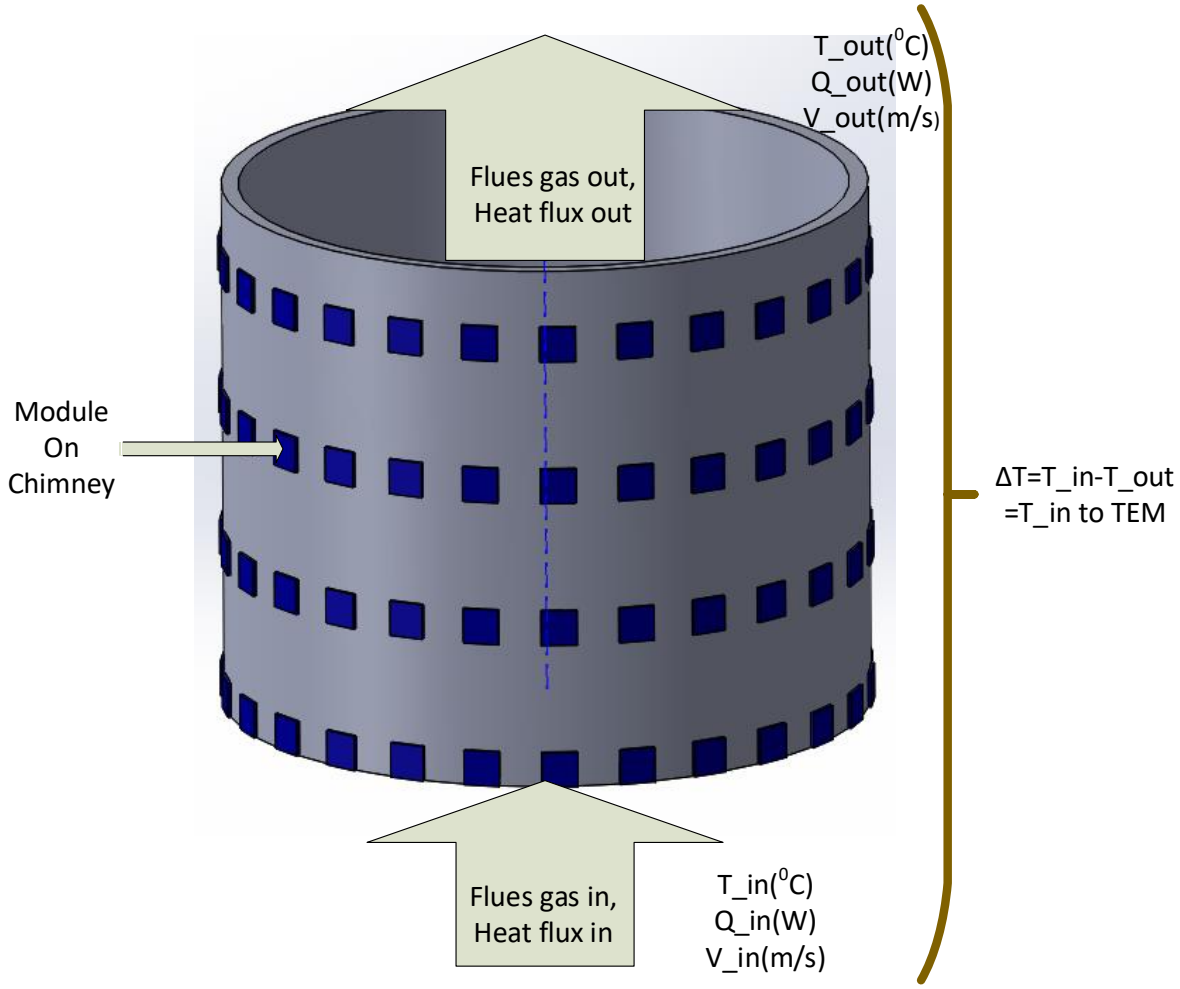

Figure 32. General design overview

From figure 32, the overview of the system where the modules are mounted on the chimney, where 26 modules fit the circumference of chimney according to the design. There is a need of heat exchanger between chimney and module; The heat exchanger, at hot side, is made

from steel or aluminium to be capable of withstanding high temperatures without degradation, and the concetration in optimization of material is on heat exchanger in this thesis. Aluminum will have some cosmetic degradation at high temperatures. The function of heat exchanger, is to create a flat surface capable of mounting a traditional module on, as well as functioning as a layer between the chimney and module, preventing overheating**.** This heat exchanger should be able to resist high temperature and have high thermoconductivity to allow heat flow, the mounting method on chimney proposed in this study, is welding the heat exchanger on chimney; then thermoelectric generator mounted on heat exchanger by means of Bolts and nuts more info or details are in [56]. Table 2 shows clearly the dimension of whole system.

Table 2. Data of Model Components of System

PARTS	SIZE(mm)				
	Length	width	Hight	diameter	thickness
Chimney			15021	600	
Heat exchanger (Hot side)	26.5	26	0.2	300 (Radius)	3
TEG Module	26	26.5			

Using the data in Table 2 above, a design of different parts for full thermoelectrics generator was made; starting on the top of figure 33 hot side heat exchanger or hot sink which should have cylindrical shape at one side; so that to be able to mate on chimney, thermoelectric module seated in heat sink, finally the system of the cold side to maintain the cold side temperature at constant value, for this study 10^0C is taken. The finned dissipater heat exchanger has been chosen, to use natural convection cooling and clapping system with bolt and nut to apply pressure. The thermoelectric module generators will be mounted on

chimney, electrically in series to increase the output voltage.in modelling and simulation, one module is considered and all material will be optimized precisely heat exchangers.

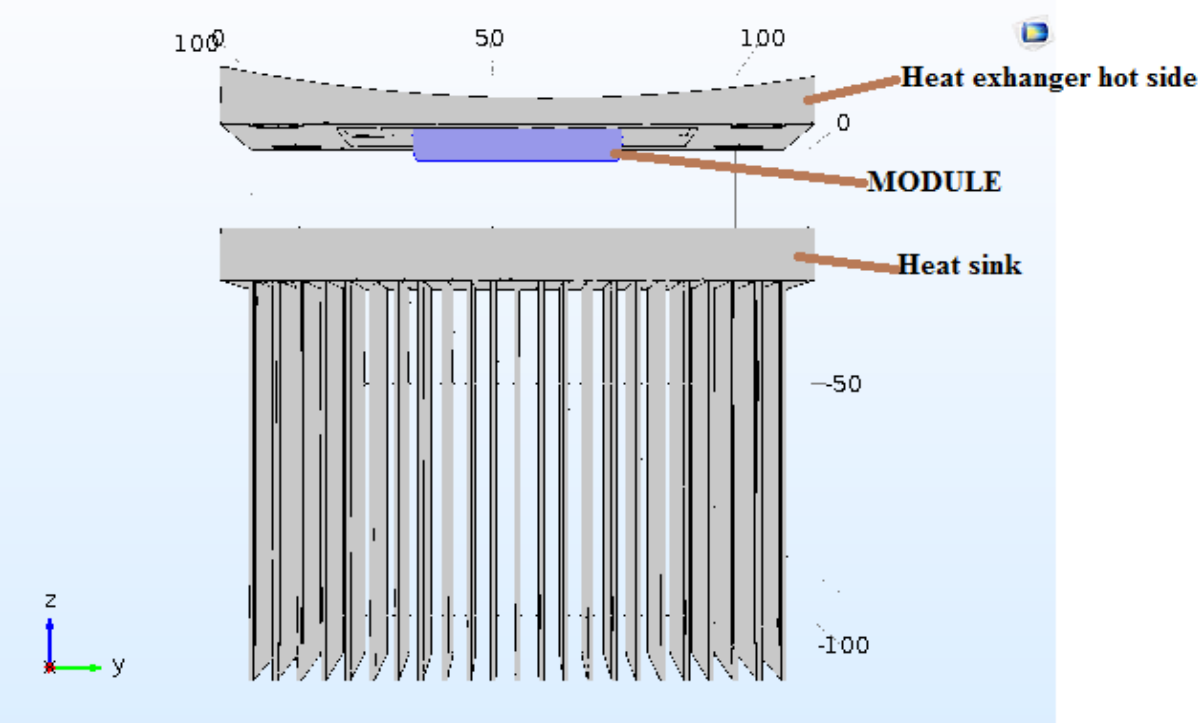

Figure 33 . Schematic view of the proposed Design of Thermoelectric Generator Model

5. MODELING OF THE DEVICES

To properly perform a thermal analysis, the practical aspects of the underlying complex phenomenon must be known and so assumptions and simplifications must be made. Taking that into consideration, steady state is assumed, the heat losses due to radiation are neglected, the gap between the thermocouples is assumed perfectly isolated, the axial heat conduction within the thermocouples is ignored since the heat transfer in the y-direction is assumed to dominate and the current flow in the thermocouple is also assumed to be one-dimensional in the y-direction [20], no parallel leakage loss. Following these assumptions, the energy balance equation for an infinitesimal element dy, depicted in figure 34, can be given by:

$$\dot{Q} - (\dot{Q}_y + \frac{d\dot{Q}_y}{dy}dy) + \frac{I^2\rho}{A}dy = 0 \tag{20}$$

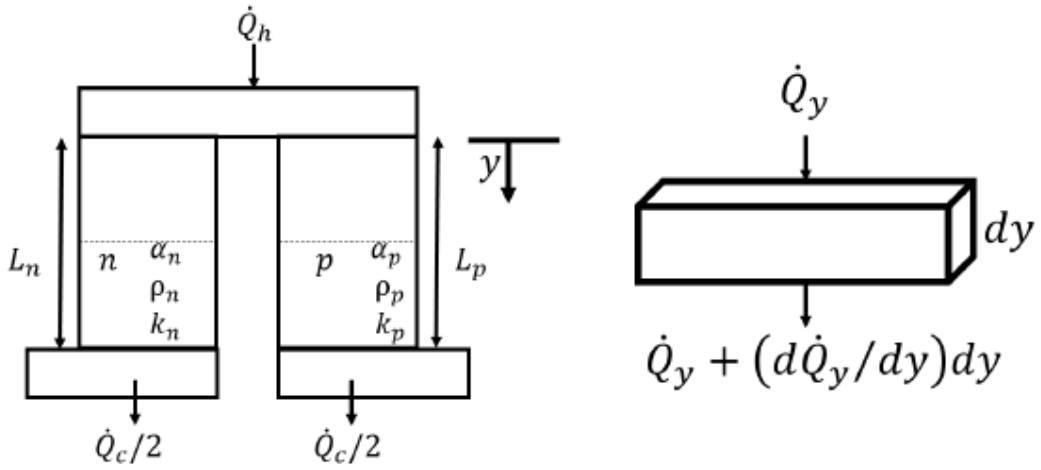

Figure 34: Schematic of the heat rate in a thermocouple *[20]*

The first term in equation (20) represents the heat transfer across the surface of the element. The second term in (20) represents the Joule heating effect, associated with the release of heat due to the passage of the electric current through the leg. The Joule heat is distributed throughout the element therefore half the heat flows towards one side and the other half goes towards the opposite side of the thermocouple. The boundary conditions are $T(y)|_{y=0} = T_h$ and $T(y)|_{y=L} = T_C$ once applied to equation 20 yield:

$$T(y) = \frac{I^2\rho y^2}{2A^2k} + \left(\frac{T_c - T_h}{L} + \frac{I^2\rho L}{2A^2k}\right)y + T_h \tag{21}$$

Which represents the temperature distribution across thermocouple. The energy balances at the hot and cold junctions of the thermocouples are given, respectively by

$$\dot{Q}_h = (\alpha_p - \alpha_n)T_h I + \left(-k_p A_p \frac{dT}{dy}|_{y=0} - k_n A_n \frac{dT}{dy}|_{y=0}\right) = 0 \tag{22}$$

$$\dot{Q}_c = (\alpha_p - \alpha_n)T_c I + \left(-k_p A_p \frac{dT}{dy}|_{y=L} - k_n A_n \frac{dT}{dy}|_{y=L}\right) = 0 \tag{23}$$

In equations (22) and (23) the first term accounts for the Peltier heat, which using the relation given by equation (3), can be written in function of the Seebeck coefficient. The second term represents the Fourier's law of thermal conduction at the boundaries, y = 0 and y = L, respectively. Practically, a thermoelectric generator is composed of three parts, heat source, thermoelectric module (TE module) and heat sink. The heat that absorbs from the heat source partially is converted to electrical power via the TE module, and the residual is released from the heat sink. Figure 35 shows its thermal network, It consists of thermal resistances Θ_H between the heat source and TE module, thermal resistance of TEM Θ_{TE}, and thermal resistance Θ_C between the TEM and the heat sink [57].

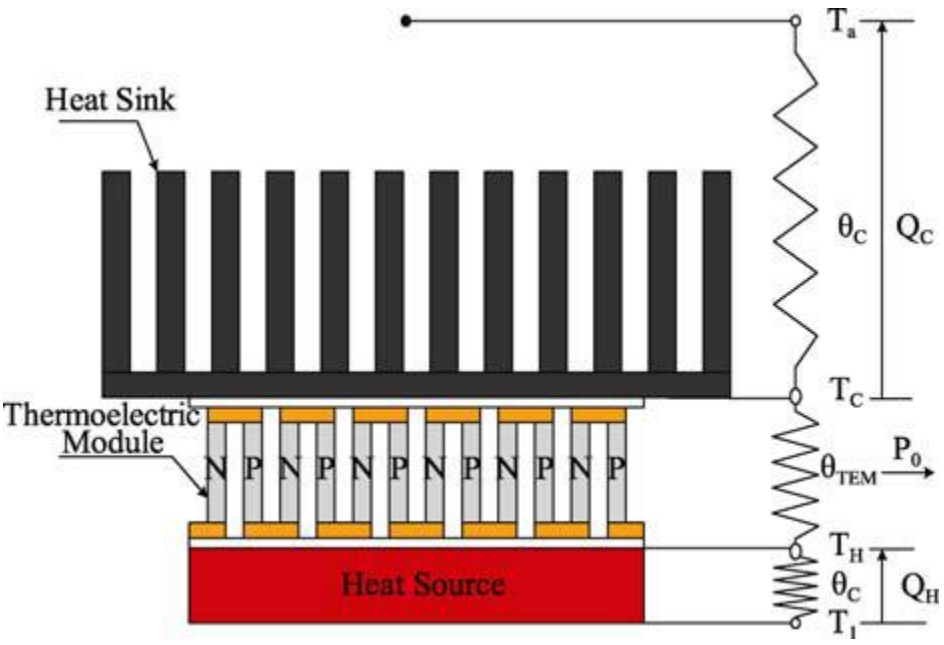

Figure 35. Structure and thermal resistor network of thermoelectric generator.

According to Figure 35, the thermal resistances Θ_h and Θ_C are defined as:

$$\Theta_h = \frac{T_1 - T_h}{Q_h} \tag{24}$$

$$\Theta_C = \frac{T_C - T_a}{Q_C} \tag{25}$$

where T_1 is the heat source temperature, T_H and T_C are the temperature of TEG hot and cold side respectively, and T_a is the ambient temperature. Q_H is the heat which TEG absorbs from the heat source, and Q_C is the heat releases from the TEG cold side. Θ_C can be defined as the heat dissipation intensity. The smaller Θ_C the higher heat dissipation intensity and the better heat dissipation are. The total thermal resistance of the *N* couples of a module, which are connected thermally in parallel, will be

$$\Theta_{TEM} = \frac{\Theta_{TE}}{N} \tag{26}$$

θ_{TE} is the thermal resistance for a single thermocouple. In the following derivation, all the thermal transfer loss, and thermal contact resistances are ignored. By employing Newton's law of heat transfer, When the system arrives at a steady state [58], equation (22) and (23) become as follow:

$$\dot{Q}_h = N\left(IT_h\alpha - \frac{1}{2}I^2R_{TE} + K\left(T_h - T_c\right)\right) = \frac{T_1 - T_h}{\Theta_h} \tag{27}$$

$$\dot{Q}_c = N\left(IT_c\alpha + \frac{1}{2}I^2R_{TE} + K\left(T_h - T_c\right)\right) = \frac{T_C - T_a}{\Theta_C} \tag{28}$$

Where,

$$R_{TE} = \frac{\rho_p L_p}{A_p} + \frac{\rho_n L_n}{A_n} + R_C \tag{29}$$

$$K = \frac{k_p A_p}{L_p} + \frac{k_n A_n}{L_n} \tag{30}$$

If we assume that *p*-type and *n*-type thermocouples are similar, we have that $R_{TE} = \frac{\rho L}{A}$ and For a general case, thermoconductivity of material is given by $K = \frac{kA}{L} = \frac{1}{\Theta}$, where $\rho = \rho_p + \rho_n$:resistivity of the material (Ω m) and $k = k_p + k_n$, R_c is contact resistance. In both Equations (27) and (28), the first terms in the square brackets represent Peltier heat

(power) generated, while the second and third terms denote Joule heat (power) and Fourier heat (power) transfer, respectively. The ratio1/2 in front of the Joule term indicates that each of the hot junction and cold junction "consumes" half of the total created Joule heat, since the TEG module has the same number of p-type elements as n-type elements. As the difference between Q_h and Q_c, the output power of the system can also be expressed in terms of the current and the external load resistance R_L, by considering the 1st law of thermodynamics across the thermoelectric module, is:

$$\dot{Q}_h - \dot{Q}_C = P_L = N[\alpha I_L (T_H - T_C) - I^2 R_{TE}] \tag{31}$$

However, the power output in Figure 12 can be defined by an external load resistance as

$$\dot{Q} = N * I^2 R_L \tag{32}$$

Equating Equations (31) and (32) with $P = V_L I$ gives the voltage as

$$V_L = NIR_L = N[\alpha(T_H - T_C) - IR_{TE}] \tag{33}$$

The maximum voltage occurs at the open circuit, where I = 0 in Equation (33), The maximum voltage is

$$V_{OC} = N\alpha(T_H - T_C) \tag{34}$$

From Equation (33), the electrical current for the module is obtained as

$$I = \frac{\alpha \Delta T}{R_{TE} + R_L} \tag{35}$$

The maximum current occurs at the short circuit, where R_L =0 in Equation (35), the maximum current for the module is

$$I_{\max} = \frac{\alpha \Delta T}{R_{TE}} \tag{36}$$

From above equation, the current I is independent of the number of thermocouples. Combining equation (32) and (35) gives:

$$P_L = \frac{N\alpha^2 \Delta T^2}{\left(R_L + R_{TE}\right)^2} R_L \tag{37}$$

Where α ($\alpha = \alpha_{pn}$) is the Seebeck coefficient difference between α_p and α_n ($\alpha = \alpha_{pn} = |\alpha_p| + |\alpha_n|$), ΔT is the temperature difference between T_H and T_C ($\Delta T = T_H - T_C$), R_{TE} is the Thermoelectric generator electrical resistance, R_L is the Thermoelectric generator load resistance. When the load resistor R_L is equal to the TEG internal resistor R_{TE}, the TEG is on matched load condition generating the maximum output power given by [59]:

$$P_{L\max} = \frac{N\alpha^2 \Delta T^2}{4R_{TE}} \tag{38}$$

In general, a thermoelectric power generator exhibits low efficiency due to the relatively small dimensionless figure-of-merit (ZT < 1) of currently available thermoelectric materials. The conversion efficiency of a thermoelectric power generator defined as the ratio of power delivered (W_e)to the heat input at the hot junction (Q_H) of the thermoelectric device, is given by $\eta = \frac{W_e}{Q_H}$ or the thermodynamic efficiency of the thermoelectric generator is given by:

$$\eta = \frac{Power\ supplied\ to\ load}{Heat\ absorbed\ at\ hot\ junction} \tag{39}$$

The power supplied to the load is just the Joule heating of the load resistor, R_L which is equal to I^2R_L. The heat absorbed at the hot junction is the Peltier term plus the heat withdrawn from the hot junction as described above. The Peltier heat is given by π I = αIT_h. If the resistance of the n-type and p-type semiconductor elements in series is R, then the current I, flowing in the circuit is just given by Ohm's Law as:

$$I = \left(\frac{V}{R_{total}} \right) = \frac{\alpha(T_h - T_c)}{R + R_L} \tag{40}$$

The heat withdrawn from the hot junction is given by the Fourier term but as there will be Joule heating from the generated current from the Seebeck voltage, some heat will also be generated and returned to the hot junction. It is usual to assume that half of the Joule heat will be transport and half will be returned to the hot junction and so [60].

Q_h =Fourier - Joule heating + half Joule heating returned

$$=kA(T_h-T_c)-I^2R+\frac{1}{2}I^2R= kA\,(T_h - T_c) -\frac{1}{2}I^2R \tag{41}$$

We can now move to calculate the efficiency by combining these terms and if the power supplied to the load is only through Joule heating to produce

$$\eta = \frac{Power\ supplied\ to\ load}{Heat\ absorbed\ at\ hot\ junction} = \frac{Power\ supplied\ to\ load}{Peltier + heat\ withdrawn from\ hot\ junction(\mathrm{Qh})}$$

$$= \frac{I^2R_L}{\alpha IT_h + kA(T_h - T_C) - \frac{1}{2}I^2R} \tag{42}$$

By inserting the value of current, voltage and heat absorbed at hot junction, all these values are in appendix C, Equation (42) become

$$\eta = \frac{\left(1-\frac{T_C}{T_H}\right)\frac{R_L}{R}}{\left(1+\frac{R_L}{R}\right)-\frac{1}{2}\left(1-\frac{T_C}{T_h}\right)+\frac{\left(1+\frac{R_L}{R}\right)^2\frac{T_C}{T_h}}{ZT_C}} \tag{43}$$

To find the maximum efficiency, this equation requires to be solved for $\frac{d\eta}{d\left(\frac{R_L}{R}\right)}=0$ With a little algebra. The result yields a relationship of $\frac{R_L}{R}=\sqrt{1+ZT}$, it can be shown that the solution is

$$\eta_{\max}=\left(1-\frac{T_C}{T_h}\right)\frac{\sqrt{1+ZT}-1}{\sqrt{1+ZT}+\frac{T_C}{T_h}} \tag{44}$$

where $T=\frac{1}{2}\left(T_h+T_c\right)$ and ZT the dimensionless figure of merit for thermoelectric is defined in equation (8). Limited by the second-law of thermodynamics, the ideal (absolute maximum) efficiency of a thermoelectric power generator operating as a reversible heat engine is Carnot efficiency [51], given by

$$\eta_{Carnot}=1-\frac{T_C}{T_H} \tag{45}$$

The maximum conversion efficiency of an irreversible thermoelectric power generator can be estimated using:

$$\eta_{\max}=\eta_{Carnot}\frac{\sqrt{1+ZT}-1}{\sqrt{1+ZT}+\frac{T_C}{T_h}} \text{ or } \eta_{\max}=\eta_{Carnot}*\eta_{r,d} \tag{46}$$

Where,

$\eta_{r,d}$ - reduced device efficiency

Using this equation, researchers can figure out the efficiency of thermoelectric devices based on how much energy was input through heat and how much energy was output by the thermoelectric material. This equation can be utilized to compare the efficiency of thermoelectric devices with other technologies. For instance, standard combustion engines have an efficiency of 33%, while current thermoelectric devices have efficiencies around 2-14%. From formula 44, it can be seen, that with a *ZT* of around 1 and temperature of the cold side of 300 K and the hot side temperature of around 600 K, an efficiency of 10% can be achieved. It is clear, that researchers need to improve the *ZT* of materials considerably. Each term in the *ZT* equation will be looked at in detail starting with the Seebeck coefficient [18].

However, there is also the maximum power efficiency. Most manufacturers have been using the maximum power efficiency as a specification for their products [61],The maximum power efficiency is obtained by letting $\frac{R_L}{R}=1$ in Equation (43). The maximum power efficiency η_{mp} is

$$\eta_{mp}=\frac{1-\frac{T_C}{T_h}}{2-\frac{1}{2}\left(1-\frac{T_C}{T_h}\right)+\frac{4\frac{T_C}{T_h}}{ZT_C}} \tag{47}$$

Note there are two thermal efficiencies: the maximum power efficiency η_{mp} and the maximum conversion efficiency $\eta_{\max}$.

5.1. HEAT EXCHANGER EFFECT AND MATERIAL OPTIMIZATION

This section is about heat exchanger and it starts on heat sink. The main goal of connecting the thermoelectric module to a heat sink is to maximize the amount of heat transfer rate from the fins. At given dimensions, width (W_f), length (L_f) and profile length (b_f) as shown in

Figure36, there are some parameters that can be optimized to minimize the thermal resistance. These parameters are the fin thickness (t_f), and fin spacing (z_f) of the heat sink [62].

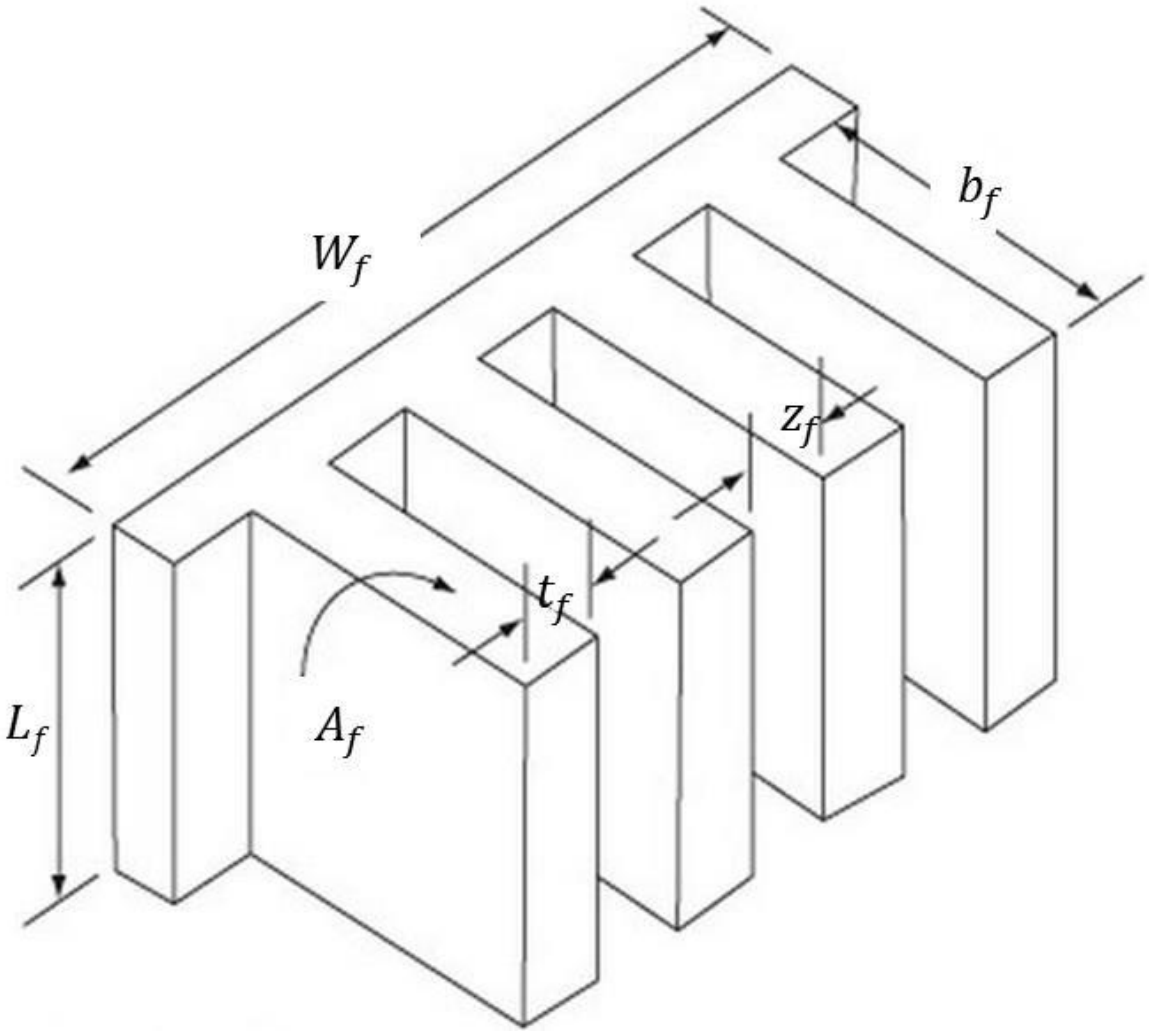

Figure 36. Multiple array heat sink

Air is employed as the coolant; The direction of the airflow is assumed to be parallel to the heat sink base, Due to the small fin spacing and low airflow rates, the airflow in typical plate fin heat sinks applied to electronic modules can be regarded as a laminar flow [63].To calculate the heat transfer coefficient the Rayleigh's number, Ra_L [64].

$$Ra_L = \frac{g\beta(|T_S - T_\infty|) * L_f^3}{\upsilon\alpha} \tag{48}$$

For the special case of air when Pr=0.72

$$h_L = \frac{k_{air}}{L_f} * 0.517 * Ra_L^{0.25} \quad (49)$$

g is the gravity, β is equal to $1/T_f$ where $T_f=(T_h+T_{amb})/2$, k_{air} is the thermal conductance of air, L_f depth of the heat exchanger and Pr is the Prandtl number.

Therefore, there must be an optimum spacing that maximizes the natural convection heat transfer from the heat sink for a given base area W_fL_f, where W_f and L_f are the width and height of the base of the heat sink, respectively, as shown in Figure36.When the fins are essentially isothermal and the fin thickness t_f is small relative to the fin spacing Z_f [65], the optimum fin spacing (Z_{opt})for a vertical heat sink is determined by Bar-Cohen and Rohsenow to be

$$Z_{opt} = L_f * 2.714 * Ra_L^{-0.25} \quad (50)$$

Number of fins are calculated as

$$n_f = \frac{W_f}{Z_{opt} + t_f} \quad (51)$$

From equation (51) fin thickness t_f may be neglected when t_f is too small compare to spacing between fins Z_f. Therefore, the laminar-based analytical method proposed by Mereu et al is used to analyze and optimize the heat sink system. For the limit of narrow channels, the airflow is considered as a fully developed flow. The total heat transfer rate can thus be obtained using [66].

$$Q_s = \frac{\rho W_f b_f Z_f{}^2 \Delta P}{1 + {}^{t_f}\!/_{Z}\, 12\mu L_f} C_p\left(T_w - T_\infty\right) \quad (52)$$

Where;

ρ -fluid density,

μ -fluid viscosity,

C_p - specific heat at constant pressure,

Δp- pressure drop across the heat sink,

T_w-maximum surface temperature of the fins, and

T_∞ -fluid inlet temperature(Air).

It should be noted that the fin surfaces are assumed to be isothermal (i.e. T_w) for simplicity. For the limit of large channels, the fin-to-fin spacing is large enough so that the airflow is approximated as a boundary layer flow. Consequently, the total heat transfer rate is expressed as [66]:

$$Q_l = 1.208 k_f W_f b_f \frac{T_s - T_\infty}{1 + {}^{t_f}\!/_{Z_f}} \left(\frac{\mathrm{Pr} L_f \Delta P}{\rho \nu^2 Z_f^2} \right)^{\frac{1}{3}} \tag{53}$$

Where,

k_f -fluid thermal conductivity,

v -fluid kinematic viscosity, and

Pr - the Prandtl number.

For a given heat sink volume $W_f \times b_f \times L_f$, there is an optimal fin-to-fin spacing Z_{opt} corresponding to the maximum heat transfer rate. The value of Z_{opt} can be obtained by intersecting the two asymptotes from equation (52) and equation (53), which yields:

$$\frac{Z_{opt}}{L_f} = 2.73 \left(\frac{\Delta P L_f^2}{\mu \alpha} \right)^{-{}^{1}\!/_{4}} \tag{54}$$

Hence, the maximum heat transfer rate Q_{max} corresponding to Z_{opt} can be obtained by substituting equation (54) into equation (52) or equation (53). Furthermore, in order to include the effect of the heat sink on the performance of the TEG, an effective heat transfer coefficient is used in this study [66]. The effective heat transfer coefficient is defined as:

$$h_{eff} = \frac{Q_{\max}}{A_B (T_w - T_\infty)} \tag{55}$$

where A_B is the base area of the heat sink. If the thermal resistance of the heat sink base is negligible, the influence of the heat sink geometry or fluid operating conditions can be

characterized by the effective heat transfer coefficient, which can be imposed as a boundary condition in the simulation of the TEG, table 3 shows different parameters used in this study.

Table 3.Properties of heat sink system *[66]*.

Properties of heat sink system	Property
Aluminum (for fin)	k_f = 237 W/m K
Air (for coolant)	$k_g = 26.3 \times 10^{-3}$ W/m K
	ρ = 1.1614 kg/m3
	$\mu = 184.6 \times 10^{-7}$ N s/m^2
	$\alpha = 22.5 \times 10^{-6}$ m^2/s
	C_p = 1007 J/kg K
	$\nu = 15.89 \times 10^{-6}$ m^2/s

The design of a TEG system normally begins with the choice of heat exchanger. This is because the heat exchangers are likely to be the physically largest components in the system; the thermoelectric module is typically small in comparison. Practical thermoelectric generators consist of hot and cold side heat exchangers and a thermoelectric module. This module consists of many individual p and n junctions wired in series to increase the total voltage [67]. The general design is shown in figure 35. When designing a TEG and corresponding heat exchangers, the sizing of these components must be carefully considered to achieve maximum power production. The system can be modeled as a thermal circuit, shown in Figure 37. At the hot side, heat ($\dot{Q}_h$) flows through a heat exchanger with thermal resistance $\Theta_{Hx,h}$ and into the TE module. Because of the Peltier and Thomson effects, there can be significant heat divergence within the TE even at steady state, such that $\dot{Q}_h \neq \dot{Q}_c$. To model this, we use

a combination of the thermal resistance Θ_{TE} and a heat sink, such that the heat leaving the TE ($\dot{Q}_c$) is less than the heat entering the TE ($\dot{Q}_h$). On the cold side, the heat leaving the TE is then dissipated by a heat exchanger with thermal resistance $\Theta_{Hx,c}$.

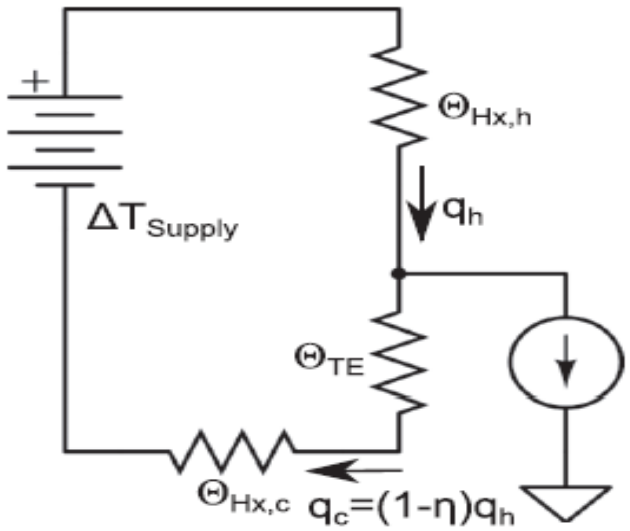

Figure 37. Equivalent thermal circuit for a thermoelectric energy harvester consisting of hot and cold side heat exchangers and a thermoelectric module *[67]*.

The temperature drops across the two heat exchangers can be written as the product of the heat flow and the thermal resistance

$$\Delta T_{Hx,h} = Q_h \Theta_{Hx,h} \quad , \quad \Delta T_{Hx,c} = (1-\eta) Q_h \Theta_{Hx,c} \tag{56}$$

These can be summed to give the total temperature drop across the two heat exchangers (ΔT_{Hx}). The combined thermal resistance Θ_{Hx} is calculated using a weighted sum of the individual heat exchanger thermal resistances

$$\Delta T_{Hx} = \dot{Q}_h \left(\Theta_{Hx,h} + (1-\eta) \Theta_{Hx,c} \right) = \dot{Q}_h \, \Theta_{Hx} \tag{57}$$

Next, the temperature drop across the TE is related to the heat entering the TE by

$$\Delta T_{TE} = \dot{Q}_h \, \Theta_{TE} \tag{58}$$

To examine the effects of ΔT_{Hx} and ΔT_{TE} on the power produced, first recall that the power is given by $P = \eta \dot{Q}_h$. If ΔT_{Hx} is zero, Equation (57) requires that the value of $\dot{Q}_h$ must be zero, so no power is produced. As ΔT_{Hx} increases, $\dot{Q}_h$ also increases .However, for a constant $\Delta T_{\sup ply}$, increasing ΔT_{Hx} causes ΔT_{TE} to decrease $(\Delta T_{\sup ply} = \Delta T_{Hx} + \Delta T_{TE})$, which decreases the efficiency η. Because the increase of ΔT_{Hx} causes two competing effects, we see that it is important to consider the relative magnitudes of, ΔT_{Hx} and ΔT_{TE}. These values are determined by the thermal resistances of the heat exchangers and the TE; it will be shown that the maximum power production is achieved when the two thermal resistances (Θ_{Hx} and Θ_{TE}) are equal. Using the thermal circuit in Figure 37 , the temperature difference across the TE can be expressed as

$$\Delta T_{TE} = \Delta T_{\sup ply} \frac{\Theta_{TE}}{\Theta_{Hx} + \Theta_{TE}} \tag{59}$$

The total $\Delta T_{\sup ply}$ can be written as

$$\Delta T_{\sup ply} = \dot{Q}_h \left(\Theta_{Hx} + \Theta_{TE}\right) \tag{60}$$

Substituting Equations (46), (59), and (60) into Equation (42) gives an expression for the power produced

$$P = \frac{\Delta T^2{}_{\sup ply} \eta_{r,d}}{T_h} \frac{\Theta_{TE}}{(\Theta_{Hx} + \Theta_{TE})^2} \tag{53}$$

Rather than consider the individual values of Θ_{Hx} and Θ_{TE}, we define the ratio $\omega = \frac{\Theta_{TE}}{\Theta_{Hx}}$. By plotting the power as a function of x in Figure 38, the power is maximized when $\omega = 1$, such that P_{max} is equation (54). The maximum power point occurs when the two thermal resistances are equal, and significant power losses are incurred when $\frac{\Theta_{TE}}{\Theta_{Hx}} \neq 1$

$$P_{\max} = \frac{\Delta T^{2}{}_{\sup ply}\eta_{r,d}}{T_h \Theta_{Hx}} \tag{54}$$

Where,

Hx-stand for heat exchanger

$\eta_{r,d}$ -reduced device efficiency (equation 46)

To minimize the denominator value of equation (54), it is clear, that thermo-resistance should be low as possible, this implies to have high thermo-conductivity, from equation (30) thermo-resistance can be reduced by decreasing the heat exchanger thickness or length(L) at the optimum value. next section shows clearly the importance of reducing this thickness.

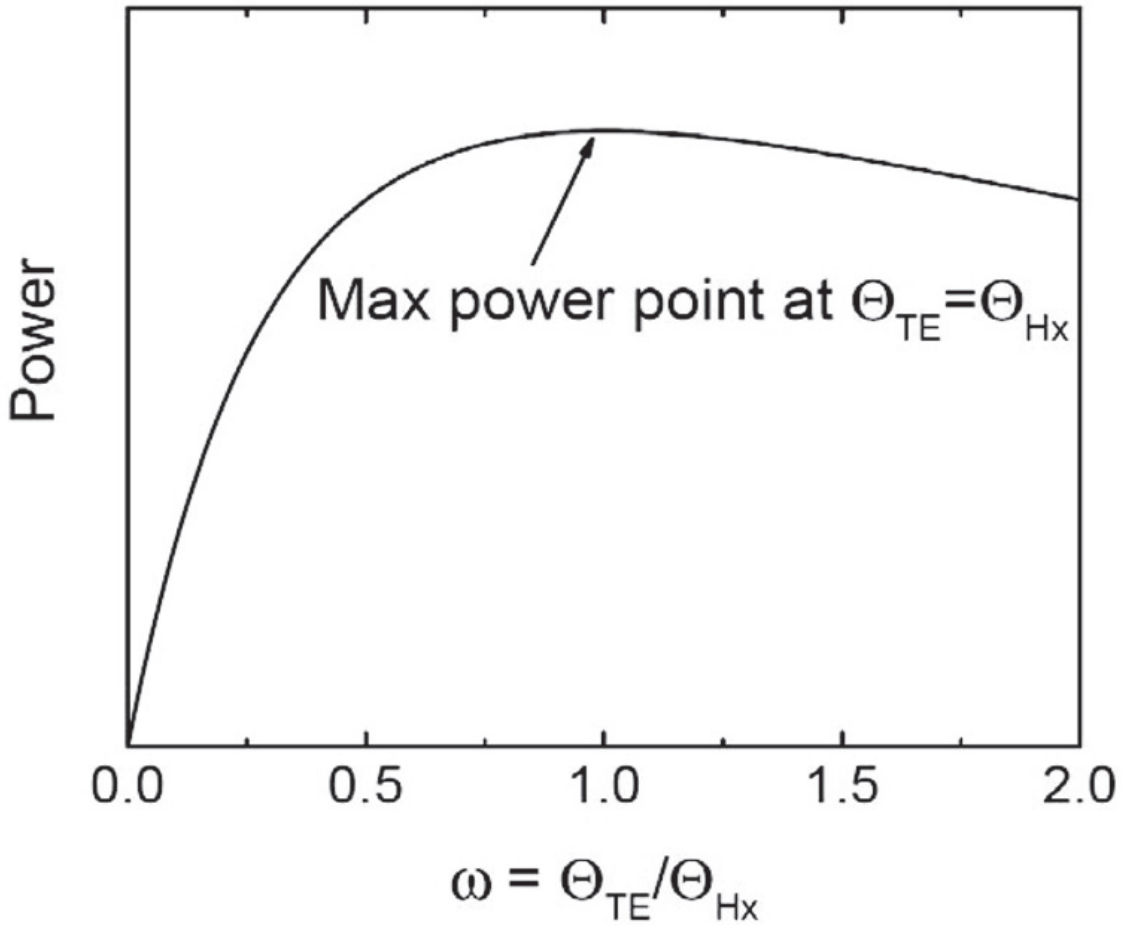

Figure 38. Variation in power as a function of the ratio of the TE and heat exchanger thermal resistances *[67]*.

5.1.1. MANUFACTURING COST CONSIDERATION

Material consideration in terms of cost, while modeling is important and it helps to use minimum cost as possible without affecting power output. This part describes how to model a thermoelectric generator with consideration of material and performance. In situations where there is excess heat (i.e., fuel/heat is free) the maximum power condition m=1 is most appropriate and yields the lowest cost. In situations where heat is costly, the maximum efficiency condition may be more appropriate [68].

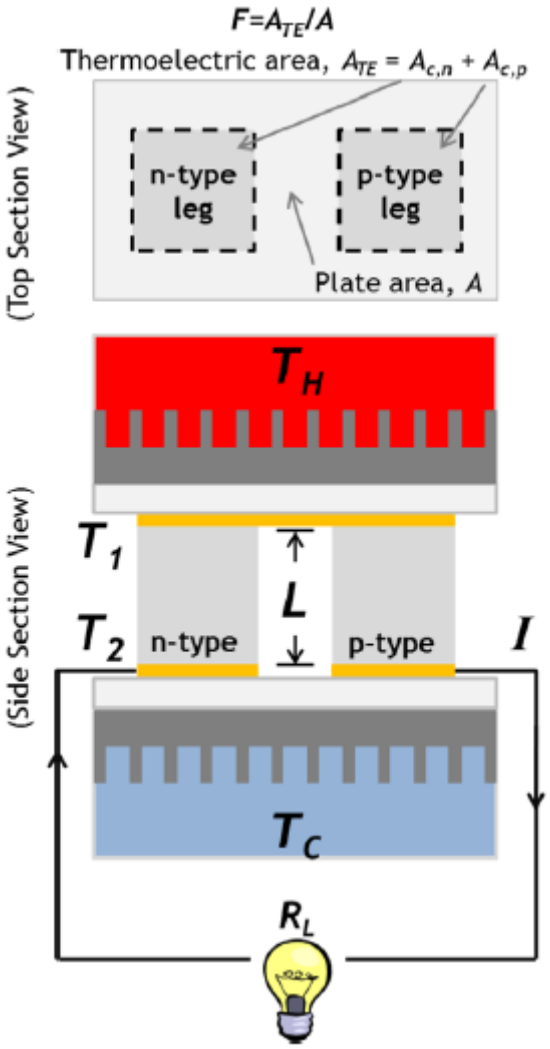

Figure 39. Diagram of thermoelectric module describing fill factor *[68]*

The fill factor, F, and the leg length, L, of a thermoelectric device are the dominant design parameters. The fill factor is the ratio of the area covered by the active thermo-electric material to the plate area, A, as illustrated in Figure 39. While it goes against traditional

thermoelectric module architecture, it is possible to envision devices with F>1. The inverse of the fill factor is known as the thermal-concentration factor. By reducing the fill factor, less active material is used, and the overall cost of the device can be reduced. In many applications, the fill factor is fixed to be above some minimum by other system constraints (e.g., mechanical robustness, voltage/areal requirements). By reducing the leg length at this fixed fill factor, less material is used, and the cost decreases. However, for a fixed heat exchanger and fixed F, as the thermoelectric leg length is reduced below some optimum, the temperature drop across the device decreases, and the output power decreases. This competition between power output and material volume suggests the existence of an optimum geometry which minimizes cost and maximizes power output [68]. Therefore, the most appropriate metric (G) for thermoelectric generators should be expressed on a $/W basis as:

$$G = \frac{C}{P_{gen}} \tag{55}$$

where,

P_{gen} -The electric power output of the generator

C -Capital cost of the device.

The capital cost includes the material, manufacturing, and heat exchanger costs. Cost of the heat available for conversion is excluded, Both C and P_{gen} are strongly dependent on L and F. A cost-performance optimization should be performed on G rather than on C or P_{gen} individually [68].

In addition to the device physics, both material and manufacturing costs influence the overall cost metric. The cost, C in Equation (55), is a function of the bulk raw material cost CB ($/kg). The manufacturing cost associated with processing bulk material $C_{M,\,B}$ ($/kg), the areal manufacturing cost $C_{M,\,A}$ ($/m^2), and the cost of both heat exchangers C_{HX} ($/(W/K)). The overall cost C is also dependent on the heat exchanger heat transfer coefficient U, the density of the active material ρ, the leg length, and area of the ceramic plates, A:

$$C = \left(\underbrace{\left(C_B + C_{M,B}\right)\rho L}_{C'''} + \underbrace{C_{M,A}}_{C''} \right) AF + C_{HX} UA \tag{56}$$

The collection of terms in the first expression is a volumetric cost C'''($/m^3), and the second term is an areal cost C''($/m^2), both of which include manufacturing costs.

As stated from above, cost is minimized by using optimum materials. In this work, referred to [68] , the pure cost of bulk material (Cm) of high manganese silicide taken is 127.51 $/kg, manufacturing cost(CMm)of 1.10 $/kg, manufacturing areal (CMA) of 168.23 $/m^2 , the cost of both heat exchangers(Chx) made in aluminum as 2.60; $/kg, and the density of the active material(ρ) equal to 4166kg/m^3 .With usage of MATLAB, considering the optimum values from table 4 the metric value or cost per unit power calculated is 0.05 $/W; this value is in the range with reference to other research made and is affordable.

The other important point is to have the optimum fill factor, the calculated one is less than 1, this shows that material has been optimized and from equation (54) the optimum power corresponds to optimum cost.in this study optimum power of TE has been considered.

Table 4 final parameter after analytical modelling

Parameter	**Value**
T_h	590^{0}C
T_C	10^{0}C
$T_{ambient}$	2^{0}C
L_{leg}	2[mm]
A	3mm^2
N	32
F (fill factor)	0.3
Voc (Open circuit voltage)	6.199 V
$P_{L\max}$ (T_{hot}= 590^{0}c, T_{cold}= 10^{0}c), calculated	11.4 W

To validate the analytical calculation modelled results COMSOL Multiphysics is used for simulation in the section 5.2, Within COMSOL Multiphysics it possible to keep the geometry creation as variable as possible. Which means in this case important geometric variables can be changed directly via a parameter list.

5.2. MODELING AND SIMULATION IN COMSOL® MULTIPHYSICS

This part is about COMSOL® modeling of thermoelectric generator, where it started by explaining briefly what is COMSOL® Multiphysics**,** then modeling follow.

COMSOL Multiphysics® is a general-purpose software platform, based on advanced numerical methods, for modeling and simulating physics-based problems. With COMSOL Multiphysics, you will be able to account for coupled or Multiphysics phenomena. With more than 30 add-on products to choose from, you can further expand the simulation platform with dedicated physics interfaces and tools for electrical, mechanical, fluid flow, and chemical applications. Additional interfacing products connect your COMSOL Multiphysics simulations with technical computing, CAD, and ECAD software [69] .The problems we want to solve in real life are always based on Multiphysics phenomena. Thus, it's required to consider interaction between two or more physics domains at one time. COMSOL Multiphysics is defined for solving these complex problems. The program offers unique user-friendly working environment and provides wide range of tools for the fast and the effective analysis. COMSOL Multiphysics allows you to minimize the needs for physical prototypes, shorten product development times and achieve substantial savings in the development process. This modeling approach helps you to develop better products and bring them faster to the market [70]. As a finite tool, this software is interesting and it gives accuracy solution, in this study Comsol Multiphysics software is used to optimize thermoelectric module.

5.2.1. WHY DO WE SIMULATE?

We simulate due to the following reasons [71] :

- Conception and understanding
  - Enables innovation
- Design and optimization
  - Achieve the highest possible performance.

- Testing and verification
    - Virtual testing is much faster than testing physical prototypes.

5.2.2. 3-D MODELING IN COMSOL® MULTIPHYSICS

First physics area to work with, here in this case; heat transfer in solid under this select thermoelectrics effect, then click **add**, after that, select kind of **study**, which is **steady state** for this case. simply, modelling of a thermoelectric generator can be done by; 3-D COMSOL® Multiphysics model of the TEG, specify materials for the model, meshing of the model, providing inputs and Simulation, 3D model building is described in the following steps:

- Parameters elaboration and geometry dimensions in table **5**, From this table of parameters, parameters can be changed easily.

Table 5. parameter in COMSOL® *Multiphysics software*

Name	Expression	Value	Description
A_pleg	3[mm^2]	3E-6 m²	P-leg area
w_pleg	sqrt(A_pleg)	0.0017321 m	P-leg width
d_pleg	sqrt(A_pleg)	0.0017321 m	P-leg depth
h_pleg	2[mm]	0.002 m	P-leg height
w_sub	24.5[mm]	0.0245 m	Substrate width
d_sub	24[mm]	0.024 m	Substrate depth
h_sub	0.2[mm]	2E-4 m	Substrate height
h_cu	0.3[mm]	3E-4 m	Copper height
h_nleg	h_pleg	0.002 m	N-leg height
k_n	2.22	2.22	N-leg thermal conducticivty
p_n	1/1.1e5	9.0909E-6	N-leg resistance
k_p	2.636	2.636	P-leg thermal conducticivty
p_p	1/3.9e4	2.5641E-5	P-leg resistance
N	32	32	Number of couples
FF	(w_nleg*d_nleg*N*2)/(w_sub*...	0.32653	Fill Factor
R_c.p	4.8e-9[ohm*m^2]	4.8E-9 Ω·m²	P-leg contact resistance
R_c.n	4.8e-9[ohm*m^2]	4.8E-9 Ω·m²	N-leg contact resistance
T_hot	590[degC]	863.15 K	Temperature hot side
T_cold	10[degC]	283.15 K	Temperature cold side
w_nleg	w_pleg	0.0017321 m	N-leg width
d_nleg	w_pleg	0.0017321 m	N-leg depth
A_te	0.5[mm]	5E-4 m	spacing
s_avg	3.34e-4[V/K]	3.34E-4 V/K	Average Seebeck coefficient
z_avg	((s_avg)^2)/((sqrt(p_n*k_n)+s...	6.9016E-4 kg²·m...	z*
A_p	d_pleg*w_pleg	3E-6 m²	P-leg area
A_n	(d_nleg*w_nleg)	3E-6 m²	N-leg area
R_int	((p_p*h_pleg)/A_p)+((p_n*h_n...	0.026355	Internal resistance
m_opt	sqrt(1+z_avg*((803.91+330.2...	1.1796 V/K	Optimum load

- Building of substrates and conducting strips at the cold side

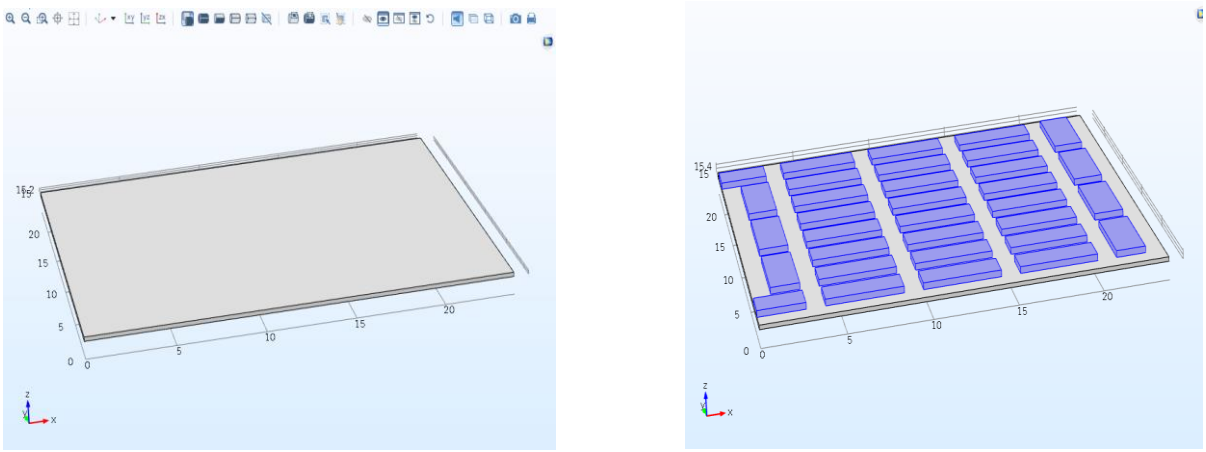

a) b)

Figure 40. a) Substrate cold side, b) Substrate and conducting strips (blues) at the cold side

The substrate in figure 40.a), is made in alumina should have high thermos-conductivity but non-electrical conductivity while the conducting strips figure 40.b) should have high electrical conductivity and thermos-conductivity.

- Pellet Couple and copper at hot side are built

P-N couples in figure41 are modelled, thermally parallel and electrically series, thermoelectric legs(P-N), as illustrate in figure 15, should be made in material which has high Seebeck coefficient, high electrical conductivity and low thermal conductivity. considering environment issue, abundance and referring to the figure 24, silicide material has been used.

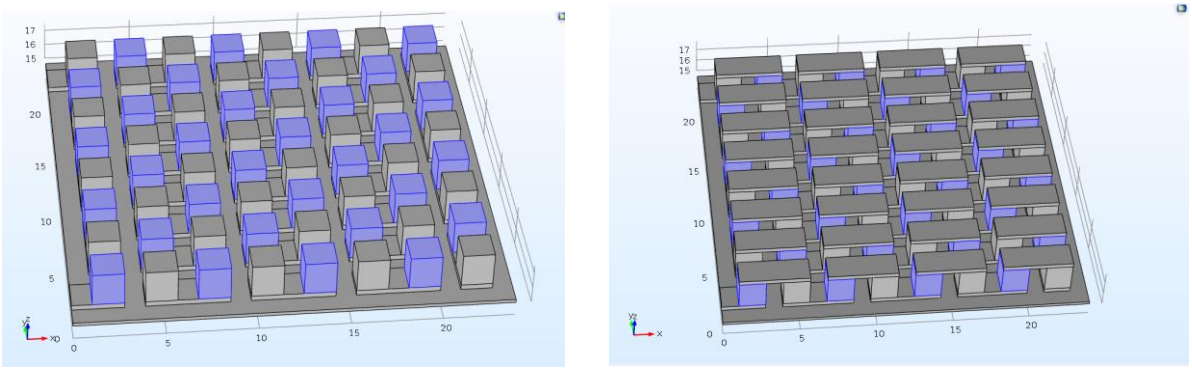

a) b)

Figure 41.a) P-N couples are built added b) Copper hot side created at hot side

- Modeling of heat sink cold side and heat exchanger hot side

The heat sink, is designed in purpose of keeping the cold surface area at the lowest temperature in this case 10^0C while ambient is average value of 2^0C .in addition this material is made in aluminium which has capacity to resist to environment (corrosion). fins are there to increase heat transfer rate and the optimum values for heat sink are in table 6.

Table 6. heat sink parameters

Part	Value	Unit
Heat sink base	26×26×1	mm
Fins	0.21×26×14	mm
Number of fins	19	-
h_{eff}	2073571.628	W/(m^2 .K)

The 2-D drawing, (figure 42), shows two principal views of the heat sink geometry, where it shows the physical dimensions and the important spacing between fins which is the key to determine the number of fins needed on any given width. the more the number of fins increases, the more it cools well but it cost more, for this work the optimum one has been taken. Next step is to develop, a 3-D view (Figure 43.a), By means of extrusion boss feature.

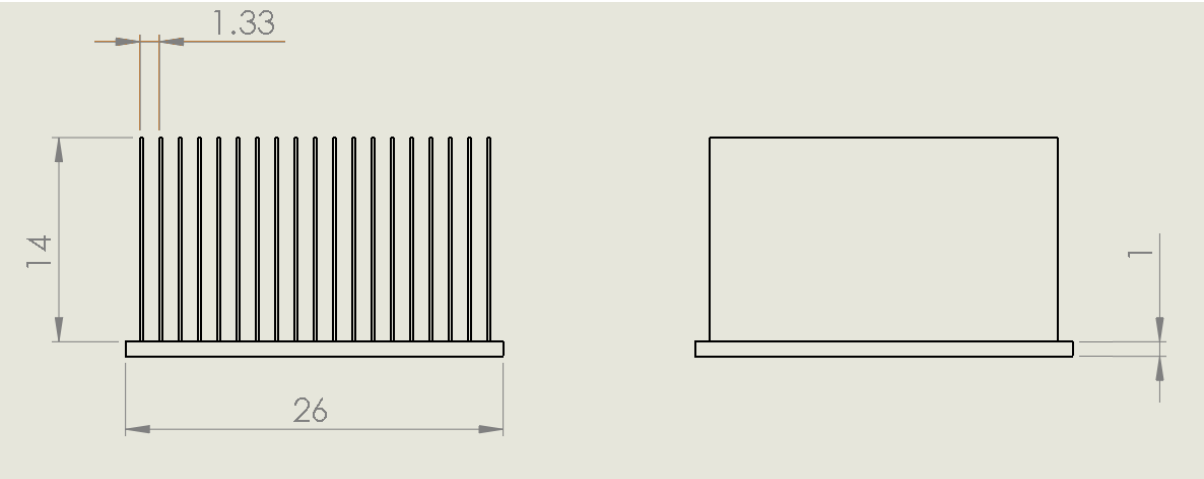

Figure 42 .2-D drawing of the heat sink geometry.

Heat exchanger at hot side Figure 43.b is modeled considering fill factor, which has been explained well in figure 39, by reducing fill factor, les active material is used and overall cost

reduced. equation 30 shows that thickness is also important, it has optimized by reducing its height with respect to the optimum power output.

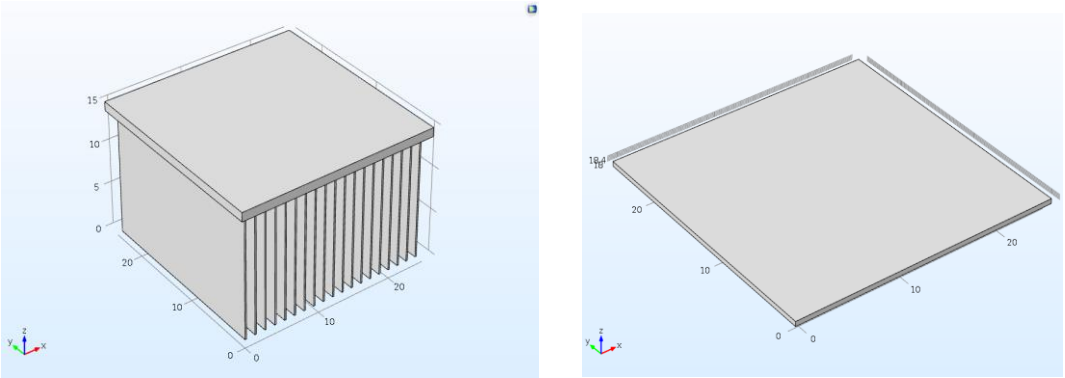

a) b)

Figure 43. a) 3-D heat sink, b) heat exchanger hot side

5.2.3. ASSIGNING MATERIALS

Before simulating the given module, material properties needed to be assigned for each geometry in thermoelectric model, COMSOL Multiphysics software has a standard set of materials in its library. Materials can however, be customized and the properties can be assigned according to the user's requirement.

The hot heat exchanger and heat sink are assigned Aluminum 3003-H18 whose material properties of thermos-conductivity is 155[W/(m*K)]. Table7, shows the difference between hot plate (substrates) and conducting strips; substrates are made in alumina(Al_2O_3) with thermos-conductivity of 27[W/(m*K)] and are electrically insulator. The well-known properties of alumina includes : low electric conductivity, resistance to chemical attack, high strength, extreme hardness (9 on the Mohs hardness scale, the highest rating being 10), and high melting point (approximately 2050 °C, or 3700 °F) [72]. Conducting strips on both sides, that connect thermoelectric legs assigned the properties of copper with electrical conductivity and thermos-conductivity of 5.998*107 [S/m], 400[W/(m*K)] respectively.

Table 7 Assigned materials for conducting strip(copper)and substrates

Copper *(mat5)*

Property	Name	Value	Unit	Property group
Electrical conductivity	sigma	5.998e7[S/m]	S/m	Basic
Heat capacity at constant pressure	Cp	385[J/(kg*K)]	J/(kg·K)	Basic
Relative permittivity	epsilonr	1	1	Basic
Density	rho	8960[kg/m^3]	kg/m³	Basic
Thermal conductivity	k	400[W/(m*K)]	W/(m·K)	Basic

substrate *(mat2)*

Property	Name	Value	Unit	Property group
Heat capacity at constant pressure	Cp	900[J/(kg*K)]	J/(kg·K)	Basic
Thermal conductivity	k	27[W/(m*K)]	W/(m·K)	Basic
Density	rho	2700[kg/m^3]	kg/m³	Basic

For the thermoelectric module simulation in COMSOL Multiphysics software, it is necessary to concentrate on thermoelectrics materials, table 8 shows, assigned material properties for p-type and n-type, like the Seebeck coefficient, thermal conductivity and electrical conductivity, the crucial element here is the function S(T) , which is shown in appendix D.

Table 8. Assignment of materials and their properties for N_leg and P_leg

N-leg Mg2Si0.4Sn0.6 *(mat4)*

Property	Name	Value	Unit	Property group
Heat capacity at constant pressure	Cp	154[J/(kg*K)]	J/(kg·K)	Basic
Density	rho	7700[kg/m^...	kg/m³	Basic
Seebeck coefficient	S	S(T)	V/K	Basic
Electrical conductivity	sigma	sigma(T)	S/m	Basic
Thermal conductivity	k	k(T)	W/(m·K)	Basic
Relative permittivity	epsilonr	1	1	Basic

P_leg(HMS) *(mat3)*

Property	Name	Value	Unit	Property group
Heat capacity at constant pressure	Cp	154[J/(kg*K)]	J/(kg·K)	Basic
Density	rho	7700[kg/m^3]	kg/m³	Basic
Seebeck coefficient	S	S(T)	V/K	Basic
Electrical conductivity	sigma	sigma(T)	S/m	Basic
Thermal conductivity	k	k(T)	W/(m·K)	Basic
Relative permittivity	epsilonr	1	1	Basic

5.2.4. MESHING

To solve the model accurately using COMSOL Multiphysics software, meshing plays a very important role. Meshing is discretization of the geometry into number of cells and nodes, All the governing equations are solved in these small discretized nodes [73]. Normal meshing has been used, since it is sufficient to simulate the problem without consuming a lot of time. The figure 44 shows the meshing that has been used in this thesis.

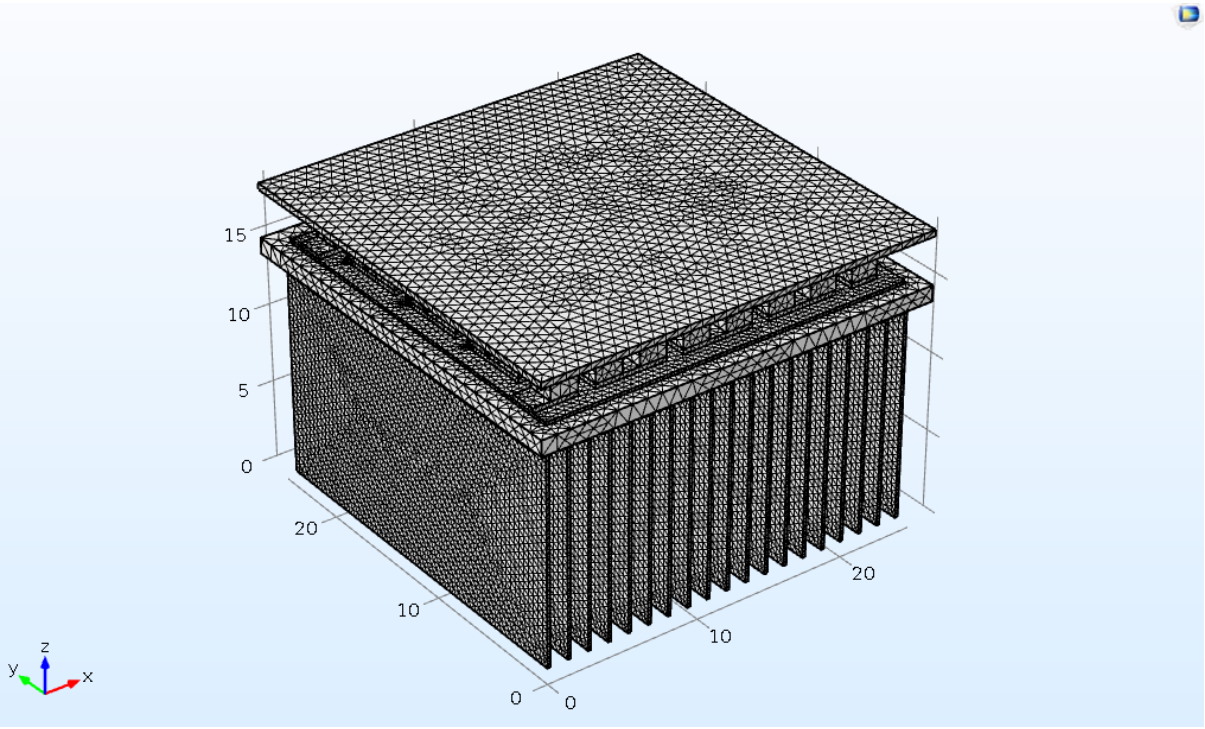

Figure 44.Meshing in COMSOL Multiphysics

Mesh size can be changed according to the user requirement. A fine mesh would give better accuracy in the result but would also consume a lot of computing power and time. So, there is always an optimum mesh size that a user can define.

5.2.5. INPUT DATA

Once meshing is done and generated for the module, inputs must be given to the module in terms of load resistance, hot side temperature and cold side temperature (effective heat transfer coefficient for heat sink), air is entering parallel to the fins. The load resistance is given in terms of geometry and the material property of the material used. The regions where these inputs need to be given is shown in the figure45.To simulating a thermoelectric generator module in COMSOL Multiphysics, it needs three boundary conditions

- Hot temperature(T_hot)
- Cold temperature or effective heat transfer coefficient(h_eff)
- Ground condition or Zero Voltage at the cold side of the N_type element.

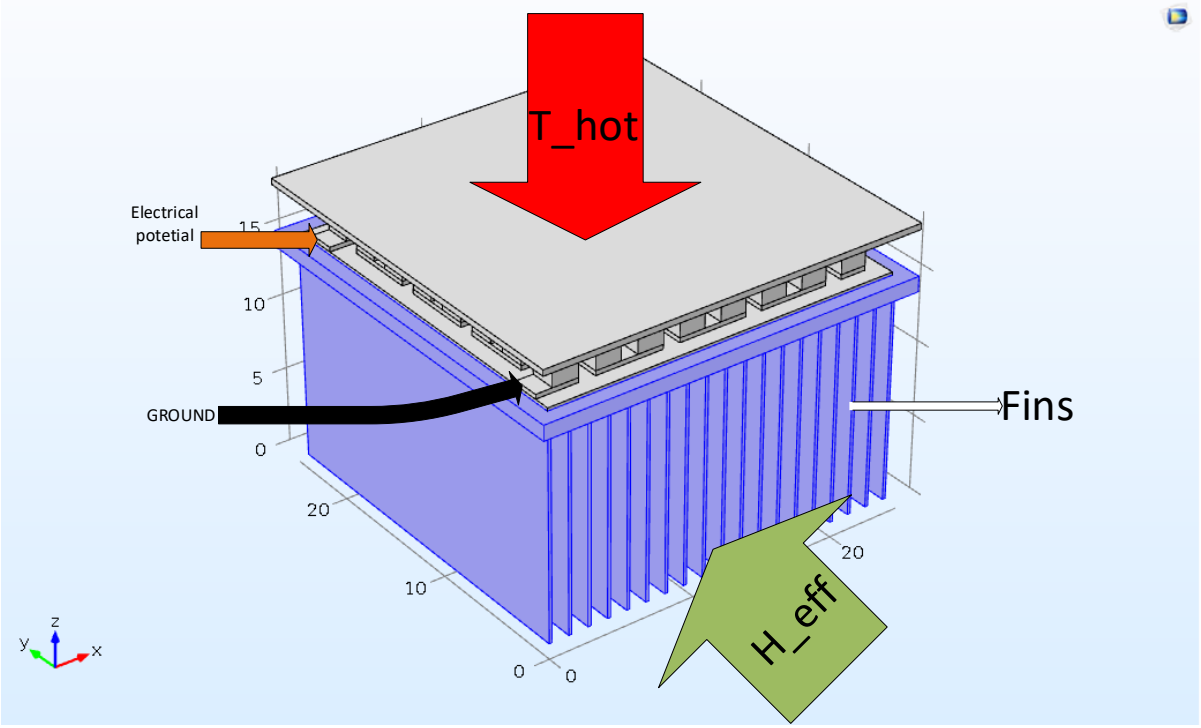

Figure 45.3D Full COMSOL model System (boundary condition)

Typically, the last boundary condition is specified at the cross section of the copper electrical conductor which connects to the load resistance. Figure 45 shows a final 3D model of thermoelectric generator composed by 32 couples, on this system which is ready to be simulated , you can find from up to down the hot heat exchanger 26×26×0.4 (mm) ,hot substrate of 24.5×24×0.2 (mm), arrays of copper at hot side (conducting materials) with 0.3

mm of height, a set thermoelements which are P_type and N_type both each has $3mm^2$as area and 2mm as height , array of copper at cold side and the substrate at cold side, finally heat sink with fins .

6. RESULTS AND DISCUSSIONS

This chapter is talking about the output results and analysis of the results. When the simulation is finished, the results of the thermoelectric generator performance, including the temperature supplied to the hot side T_hot, the generated current I, the output power P, open circuit voltage Voc, and the efficiency, were obtained. Figure 46 shows a temperature distribution of the thermoelectric module; the hot temperature has been applied to the upper side as you can see and for the cold side temperature as we are using heat sink to cool, effectiveness heat transfer coefficient is used instead of T_cold, ambient temperature which has been taken is 2^0C and the surface temperature at the cold substrate side 10^0C. As indicated in Figure 46 the temperature distributions are the same at the same level(Height) in all thermoelectric elements due to its parallel thermally arranged and clearly the cooling is good.

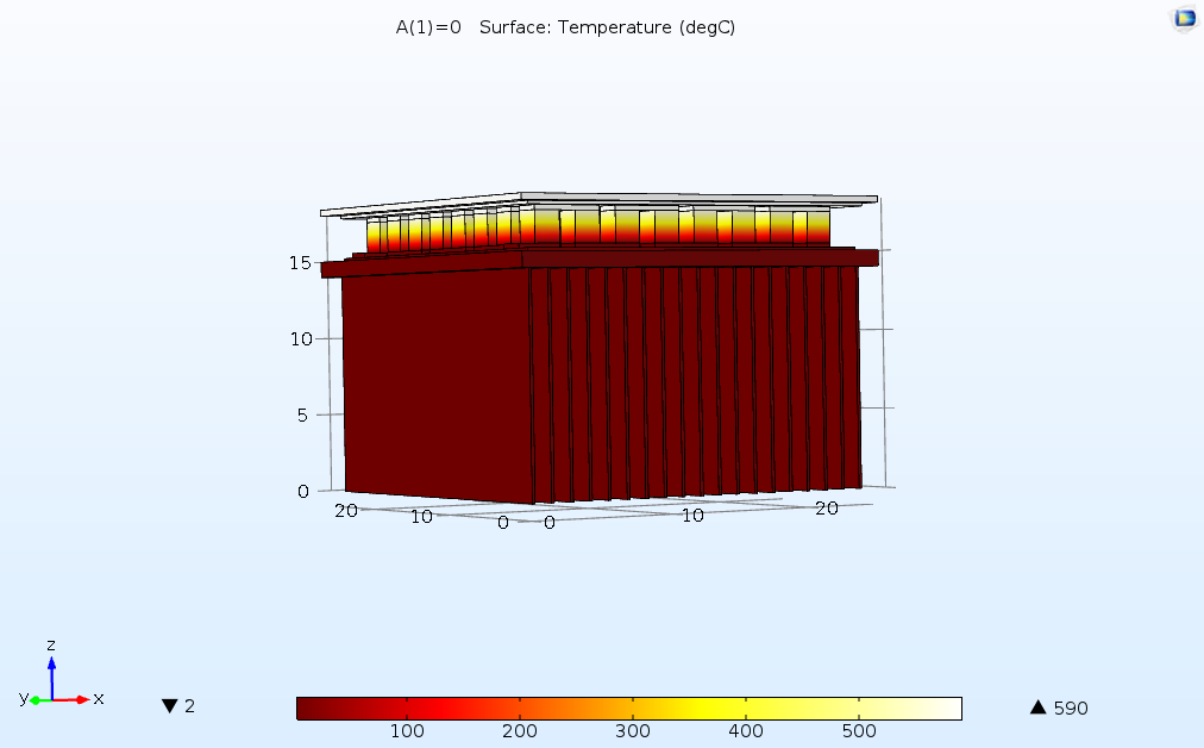

Figure 46. temperature distribution *(590^{O}C* and *2^{0}C)* here 2^0c is ambient temperature

Figures 47 shows the voltage distribution, how it varies with respect to different parameters; for instance, it shows electrical voltage distribution of the thermoelectric module, where the voltage increases with increase number of thermoelectric element couples, this is due to its electrically arranged in series. This proves that, once number of couples increase, electrical potential differences increases. Further analysis shows that the temperature difference is an important parameter; once increases, output voltage increases. There are different parameters that can be changed to get a desired output voltage such as ratio of area to the length of pellet, temperature differences, material properties, number of pellet couples(N), etc.

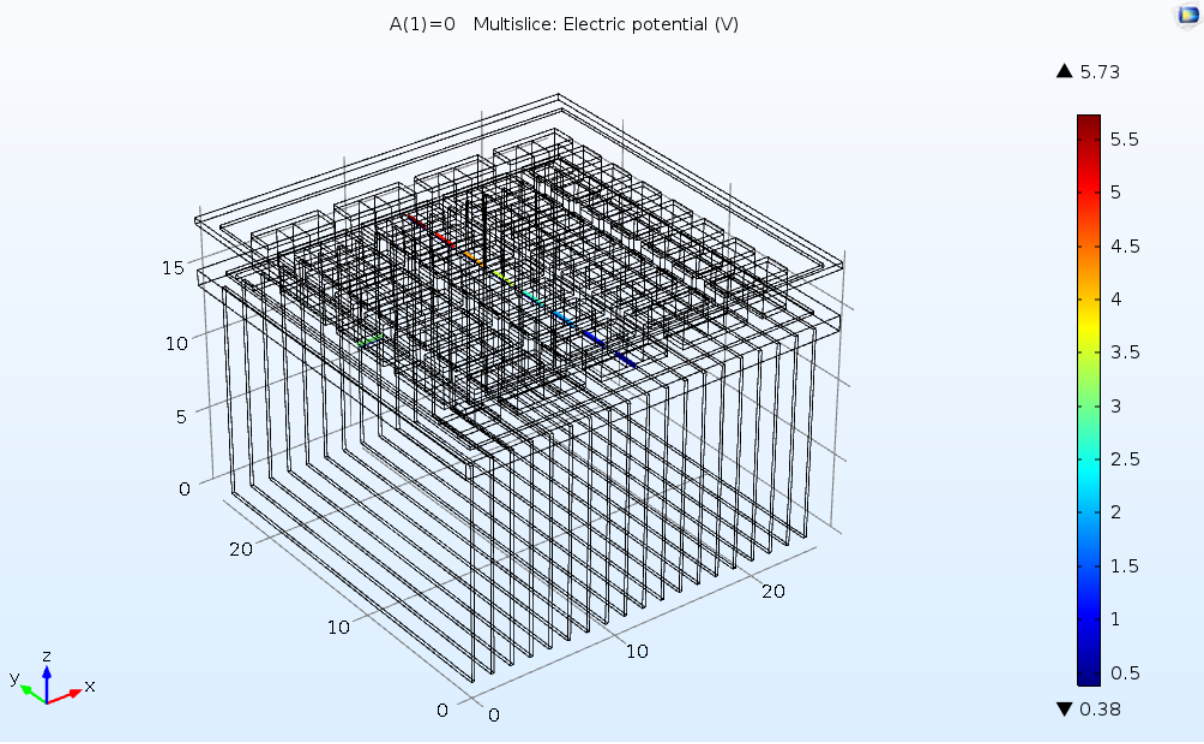

Figure47.Voltage distribution *of the thermoelectric module* (T_{hot}=590^{0}c,T_{cold}= 10^{0}c,$T_{ambient}$=2^{0}c)

Figure 48 shows the curve of output voltage versus electric current, where it goes decreasingly, the output voltage is maximum when the circuit is open; once the load applied the open circuit voltage decreases linearly, this means that maximum voltage minus drop voltage due to the load, equation33.

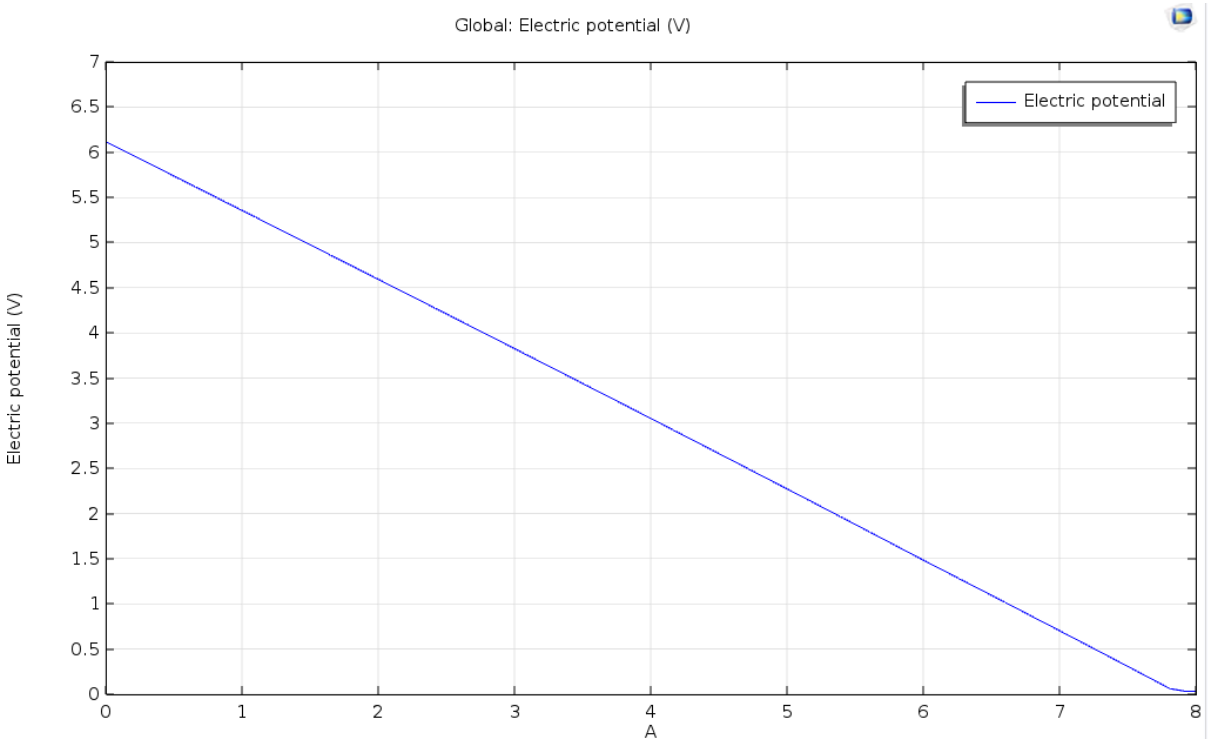

Figure 48. Electrical potential curve *(T_{hot}= 590^{0}C, T_{cold}= 10^{0}C,$T_{ambient}$=2^{0}C)*

Figure 49 shows the output power from the thermoelectric module versus electrical current, obviously, While the electrical current is increasing the power increases till maximum power point. After optimum point the power decreases as the electrical current continuous to increase.as the objective of this thesis, this maximum of 12.1W is obtained with optimum material; at optimum thickness or height of thermoelectric legs, substrates, hot heat exchanger and heat sink, this power is not exactly as the calculated one; the difference is small which is due to the contact resistance error. This simulated power output of 12.1 W was found with usage of heat sink as cooling system, which is not different to power found without heat sink (appendix E), this means that the designed cooling system is successfully.

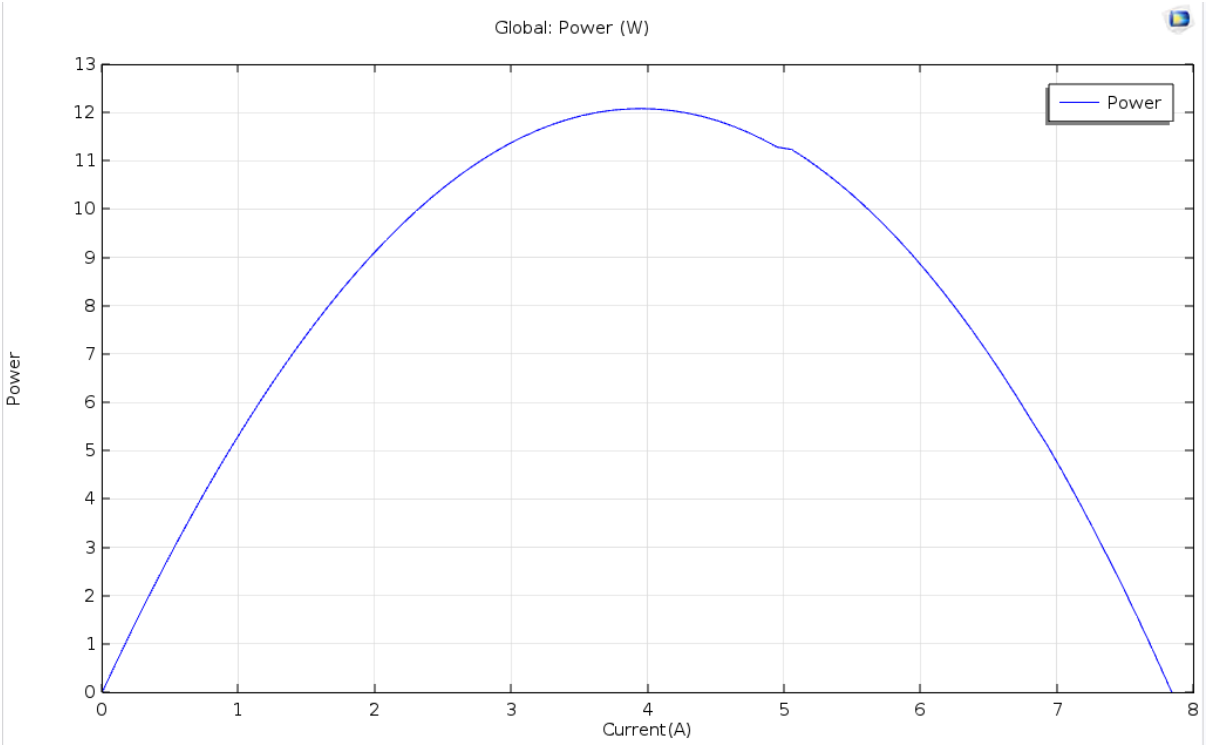

Figure 49.Power versus current

Table 9 shows output results of power and voltage with respect to different hot temperature, this proves that when temperature difference increase both output maximum power and open circuit voltage increase. These results were taken from simulated optimum module, more details are in appendix A and B, where you may find also the simulated results without both heat exchanger in appendix E.

Table 9 output power and voltage, with respect to the temperature

Temperature(^{0}C)	Power(W)	Open circuit voltage(V)
T_hot1= 210	1.4	1.8
T_hot2=400	5.8	3.7
T_hot3=590	12	5.73

Obviously in figure 50, power and efficiency are maximum at the same time, the results show clearly power and efficiency increase and decrease simultaneously, while the current is increasing. in both cases, electrical potential voltage does not change its directions, it means that, continues to decrease when the current increases.

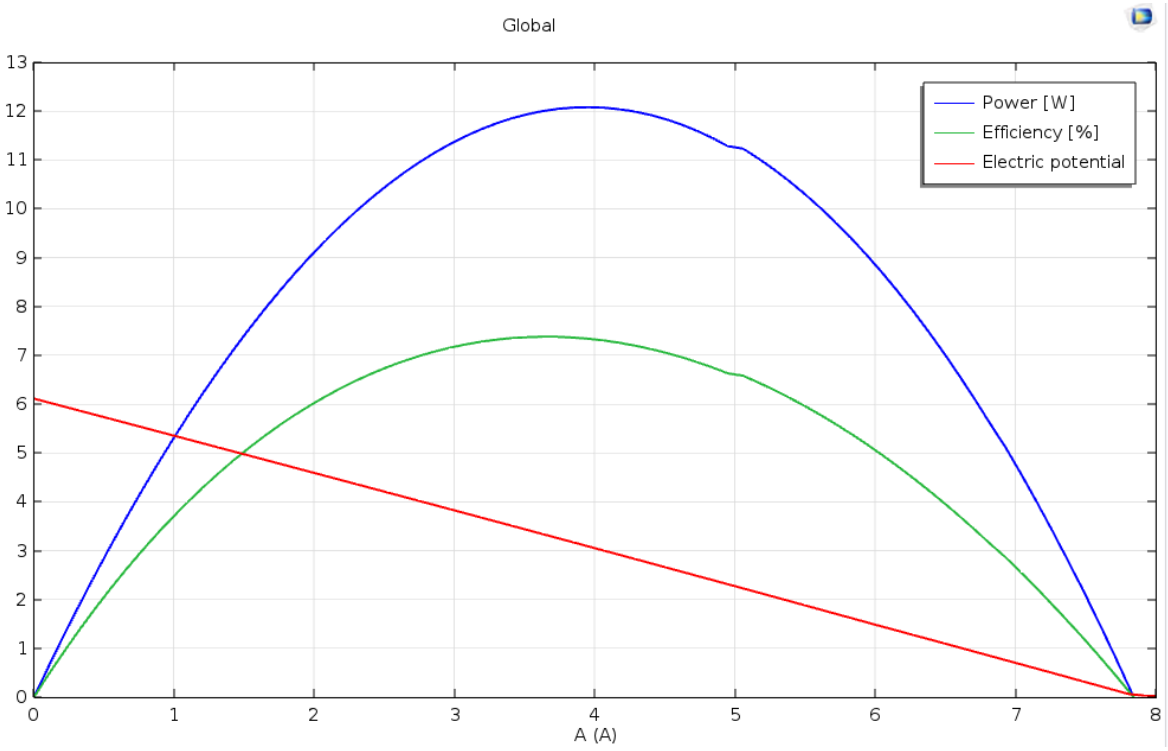

Figure 50.Power-current, voltage-current and efficiency-current

The open-circuit voltage V_{OC} is the voltage when no current is drawn by the load, while the short-circuit current I_{SC} is the current when the TEG's terminals are shorted together. The maximum power point lies at the point when $I_{load}=I_{SC}/2$ or $V_{load}=V_{OC}/2$ and is established when the equivalent electrical load resistance in the external circuit connected to the TEG exactly equals the internal electrical resistance R_{int} of the TEG. R_{int} $(R_{TE})$is the inverse slope of the *V-I* line and its absolute value is dependent on the temperature at which the TEG is operating and hence does not have a fixed value. When the TEG is operated to the left of the maximum power point around 12.1W in Figure 50, reduced current flows through the TEG and the effective thermal conductivity of the TEG (which depends also on the current flow, due to the parasitic Peltier effect) decreases. Under this condition, the thermal energy conducted via the TEG is less than that at the maximum power point and hence a lower thermal load is imposed on the overall system. This is advantageous in most circumstances since it leads to increased

thermal efficiency of the system. When the TEG is operated to the right of the maximum power point then the thermal conductivity increases and the thermal energy conducted via the TEG is greater than that which flows at the maximum power point. Operation in the region to the right-on Figure 50, leads to a reduced thermal efficiency of the system [74].

7. CONCLUSIONS

Waste heat from industries, when are not captured, are useless and contribute to global warming, there are a lot of methods to recover the waste heat generated from local industries but here in this project, research was made on thermoelectric generator for waste heat recovery; which is the renewable energy source.

Thermoelectrics effect are the way electrical potential is generated, by presence of temperature difference and vice versa, and this result depend on material properties of thermocouples and their size, I mean areas and lengths; High manganese silicide(HMS) has been used to make thermoelements materials .

Design which has been done, including the design and modeling of thermoelectric generator, Heat exchanger on both sides; hot heat exchanger and heat sink (cold side) which helps to predict the real system, it was based on the properties of waste heat from local industries; like temperature range to work with and the Cost per optimum power, where the obtained optimum power was reached with usage of optimum materials. Simulation done by using Comsol Multiphysics is good because it doesn't consume materials and it is easy to edit when you want to change any parameters.

Results found are good and there are showing that once temperature difference increases output also increase, the generated electrical power changes with change in temperature differences, so this can be conditioned (boost converter) and supplied to the electronics devices or can be used for other purposes to increase the overall efficiency in the plant, this shows that manufacturing and production industries, should use or adopt this system to save environments. As recommendation, University of Agder should install material science laboratory, to have more practice in thermoelectric fabrication or making; as it is needed to work on figure of merit ZT physically to improve the performance.

8. REFERENCES

[1] Jiin-Yuh Jang, Ying-Chi Tsai, "Optimization of thermoelectric generator module spacing and spreader thickness used in a waste heat recovery system," *Elsevier,* no. 51, pp. 677-689, 2012.

[2] Laia Miró, Jaume Gasia, Luisa F. Cabeza, “Thermal energy storage (TES) for industrial waste heat (IWH) recovery:A review,” *Elsevier,* p. 285, 2016.

[3] Tongcai Wang, Weiling Luan ⇑, Wei Wang, Shan-Tung Tu, "Waste heat recovery through plate heat exchanger based thermoelectric generator system," *Elsevier,* p. 860, 2014.

[4] Cynthia Haddad, Christelle Périlhon, Amélie Danlos, Maurice-Xavier François,Georges Descombes, "Some efficient solutions to recover low and medium waste heat:competitiveness of the thermoacoustic technology," in *The International Conference on Technologies and Materials for Renewable Energy, Environment and Sustainability, TMREES14*, Paris, 2014.

[5] S. Spoelstra, M.E.H. Tijani, "Thermoacoustic heat pumps for energy savings," in *Presented at the seminar "Boundary crossing acoustics" of the Acoustical Society of the Netherlands*, Netherlands, 2005.

[6] Fitriani, R.Ovik , B.D.Long , M.C.Barma , M.Riaz , M.F.M.Sabri , S.M.Said ,, "A reviewonnanostructuresofhigh-temperaturethermoelectric materialsforwasteheatrecovery," *Elsevier,* p. 636, 2016.

[7] BCS, Incorporated, "Waste Heat Recovery:Technology and Opportunities in U.S. Industry," U.S. Department of Energy’s Office of Energy Efficiency and Renewable Energy, Industrial Technologies Program (ITP), United state of amarica, 2008.

[8] *WASTE HEAT TO POWER SYSTEMS,* 2012.

[9] KEIICHI SASAKI, DAISUKE HORIKAWA,and KOICHI GOTO, "Consideration of Thermoelectric Power Generation by Using Hot Spring Thermal Energy or Industrial Waste Heat," *Journal of ELECTRONIC MATERIALS,,* Vols. Vol. 44, No. 1, 2015, p. 391, 2014.

[10] BITSCHI, ANDREAS, Modelling of thermoelectric devices for electric power generation, ETH ZURICH: SWISS FEDERAL INSTITUTE OF TECHNOLOGY ZURICH, 2009.

[11] Takla, Marit, "Recovering Industrial Waste Heat by the Means of Thermoelectricity," Department of Chemistry Norwegian University of Science and Technology, Trondheim, 2010.

[12] Shigeyuki Nakamura, Yoshihisa Mori and Ken'ichi Takarabe, "Mg2Si Thermoelectric Device Fabrication with Reused-silicon," in *Proc. Int. Conf. and Summer School on Advanced Silicide Technology 2014*, Okayama, 2014.

[13] Dan Mastbergen, Dr. Bryan Willson,, "Generating Light from Stoves using a Thermoelectric Generator," Engines and Energy Conversion Laboratory Department of Mechanical Engineering Colorado State University, USA.

[14] Li, Ling Bing Kong • Tao Li •Huey Hoon Hng • Freddy Boey Tianshu Zhang • Sean, Waste Energy Harvesting Mechanical and Thermal Energies, Springer Heidelberg New York Dordrecht London: Springer, 2014.

[15] Ltd., Elsevier Science, "Thermoelectric Materials: Principles,Structure, Properties, and Applications," *Elsevier,* pp. 1-11, 2002.

[16] G. Chen, MIT, [Online]. Available: www3.nd.edu/~sst/teaching/AME60634/lectures/AME60634_F13_thermoelectric.pdf. [Accessed Wednesday january 2017].

[17] Bos, Jan-Willem, "Thermoelectric materials:efficiencies found in nanocomposites," Bos, Jan-Willem, Edinburgh, 2012.

[18] Shams, Rafay Uz Zaman, "Thermoelectric Properties of Materials Based on Double Filled Type-I Clathrates," University of Waterloo, Waterloo, Ontario, Canada, 2015.

[19] Astronomy, Department of Physics and, [Online]. Available: www.phy.olemiss.edu/~cremaldi/PHYS417/Seebeck%20and%20Peltier%20Effects.pdf. [Accessed Friday January 2017].

[20] Vale, Sónia Cristina Azevedo, "Thermoelectric generator from space to automotive sectormodel and design for commercial and heavy duty vehicles," 2015.

[21] Diana Enescu, ElenaOtiliaVirjoghe, "A review on thermoelectric cooling parameters and performance," *Elsevier,* no. 38, p. 903–916, 2014.

[22] Oliveira, José Rui Camargo and Maria Claudia Costa de, "Principles of Direct Thermoelectric Conversion," InTech, University of Taubaté, 2011.

[23] HÖGBLOM, OLLE, "Multiscale Simulation Methods for Thermoelectric Generators," CHALMERS UNIVERSITY OF TECHNOLOGY, Gothenburg, Sweden, 2016.

[24] Dziurdzia, Piotr, "Modeling and Simulation of Thermoelectric Energy Harvesting Processes," InTech, Poland, 2011.

[25] BITSCHI, ANDREAS, "Modelling of thermoelectric devices for electric power generation," Technical University of Vienna, ETH ZURICH), 2009.

[26] Chhatrasal Gayner, Kamal K. Kar, "Recent advances in thermoelectric materials," *Elsevier,* pp. 331-335, 2016.

[27] Skomedal, Gunstein, "Thermal durability of novel thermoelectric materials for waste heat recovery," University of Agder, Kristiansand, 2016.

[28] Alexandre Polozine, Susanna Sirotinskaya, Lírio Schaeffer, "History of development of thermoelectric materials for electric power generation and criteria of their quality," *Sept./Oct. 2014,* 9 September 2014.

[29] Truong, Dao Y Nhi, "Thermoelectric Properties of Higher Manganese Silicides," University of Waterloo, Waterloo, Ontario, 2015.

[30] Skomedal, Gunstein, "Thermoelectric Materials for Waste Heat Recovery," University of Agder, Grimstad,Norway, 2013.

[31] R. Nave. [Online]. Available: http://hyperphysics.phy-astr.gsu.edu/HBASe/thermo/thercond.html. [Accessed 31 January 2017].

[32] Li, Zhongliang Ouyang and Dawen, "Modelling of segmented high-performance thermoelectric generators with effects of thermal radiation, electrical and thermal contact resistances.," www.nature.com/scientificreports, Tuscaloosa, AL 35487, United States., 2016.

[33] Ahmed, Basel I. Ismail and Wael H., "Thermoelectric Power Generation Using Waste-Heat Energy as an Alternative Green Technology," *Recent Patents on Electrical Engineering,* Vols. Vol. 2, No. 1 29, pp. 27-39, 2008.

[34] Mikhail I. Fedorov, Vladimir K. Zaitsev, "Sigma-Aldrich," Sigma-Aldrich Co. LLC. All Rights Reserved, 2017. [Online]. Available: http://www.sigmaaldrich.com/technical-documents/articles/material-matters/thermoelectric-materials.html. [Accessed 3 february 2017].

[35] Palmqvist, Yi Ma • Richard Heijl • Anders E. C., "Composite thermoelectric materials with embedded nanoparticles," *Springer Science+Business Media,* p. 2767–2778, 2012.

[36] v. von, "Control and Optimization of a DC-DC Converter for Thermoelectric Generators," der Technischen Universität Berlin, Berlin, , 2016.

[37] *On Thermoelectric Properties of P-Type Skutterudites,* March 21, 2012.

[38] Mori, Kunihito Koumoto • Takao, Thermoelectric Nanomaterials Materials Design and Applications, vol. 182, London, 2013, p. 135.

[39] J. YANG, "Thermoelectric Properties of CoSb3-BASED SKUTTERUDITES," © copyright by JIAN YANG, Boston , 2010.

[40] Palmqvist, Yi Ma • Richard Heijl • Anders E. C., "Composite thermoelectric materials with embedded nanoparticles," *Springer,* p. 2767–2778, 2012.

[41] Kofstad., Bjørn Pedersen Per K., "Store norske leksikon," 16 august 2016. [Online]. Available: https://snl.no/silisium. [Accessed 02 February 2017].

[42] ZUO Lei, FU Gaosheng, YU Liangyao, "Thermoelectric Materials and Thermal Spray Process for Vehicle Waste Heat Recovery," *J Automotive Safety and Energy,* vol. Vol. 7 No. 2, pp. 135 - 150, 2016.

[43] Fedorov, M.I., "THERMOELECTRIC SILICIDES:PAST, PRESENT AND FUTURE," *Journal of Thermoelectricity №2,* pp. 51-60, 2009.

[44] Liu, Jian He and Yufei, "Oxide thermoelectrics: The challenges, progress, and outlook," *Materials Research Society,* vol. Vol. 26, pp. 162-1772, Aug 14, 2011.

[45] LeBlanc, Saniya, "Thermoelectric generators: Linking material properties and systems engineering for waste heat recovery applications," *Elsevier,* p. 26–35, 2014.

[46] R. A. Hayati Mamura, "Application of a DC–DC boost converter with maximum power point tracking for low power thermoelectric generators," *Elsevier Ltd,* vol. 97, p. 265–272, 2015.

[47] AravindKaruppaiah, Ganesh, Dileepan, Jayabharathi, "Fabrication and Analysis of Thermo Electric Generator For Power Generator," *IJIRSET,* vol. 3, pp. 1508-1513, 2014.

[48] Ssennoga Twaha, Jie Zhu, Yuying Yan, Bo Li, "A comprehensive review of thermoelectric technology: Materials, applications, modelling and performance improvement," *Elsevier,* vol. 65, p. 698–726, 2016.

[49] KARRI, MADHAV A, "THERMOELECTRIC POWER GENERATION SYSTEM OPTIMIZATION STUDIES," Madhav A. Karri, 2011.

[50] Shammas, Chris Gould and Noel, "Three Dimensional TCAD Simulation of a Thermoelectric Module Suitable for use in a Thermoelectric Energy Harvesting System," *InTech,* pp. 31-42, 2012.

[51] Basel I. Ismail, Wael H. Ahmed, "Thermoelectric Power Generation Using Waste-Heat Energy as an Alternative Green Technology," *Bentham Science Publishers Ltd.,* pp. 27-39, 2009.

[52] Govardhan Neeli, Dilip Kumar Behara, Meda Kalyan Kumar, "State of the Art Review on Thermoelectric Materials," *International Journal of Science and Research,* vol. 5, pp. 1833-1844, 2016.

[53] D.M. Rowe, G.Min, "Design theory of thermoelectric modules for electrical power generation," *IEE,* vol. 143, pp. 351-356, 1996.

[54] Jaluria, Yogesh, Design and Optimization of Thermal Systems, Second Edition, 2007.

[55] "pipeflowcalculations," [Online]. Available: http://www.pipeflowcalculations.com/tables/flue-gas.php. [Accessed 23 february 2017].

[56] Vegard Haukaas, "Waste heat recovery Design, modeling and feasibility of thermoelectric power generation," University of Agder, Grimstad, 2016.

[57] Ze-Guang Zhou, Dong-Sheng Zhu, Hong-Xia Wu and Hong-Sheng Zhang, "Modeling, Experimental Study on the Heat Transfer Characteristics of Thermoelectric Generator," *Journal of Thermal Science,* vol. 22, no. 1, p. 48−54, 2013.

[58] Li, Zhongliang Ouyang & Dawen, "Modelling of segmented high-performance thermoelectric generators with effects of thermal radiation, electrical and thermal contact resistances," *Scientific Reports,* pp. 1-12, 2016.

[59] Raşit Ahıska, Hayati Mamur, "A review: Thermoelectric generators in renewable energy," *INTERNATIONAL JOURNAL of RENEWABLE ENERGY RESEARCH,* vol. 4, pp. 128-136, 2014.

[60] Paul, Douglas, "Thermoelectric Energy Harvesting," InTech, 2014.

[61] Lee, HoSung, "Thermoelectric Generators," [Online]. Available: homepages.wmich.edu/~leehs/ME539/Thermoelectric%20Contact%20Resistances.pdf. [Accessed 15 february 2017].

[62] Fagehi, Hassan, "OPTIMAL DESIGN OF AUTOMOTIVE EXHAUST THERMOELECTRIC GENERATOR," Hassan Fagehi, Western Michigan University, 2016.

[63] C.-I. H. ,. W.-H. C. Chien-Chang Wang, "Design of heat sink for improving the performance of thermoelectric generator using two-stage optimization," *Elsevier,* p. 236e245, 2012.

[64] Lee, HoSung, Thermal Design - Heat Sinks, Thermoelectrics, Heat Pipes, Compact Heat Exchangers, and Solar Cells, ProQuest Ebook Central, 2010.

[65] [Online]. Available: http://mechfamilyhu.net/downloads/Heat%20Transfer1&2/books/Heat.And.Mass.Trafer%20by%20chapter/cen58933_ch09.pdf. [Accessed 15 March 2017].

[66] Chien-Chang Wang, Chen-I Hung, Wei-Hsin Chen, "Design of heat sink for improving the performance of thermoelectric generator using two-stage optimization," *Elsevier,* vol. 39, no. 1, p. 236–245, 2012.

[67] Lauryn L. Baranowski, G. Jeffrey Snyder, and Eric S. Toberer, "Effective thermal conductivity in thermoelectric materials," *JOURNAL OF APPLIED PHYSICS 113, 204904 (2013),* pp. 1-12, 2013.

[68] Saniya Le Blanc, ShannonK.Yee , MatthewL.Scullin , ChrisDames, "Material and manufacturing cost considerations for thermoelectrics," *Elsevier,* p. 313–327, 2014.

[69] COMSOL Inc, "COMSOL," [Online]. Available: https://www.comsol.com/comsol-multiphysics. [Accessed 08 March 2017].

[70] HUMUSOFT s.r.o., [Online]. Available: http://www.humusoft.cz/comsol/. [Accessed 08 march 2017].

[71] COMSOL, [Online]. Available: https://www.comsol.com/video/simulate-thermoelectric-devices-tecs#. [Accessed 23 March 2017].

[72] The Editors of Encyclopædia Britannica, "Encyclopædia Britannica," [Online]. Available: https://global.britannica.com/science/alumina. [Accessed 25 April 2017].

[73] Shripad Dhoopagunta, "ANALYTICAL MODELING AND NUMERICAL SIMULATION OF A THERMOELECTRIC GENERATOR INCLUDING CONTACT RESISTANCES," Western Michigan University, Michigan, 2016.

[74] Andrea Montecucco , Jonathan Siviter, Andrew R. Knox, "The effect of temperature mismatch on thermoelectric generators electrically connected in series and parallel," *Elsevier Ltd,* pp. 47-54, 2014.

Appendix A – Silicide module Temperature and voltage distribution at T_hot=210^{0}C

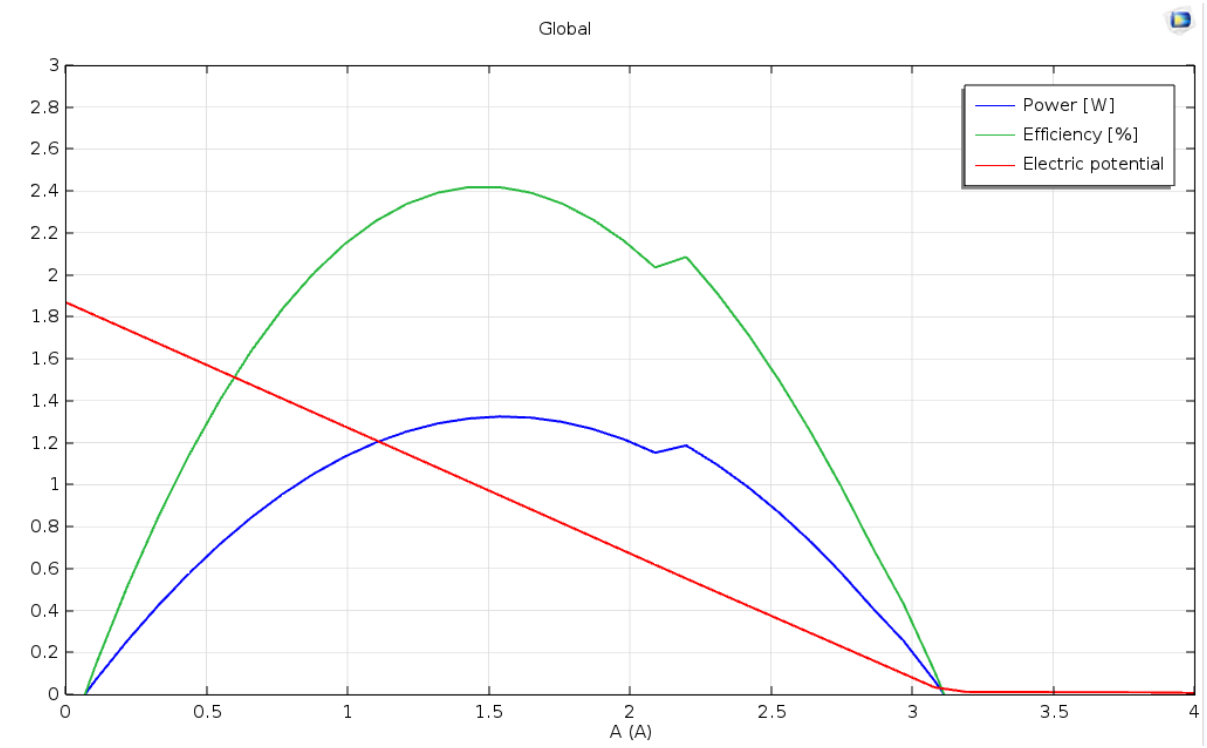

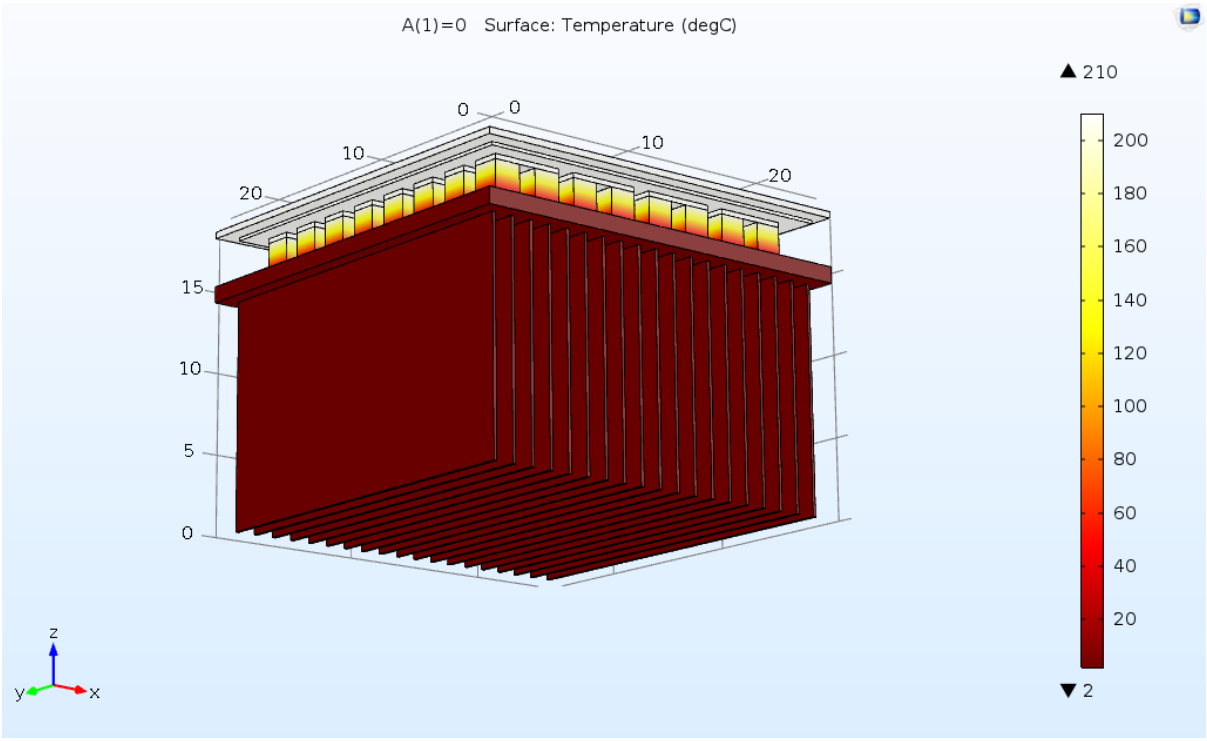

Appendix B – Silicide module Temperature and voltage distribution at T_hot=400^{0}C

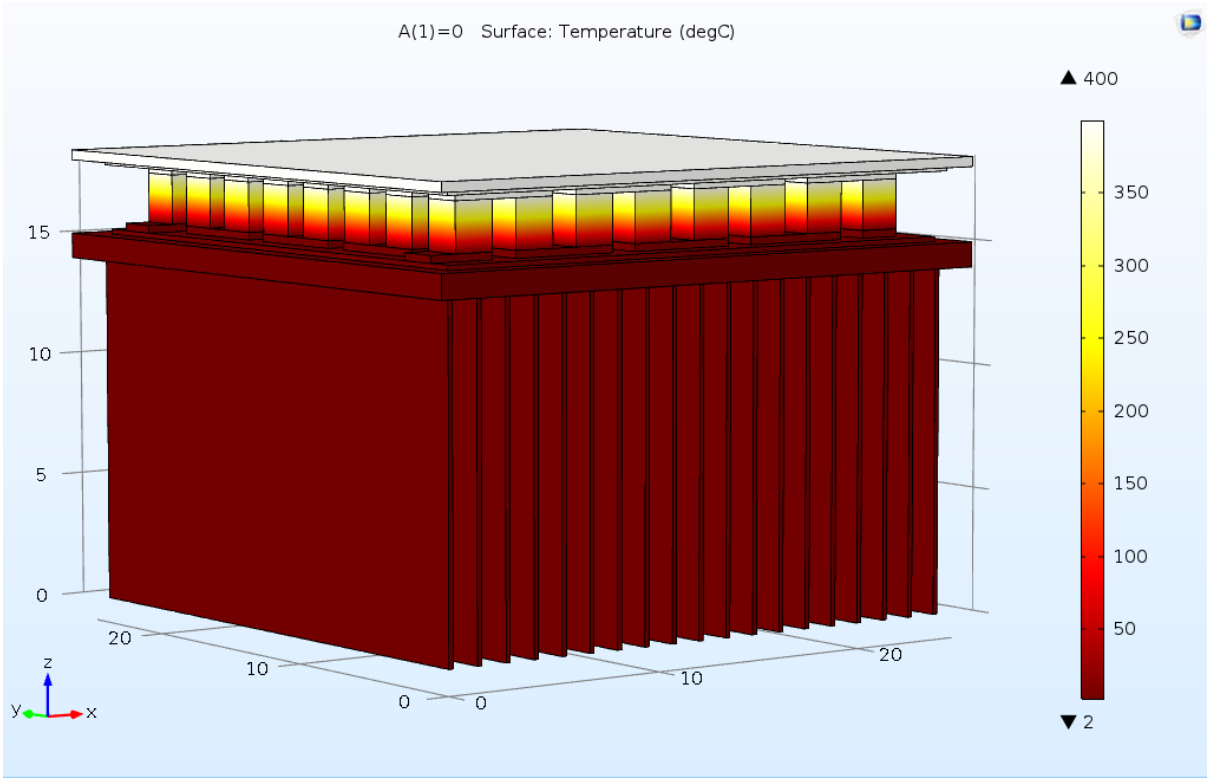

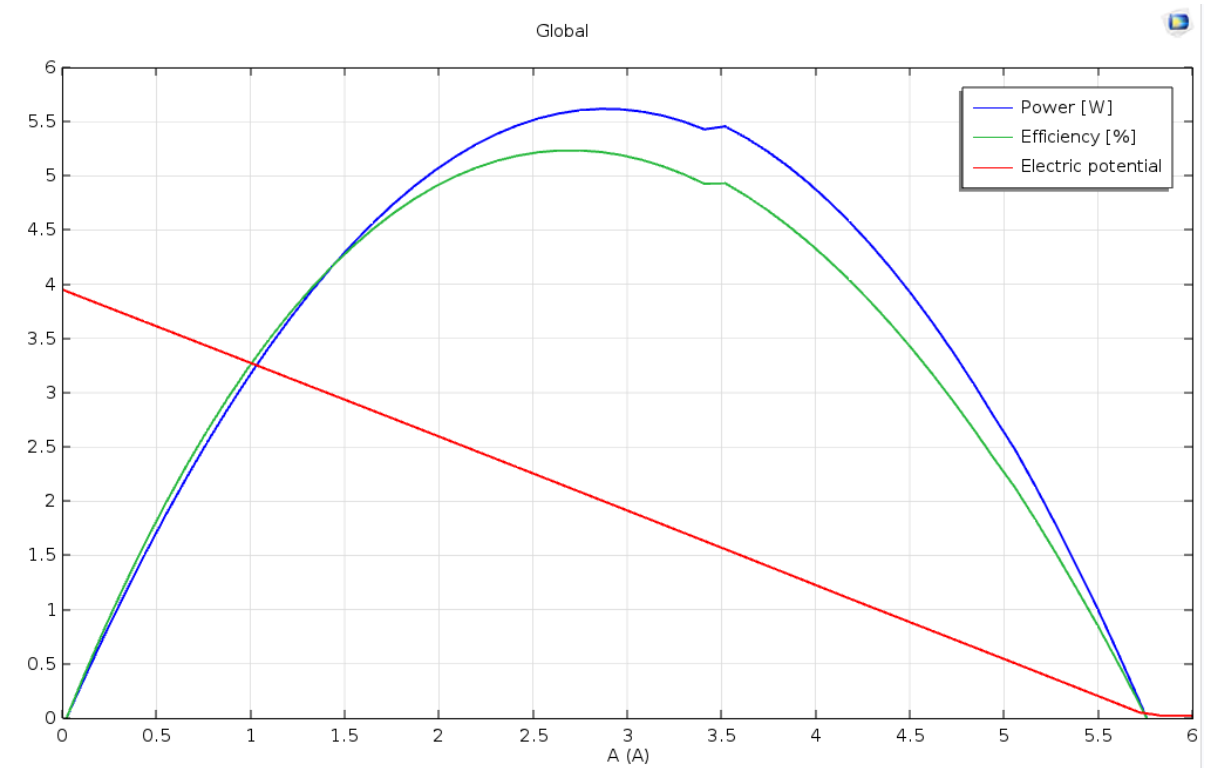

Appendix C –Some basic formulas

$$V = \frac{N\alpha\Delta T}{\frac{R_L}{R}+1}\left(\frac{R_L}{R}\right)$$

$$\dot{W} = \frac{N\alpha^2\Delta T^2}{R}\frac{\frac{R_L}{R}}{\left(1+\frac{R_L}{R}\right)^2}$$

$$\eta_{th} = \frac{\dot{W}}{\dot{Q}_h} \qquad , \dot{Q}_h - \dot{Q}_C = P_L = N[\alpha I_L(T_H - T_C) - I^2 R_{TE}]$$

Appendix D-Seebeck coefficient Properties for P_leg and N_leg

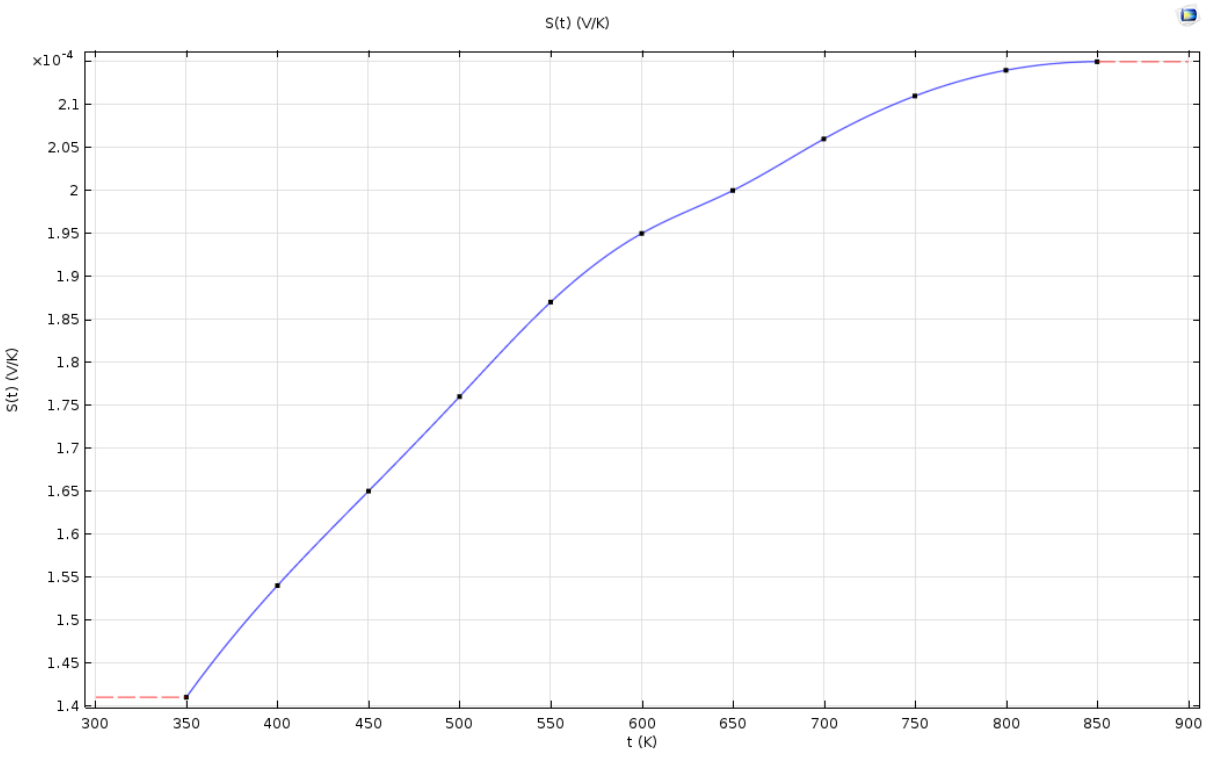

Figure of Seebeck coefficient curve for P_leg materials

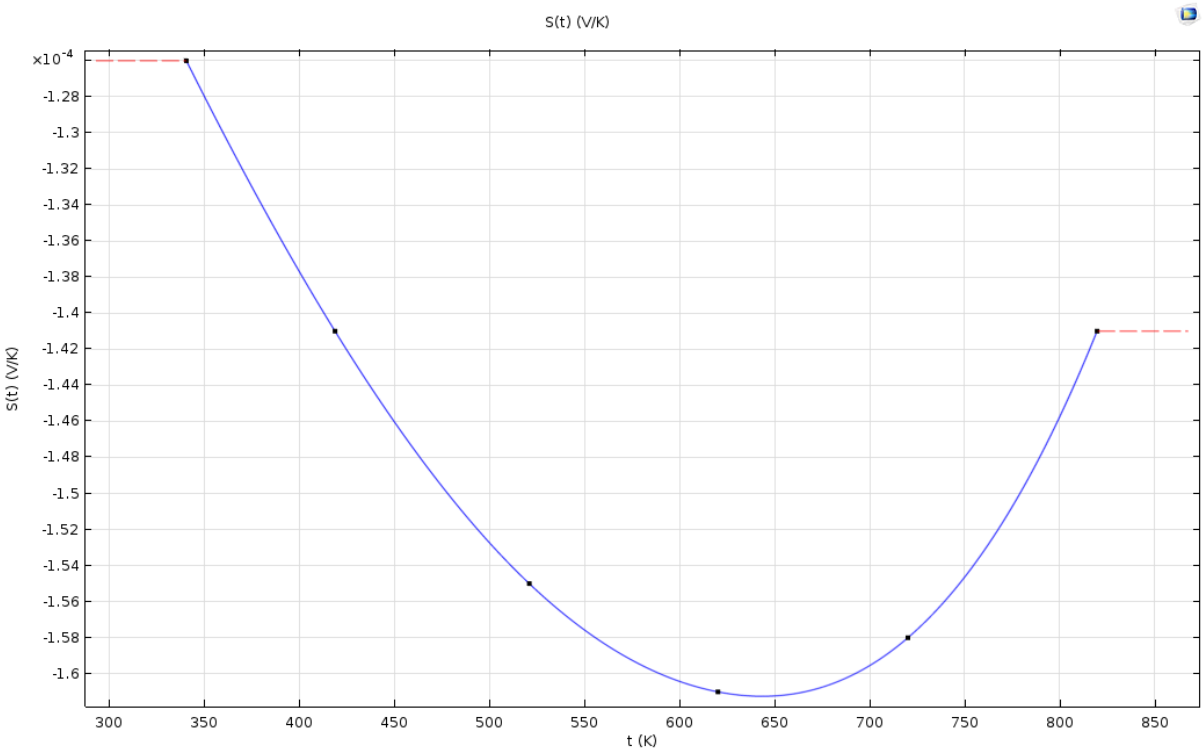

Figure of Seebeck coefficient curve for N_leg materials

Appendix E-Silicide Module Temperature and voltage distribution at T_hot=490^{0}C without heat exchanger and heat sink, T_Cold =10^{0}C

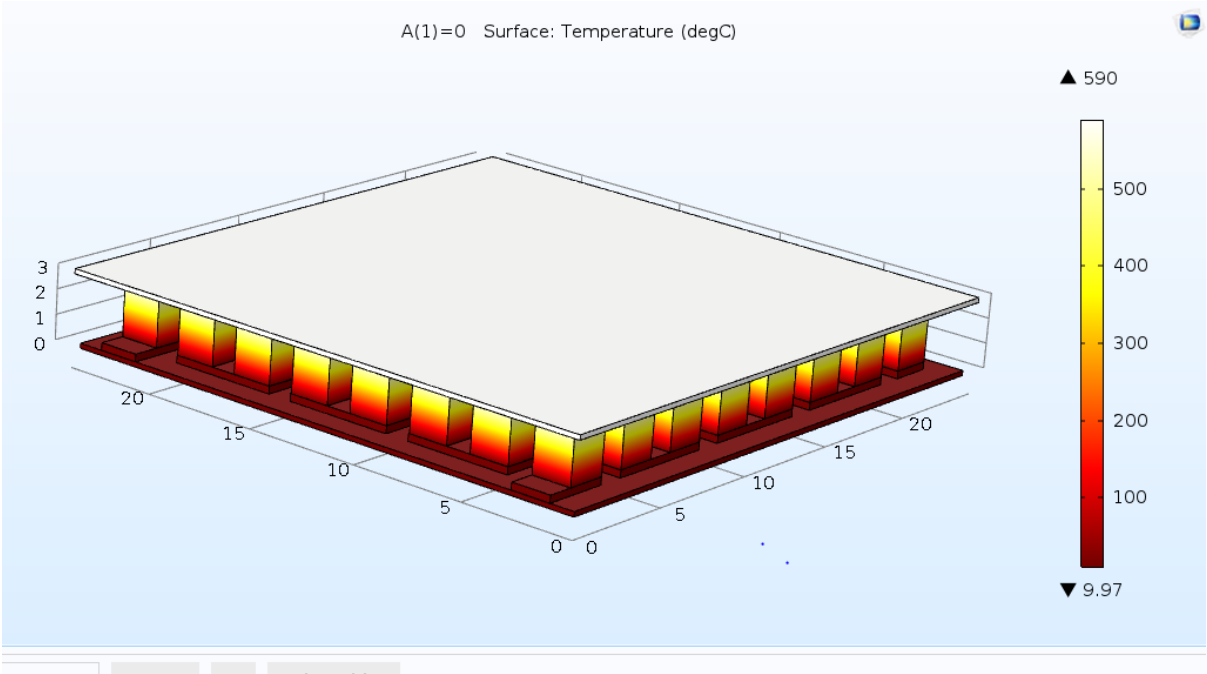

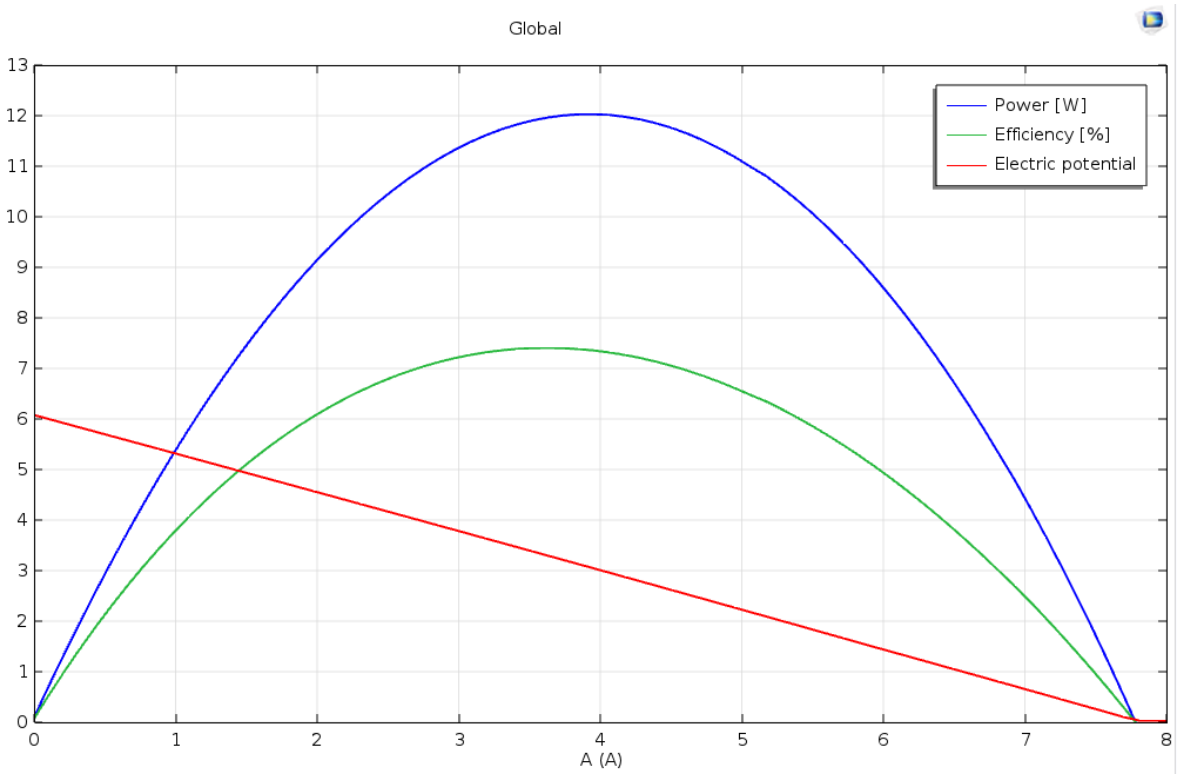
Global
Power [W]
Efficiency [%]
Electric potential
A (A)
0
1
2
3
4
5
6
7
8
9
10
11
12
13